MOLECULAR CONTROL OF GROWTH CONE PROTRUSION, ADHESION AND INVADOSOME FORMATION

by

Miguel Santiago-Medina

A dissertation submitted in partial fulfillment of

the requirements for the degree of

Doctor of Philosophy

(Neuroscience)

at the

UNIVERSITY OF WISCONSIN - MADISON

2013

Date of final oral examination: 11/22/13

The dissertation is approved by the following members of the Final Oral Committee:

Timothy Gomez, Professor, Neuroscience

William Bement, Professor, Zoology

Corinna Burger, Professor, Neuroscience

Erik Dent, Associate Professor, Neuroscience

Mary Halloran, Professor, Zoology

Luis Populin, Associate Professor, Neuroscience

ACKNOWLEDGEMENTS

I am deeply appreciative of the guidance received from my mentor, Timothy Matthew Gomez, for without it, I would not be the scientist I am today. I would also like to acknowledge the members of my graduate committee, Erik Dent, Mary Halloran, Bill Bement, Corinna Burger and Luis Populin for their attentiveness, patience and discussion over the years. In addition, I am thankful to Jenny Dahlberg, Mallory Musolf, Tera Holt, Sara Patterson and Abbey Thompson for all their hard administrative work. I would also like to extend gratitude towards past and present members of the Gomez lab, in particular, Bridget Jacques-Fricke, Jonathan Myers, Patrick Kerstein and Robert Nichol for their encouragement and entertainment over the years. I would also like to thank the undergraduate students of the lab, Anna Drewry, Allison Ducharme-Smith and Erik Thornton for their youthful energy.

I wouldn't be the person I am today if it wasn't for my wonderful and uplifting friends. They provided me with kindness and fun, making life sweeter. I would like to thank my old friends, Charles Rubert, Juan Rodriguez and his family and Pankaj Sahai for their constant encouragement ever since college graduation. I would like to thank my Madison friends, Jesus Mena, Elliot Merriam, Ginny Hu, Kendra Taylor, Matt Millette, Allison Schaser and Sayantanee Biswas. I'd like to thank my parents, Miguel Santiago and Yasin Cruz along with my siblings Leugim and Yacila Santiago for always helping me put things into perspective. I am also grateful for the kindness I have received from my girlfriend's family, Donna Gregus and Mark Terner.

Most of all, I would like to acknowledge the lovely Kelly Gregus for not only always believing in me but always being there and, really, just making everything better.

TABLE OF CONTENTS

CHAPTER 1

Introduction

General overview of growth cone motility

During embryonic development, the guidance of axons and dendrites, collectively called neurites, is critical to the formation of a functional nervous system. Growth cones at the tips of neurites both extend and navigate these neuronal processes to their pre- and post-synaptic targets by integrating signals generated through receptor interactions with diffusible and surface-bound guidance cues. Surface-bound cues found on neighboring cells, such as cell adhesion molecules (CAMs), or assembled into the extracellular matrix (ECM) act as both signaling proteins and adhesives for the growth cone (Lowery and Van Vactor, 2009). Importantly, the effects of the ECM and CAMs are likely modulated by simultaneous interactions with diffusible chemotropic factors such as morphogens, neurotrophic factors and neurotransmitters. Therefore, growth cones must integrate signals generated by multiple ligand-receptor interactions and transduce these convergent intracellular signals into the proper guidance behavior (Kolodkin and Tessier-Lavigne, 2011). These signals elicit the corresponding navigational action by reorganizing the cytoskeleton and modifying the membrane composition of the growth cone (Dent et al., 2011).

The growth cone cytoskeleton is comprised of microtubules, neurofilaments and actin filaments. Microtubules extend into the central (C) domain of the growth cone providing structural integrity and a scaffold for transport of molecules to and from the growth cone. The peripheral (P) domain of the growth cone contains globular (monomeric) and filamentous actin (G-actin and F-actin, respectively), and gives rise to the actin-rich protrusions known as filopodia and lamellipodia. Filopodia are transient antenna-like protrusions that emanate from the growth cone and are composed of

densely bundled F-actin. Lamellipodia are thin veil-like extensions of plasma membrane that arise between filopodia and consist of a network of branched and cross-linked actin filaments. Within the P domain, the actin cytoskeleton polymerizes by the addition of G-actin to the barbed ends of F-actin. Because the barbed ends of F-actin are oriented towards the leading edge, the addition of G-actin causes the rearward treadmilling of actin filaments towards the C domain. Actin retrograde flow is further regulated by the contraction of F-actin by molecular motors such as myosin. Depolymerizing factors such as ADF/cofilin, sever actin monomers at the rear of actin filaments, producing a pool of readily available actin monomers to continue the process of actin polymerization. Within the P domain, actin polymerization occurs as a continuous process balanced by the availability and addition of G-actin to actin filaments, actomyosin contractility and the disassembly of actin at the rear of filaments. The actin polymerization within filopodia and lamellipodia along with the adhesion of these protrusions to the ECM are a major determinant of growth cone motility and axon guidance.

As mentioned above, the adhesion of nascent filopodial and lamellipodial protrusions is important for growth cone motility and guidance. The adhesion of growth cones to ECM proteins occurs at specialized contact sites referred to as point contacts (PCs) (Gomez et al., 1996; Renaudin et al., 1999). In PCs, transmembrane integrin receptors tether the ECM to the intracellular F-actin network generating the traction forces necessary for membrane protrusion and directed neurite outgrowth. Because PCs anchor the actin cytoskeleton to the substratum to generate traction forces they are known as molecular clutches (Mitchison and Kirschner, 1988). These clutch sites slow

the retrograde flow of actin, resulting in increased actin filament elongation due to continuous polymerization. Since restraining actin retrograde flow regulates membrane protrusion, the distribution and dynamic turnover of PCs may have important roles in controlling the rate and direction of neurite outgrowth (Suter and Forscher, 2000). Importantly, evidence indeed suggests that axon guidance cues control the rate and direction of neurite outgrowth by modulating substratum–cytoskeletal coupling (Woo and Gomez, 2006; Woo et al., 2009). Additionally, multiple signaling pathways modulated within the protein complex of adhesions, known as the adhesome, regulate diverse cellular processes, including cytoskeletal dynamics (Harburger and Calderwood, 2009). Therefore, the regulation of cell surface integrin receptor expression and function can have diverse effects on cell motility by influencing a wide variety of associated adaptor and signaling proteins. For example, integrin activation and clustering within PCs may locally control actin polymerization by targeting factors such as the guanine nucleotide exchange factors (GEFs) to activate Rho GTPases, which in turn activate kinases that directly modulate the cytoskeleton and membrane composition of navigating growth cones.

PART I: The role of PAK in growth cone motility and axon guidance

P21- Activated Kinase (PAK)

PAK proteins are a conserved family of serine/threonine kinases that lie downstream of the Rho family GTPases, Rac1 and Cdc42 (Bokoch, 2003). PAK proteins are classified into two families depending on the sequence homology among members. The group I PAKs consist of PAK1, PAK2 and PAK3, whereas group II consists of PAK4, PAK5 and PAK6 (Arias-Romero and Chernoff, 2008). The members of both groups contain an N-terminal Rac and Cdc42 binding site known as the p21 binding domain (PBD) and a C-terminal catalytic domain. Group I PAKs additionally contain an auto-inhibitory domain (AID) that overlaps partially with the PBD as well as proline-rich domains responsible for adaptor protein interactions which are absent in group II members. Since PAKs bind many adaptor proteins and downstream effectors, they regulate numerous cellular processes implicated in cell migration. For example, PAKs regulate cell motility through direct modulation of the actin binding proteins myosin and cofilin as well through the direct phosphorylation of the adhesion protein paxillin (PXN). Because PAKs can regulate both cytoskeletal and adhesion dynamics they are key proteins in the coordination of cytoskeletal based membrane protrusion and the stabilization of such protrusions to the ECM. Many studies have investigated the role of PAK in non-neuronal cell motility, however, little is known about the functions of PAKs in neuronal growth cone motility and guidance. Understanding how the spatial and temporal activity of PAK isoforms influence growth cone adhesion and motility downstream of guidance cues is crucial to our understanding of neural development.

Importantly, PAK disfunction is implicated in neuronal development and degenerative diseases. For example, several mutant forms of PAK3 lead to dendritic spine abnormalities, which are associated with mental retardation (Boda et al., 2004).

Regulation of cell adhesion by PAK

Modulation of integrin-dependent adhesions and the downstream signals coordinated at growth cone PCs is a fundamental regulatory mechanism that controls axon guidance (Myers et al., 2011; Robles and Gomez, 2006; Woo and Gomez, 2006). Cell-substratum adhesion complexes function both as anchorage points to stabilize new protrusions, but also as signaling centers that coordinate diverse cellular processes, including new protrusion formation (Huveneers and Danen, 2009; Mitra et al., 2005). Within PCs are a myriad of signaling proteins that modulate adhesion assembly and disassembly (collectively referred to as adhesion dynamics). Structural proteins such as PXN are involved in direct linking of actin filaments to integrin receptors. Paxillin is a multi-domain molecular scaffolding protein that serves as a nexus to integrate and coordinate signals generated from diverse stimuli (Deakin and Turner, 2008). The C-terminal half of PXN mediates focal adhesion targeting, whereas the N-terminal half of PXN contains five LD (leucine- and aspartate-rich) motifs and multiple Ser/Thr phosphorylation sites, which mediate interactions with a variety of proteins, including PAKs. One key target of PAKs is phosphorylation of PXN at S273, which activates Rac1 to promote adhesion turnover (Nayal et al., 2006).

PAKs link to PXN at adhesions by binding to a Rac- and Cdc42-specific guanine nucleotide exchange factor, termed PIX (PAK-interacting exchange factor) (ten Klooster

et al., 2006). The LD4 domain of PXN recruits a signaling complex composed of G-protein-coupled receptor kinase interacting protein (GIT), which binds to PIX-PAK. The binding of the GIT-PIX-PAK complex to PXN is regulated by the PAK dependent phosphorylation of S273-PXN (Nayal et al., 2006). Interestingly, PAK phosphorylation of S273-PXN appears to destabilize adhesions. In motile cells, PAK promotes adhesion formation through its N-terminal, regulatory domain, and promotes adhesion dissolution and turnover through its kinase activity (Manser et al., 1998). The interaction between PAK and PIX is crucial for lamellipodia formation as well as stabilization and does not require PAK catalytic activity. This suggests that one function of PIX may be to recruit PAKs to adhesions as scaffolding proteins. For example, PAK recruitment to adhesions can promote the activation of Rac through its association with PIX, which in turn acts as a GEF for Rac activation (Obermeier et al., 1998). In a localized feedback loop, cell motility may be enhanced due to both Rac activation and adhesion turnover through PAK phosphorylation of PXN. Moreover, PAK and Rac compete for PIX binding within a cell to control adhesion dynamics and motility (ten Klooster et al., 2006).

Regulation of cell motility by PAK

The assembly and organization of actin filaments and microtubules within growth cones control motility and guidance. Protrusion of the leading edge membrane, which drives the exploratory behaviors of filopodia and lamellipodia, depends on actin polymerization. As discussed above, leading edge protrusion is controlled by a balance of myosin II dependent retrograde flow of F-actin and F-actin polymerization. There are many actin-binding proteins that regulate F-actin polymerization. Cofilin regulates actin

polymerization by severing or depolymerizing actin filaments. Interestingly, both myosin II and cofilin activity are regulated by PAK through LIM kinase and myosin light chain (MLC) kinase, respectively (Bokoch, 2003). While several studies have shown that LIM kinase, cofilin and myosin activity are important regulators of growth cone motility, little is known about the mechanistic link between PAK and its targets in growth cones.

Different PAK isoforms regulate various aspects of neuronal morphogenesis. For example, PAK1 is important in the formation of both axons and dendrites (Daniels et al., 1998; Hayashi et al., 2002), whereas PAK3 is involved in neuronal migration (Cobos et al., 2007). Fitting with a role in neuronal migration, PAK3 overexpression in neurons increases lamellipodia formation (Obermeier *et al.* 1998). Growth cones with altered PAK kinase activity exhibit less dynamic filopodia when compared to wild-type cells. Since filopodia play an important role as exploratory structures, altered PAK function may allow growth on to repulsive substrata as well as disrupt axon pathfinding. Indeed, inhibition of PAK kinase activity in neuroblastoma cells causes axons to extend onto repulsive ECM molecules (Marler et al., 2005). This is consistent with findings from our own work showing that PAK regulates filopodial tip elongation (Robles et al., 2005; Santiago-Medina et al., 2013). While the specific isoform of PAK that is involved in filopodial extension by *Xenopus* spinal neurons was uncertain, other studies have shown that constitutively active PAK1 (Sells et al., 2000) and wild-type PAK2 (Marler et al., 2005) induce the formation of filopodia. Interestingly, these various effects on neuronal morphology are not only dependent on kinase activity but also on the N-terminal scaffolding domains of PAKs.

PAKs are multi-functional proteins that regulate cell motility and adhesion through

their interactions with different adaptor proteins in addition to their catalytic activity on downstream targets. In fact, several downstream effectors of PAK have been implicated in neurite outgrowth. For example, LIM Kinase is a prominent downstream target of PAK that modulates neurite extension by phosphorylating and inhibiting cofilin, which promotes actin severing (Aizawa et al., 2001; Endo et al., 2007; Endo et al., 2003). Balanced cofilin activity is necessary for optimum neurite outgrowth, as overactivation or inhibition of cofilin activity significantly reduces growth cone motility and neurite extension (Fass et al., 2004; Marsick et al., 2010; Vitriol and Zheng, 2012). This strongly suggests that PAK activity is critical for the proper balance of cofilin activity and cofilin-mediated actin severing. Similarly, PAK can regulate myosin activity and control the rearward pull on the actin cytoskeleton. Activated PAK can promote cellular relaxation by phosphorylating and inactivating myosin light chain kinase which now can no longer phosphorylate the regulatory myosin light chain (R-MLC) of myosin II to control actin contractility. Conversely, active PAK can also induce contractility by directly phosphorylating R-MLC, activating myosin tension (Bokoch, 2003).

Regulation of axon guidance by PAK

During nervous system development, nascent neurites are guided to their targets by a myriad of attractive and repulsive cues. This molecular instruction arises from the pairing of ligands with receptors, such as Slit with Robo, Semaphorin with Neuropilin, Netrin with DCC, and Ephrin with Eph. Activation of all these guidances receptors converges onto the Rho GTPases, which modulate cytoskeletal proteins and integrin-based adhesions (Nakamoto et al., 2004). The influence of PAK on both cytoskeletal

remodeling and adhesion dynamics supports its role as a key modulator of growth cone guidance. Indeed, evidence suggests that PAK can balance both repulsive and attractive axon guidance, likely by functioning differentially in specific signaling pathways to mediate guidance.

The first evidence of PAK function in axon guidance came from Drosophila mutants where photoreceptor and olfactory axon pathfinding was disrupted (Ang et al., 2003; Hing et al., 1999). Axons with genetically altered PAK function exhibit increased fasciculation and undertake disorganized and circuitous trajectories, resulting in ectopic targeting. Importantly, correct growth cone steering and neurite projection to targets requires both PAK kinase activity and PAK binding to Nck. The regulation of filopodial dynamics by PAK is also believed to influence growth cone guidance in this system (Kim et al., 2003). In addition, PAK function can induce both axon repulsion (via UNC-5) and attraction (via DCC) downstream of Netrin signaling (Lucanic et al., 2006; Shekarabi et al., 2005). Moreover, both Semaphorin and Slit, which are important chemorepulsive guidance cues, require PAK function for their inhibitory effects on growth cones (Aizawa et al., 2001; Fan et al., 2003). Interestingly, Rac1, an upstream activator of PAK, is sequestered and rendered inactive by the Semaphorin receptor PlexinA1, which results in growth cone collapse and repulsive turning (Hu et al., 2001; Vikis et al., 2002). Nearly all these studies suggest that Nck, Rac and PAK function together in a protein complex to regulate the actin cytoskeleton downstream of guidance cues. Finally, in retinal ganglion cells, Ephrin-A1 binding to the EphA receptor can influence guidance by interfering with Rac and Cdc42 dependent PAK activation while simultaneously enhancing RhoA induced growth cone repulsion (Shamah et al., 2001).

PART II: The role of invadosome-like structures in growth cones

The mechanisms mentioned thus far concentrate on the effect of the extracellular environment in eliciting growth cone motility through cytoskeletal and adhesion remodeling. However, an equally important mechanism that likely works in parallel with cytoskeletal and adhesion signaling is the modification of the extracellular environment as a result of the interaction between the growth cone and said environment. In other words, axon guidance depends on the ability of the growth cone to actively remodel its extracellular environment in response to environmental factors and guidance cues. Extracellular modifications include the remodeling of the ECM which surrounds the growth cone as well as the ligands and receptors present in the environment and cell membrane respectively. Importantly, these modifications are carried out by the expression and secretion of varying proteases from the navigating growth cone. In both scenarios, extracellular protease activity may regulate how the growth cone both perceives and responds to the environment throughout axon guidance in developing neuronal systems. Other cell types such as monocytes, osteoclasts, and cancer cells form structures known as invadosomes which serve as adhesion and proteolytic sites. Previous studies have shown the importance of neuronal protease expression and secretion in axon guidance yet no study has ever shown the existence of invadosomes in growth cones.

Invadosomes

Podosomes and invadopodia are cell-matrix contact sites with the ability to

degrade ECM components and, when given the right environment, form 3D filopodia-like protrusions (Murphy and Courtneidge, 2011). The terms podosome and invadopodia are often used interchangeably, although they typically refer to the structures formed in normal and cancer cells, respectively. While evidence suggests important distinctions between the two (Oser et al., 2011), they are collectively referred to as invadosomes when describing adhesive structures involved in ECM degradation and invasion (Linder et al., 2011). Similar to filopodia, invadosomes are characterized by an F-actin rich core together with several actin bundling proteins and regulators of actin polymerization. For example, invadosomes contain the actin bundling proteins fascin and α-actinin; the actin regulatory proteins cortactin, N-WASP and Arp2/3; as well as the signal modulators Src, protein kinase C (PKC) and $PI(3,4)P_2$; and certain integrin and growth factor receptors (Albiges-Rizo et al., 2009; Boateng and Huttenlocher, 2012; Yamaguchi and Oikawa, 2010). However, invadosomes are distinct from filopodia in several ways. For example, invadosomes appear as long lived F-actin rich accumulations situated on the ventral surface of cells, typically away from the leading edge. In 3D environments, invadosomes penetrate into the underlying ECM to promote cell migration through tissues or 3D matrices. To facilitate ECM degradation, invadosomes express both cell surface and secreted proteases (Murphy and Courtneidge, 2011). Finally, two key scaffolding proteins that distinguish invadosomes are the adaptor proteins, Tyr kinase substrate with four SH3 domains (Tks4) and its homolog, Tks5 (Courtneidge, 2012).

Invadosome assembly is induced by growth factors that activate Src kinases and PKC, which may function in cooperation with integrin signaling (Boateng and

Huttenlocher, 2012). Phosphorylation of key invadosome-associated proteins, like Tks5 and cortactin (Cttn) initiate invadosome formation and proteolytic activity (MacGrath and Koleske, 2012). The extent of ECM degradation by invadosomes varies by cell type and substrate. The most degradative cells are Src-transformed metastatic cells, but normal cells such as smooth muscle cells, monocytic cells, and osteoclasts form invadosomes that degrade the ECM (Linder et al., 2011). Importantly, the types of pericellular proteases presented or released at invadosomes will determine the types and extent of protein cleavage. For example, several proteases cleave and remodel ECM components like collagen (Col), laminin (LN) and chondroitin sulfate proteoglycan (CSPG) to facilitate cell migration through interstitial spaces (Stamenkovic, 2003; Yong et al., 2001). However, invadosomes may also induce the specialized proteolysis of proteins to activate ligands, such as conversion of pro-BDNF to BDNF (Je et al., 2012), or alter receptor function, such as cleavage of the extracellular domain of DCC (Bai et al., 2011; Galko and Tessier-Lavigne, 2000) or APP receptors (Yong et al., 2001). Finally, evidence suggest that invadosomes not only penetrate the ECM by proteolysis, but can also physically displace the basement membrane (Hagedorn et al., 2013).

Extracellular proteases

There are many proteases involved in the degradation of extracellular proteins such as the matrix metalloproteases (MMPs), a disintegrin and metalloproteases (ADAMs) and plasmin. MMPs and ADAMs belong to the metzincin family of proteases due to the presence of a conserved Met residue and zinc ion at their catalytic active site (Rivera et al., 2010). Plasmin, on the other hand, is a serine protease that is secreted

from cells as a zymogen called plasminogen (Gutierrez-Fernandez et al., 2009). Although all three types of proteases mentioned function by degrading extracellular proteins, they are differentially localized throughout the cell. For example, plasmin along with certain MMPs are secreted into the pericellular space whereas other MMPs (MT-MMPs) and the majority of ADAMs are transmembrane proteins. These proteases are capable of degrading a wide variety of ECM proteins, such as LN, FN, Coll, CSPG and tenascin-R as well as execute the juxtamembrane cleavage of membrane-associated proteins such as receptors (Rivera et al., 2010). For this reason, certain proteases such as ADAM10 and 17 are referred to as sheddases. Since most of the proteases mentioned are initially expressed as zymogens, a common post-translational regulatory mechanism for their activation is the proteolytic removal of an inhibitory pro-domain. The removal of pro-domains can be accomplished by active MMPs and plasmins as well as intracellular proteases such as furins. Lastly, protease activity can be further regulated by the interaction of active proteases with endogenous tissue inhibitors of metalloproteases (TIMPs). TIMPs block proteolytic activity by binding to the catalytic site of MMPs and ADAMs thus sequestering all proteolytic active sites (Ould-yahoui et al., 2009). Interestingly, all three types of pericellular proteases as well as their endogenous inhibitors, the TIMPs, have been implicated in growth cone motility.

Extracellular proteases in growth cone motility and guidance

Pericellular proteases were once believed to regulate axon extension by simply degrading the surrounding matrix to create a passage for axonal outgrowth (Ethell and Ethell, 2007; Muir, 1994; Sarig-Nadir and Seliktar, 2010; Zuo et al., 1998). For example,

plasmin secreted from PC12 growth cones can degrade LN-1 resulting in increased neurite initiation and length (Gutierrez-Fernandez et al., 2009). However, recent studies performed both *in vitro* and *in vivo* now suggest that proteolytic cleavage is directed toward specific ligands in the environment, as well as receptors on growth cones to activate or terminate motility (Chen et al., 2007; Fambrough et al., 1996; Hehr et al., 2005; Schimmelpfeng et al., 2001; Webber et al., 2002). Additional evidence suggests that pericellular proteases act to reveal cryptic sites in molecules that are otherwise inert in axon guidance, as well as release neurotrophic factors that may associate with the ECM (McFarlane, 2003; Yong et al., 2001). For example, MMP2 cleavage of the LN-5 γ2 subunit reveals a cryptic site on the α3 subunit which enhances the migration of epithelial cells (Giannelli et al., 1997). Similarly, MMP9 activity exposes a cryptic site in collagen IV that potentiates endothelial cell migration (Xu et al., 2001).

Besides a role in ECM remodeling, pericellular proteases function upon and in response to guidance cues. Neurotrophic factors such as NGF and BDNF can upregulate MMP transcription and translation. MMPs, in turn, regulate neurotrophic factor activity. For example, in rat cortical neurons, BDNF stimulation augments MMP9 activity through an increase in mRNA and protein synthesis (Kuzniewska et al., 2013). In turn, MMP9 along with MMP14/MMP2 cleave pro-BDNF and pro-NGF into the corresponding mature forms, respectively (Je et al., 2012; Saygili et al., 2011). Additionally, plasmin can also proteolytically remove the pro-domains of neurotrophins (Lee et al., 2001). Extracellular proteases can also regulate growth cone motility by cleaving both guidance cues and their receptors. In culture, both MMP2/9 and ADAM10 regulate Eph/ephrin induced growth cone repulsion by cleaving the receptor and ligand,

respectively (Hattori et al., 2000; Lin et al., 2008). Eph/ephrin activation also triggers growth cone repulsion through ADAM10-dependent NCAM cleavage (Brennaman et al., 2013). Additional findings demonstrate that ADAM-dependent ectodomain shedding of DCC, $p75^{NTR}$ and transmembrane semaphorin can also regulate growth cone motility (Browne et al., 2012; Galko and Tessier-Lavigne, 2000; Kanning et al., 2003). Importantly, the role of proteases in regulating receptor-ligand interactions during axon guidance has been shown in developing animals across species. For example, in Xenopus, inhibition of ADAM10 activity within the neuroepithelial cells along the pathway of growing RGC axons leads to axon guidance errors (Chen et al., 2007; Hehr et al., 2005). In Drosophila, both ADAM and MMP activity contribute to proper axon guidance. Flies that carry loss-of-function mutations in ADAM10 show axon stalling during development due to a decrease in Slit/Robo proteolytic cleavage (Fambrough et al., 1996; Schimmelpfeng et al., 2001). Additionally, in Drosophila motor neurons, MMP2 dependent processing of Sema-1a controls axon fasciculation as determined by MMP2 mutants and TIMP overexpression (Miller et al., 2008). Lastly, metalloproteases regulate Netrin/DCC-mediated commissural and motor axon guidance in mice through the generation of transmembrane DCC stubs (Bai et al., 2011).

Introduction to the dissertation

Throughout my thesis work, I have studied a mechanism important in the regulation of growth cone motility as well as identified a previously uncharacterized structure in growth cones, which I explain in chapter 2 and 3, respectively. The study mentioned in chapter 2 was published in the Journal of Cell Science whereas the study described in chapter 3 is in its final stage of preparation.

The study explained in chapter 2 describes how the Rho-GTPase effector and scaffolding protein, PAK, can regulate growth cone motility by modulating the actin cytoskeleton and adhesion dynamics. In this first study, I found that PAK2 and 3 are the dominant isoforms expressed in spinal neurons and that they localize differentially throughout the growth cone. I also provide evidence that the adaptor protein and GEF, PIX is also present in growth cones and localizes with PAK at PCs. To determine the importance of the association of PAK and PIX at growth cone PCs, I used an 18 amino acid long cell permeable peptide (PAK18) designed to disrupt the binding of PAK and PIX. Surprisingly, I found that low doses of PAK18 increases growth cone protrusion, size and motility whereas high doses result in growth cone collapse and neurite retraction. I determined that the dose-dependent biphasic effect of PAK18 on neurite outgrowth was mostly attributed to cofilin and myosin mediated actin polymerization regulation and not adhesion dynamics. Expressing mutated versions of PAK2 and 3, I further demonstrated that PAK2 is the predominant PAK isoform involved in neurite outgrowth. Lastly, I examined the role Rac activation through PIX has as a result of PAK18 stimulated outgrowth. Interestingly, in response to PAK18, Rac does contribute

to neurite acceleration as determined by a decrease in outgrowth from growth cones expressing a dominant negative form of Rac.

In chapter 3, I identify and characterize a novel growth cone structure that resembles the adhesion and proteolytic sites known as podosomes and invadopodia (collectively known as invadosomes) of immune and cancer cells, respectively. Using both fixed and live cell imaging, I determined that growth cones from a variety of sources and on a variety of substrata form invadosomes that appear as F-actin rich foci. These invadosomes form within the growth cone central domain and are predominantly stable, long-lived structures. Importantly, the growth cones of commissural interneurons within the intact spinal cord of Xenopus embryos form invadosomes. I further characterized growth cone invadosomes by assessing the actin polymerization and actin-modulatory proteins within these structures. I found many F-actin modulatory proteins in invadosomes including cortactin, Src and Tks5, which are well known invadosomal markers in non-neuronal cells. Next, I measured the formation and stability of invadosomes in response to Src and Tks5 perturbation and discovered their importance in growth cone invadosome maintenance. To determine if invadosomes protrude into 3D space, I used structured illumination microscopy (SIM) to obtain a 3D rendering of growth cones *in vitro* and *in vivo*. The observations I obtained using SIM demonstrated that invadosomes are indeed 3D protrusions that emanate from the growth cone surface. Lastly, to determine if growth cone invadosomes contain proteases that are capable of remodeling the ECM, I immunolabeled for MMPs as well as cultured spinal explants on fluorescently conjugated gelatin. As expected, invadosomes contain both MMP14 and the ability to degrade the ECM.

References

Aizawa, H., Wakatsuki, S., Ishii, A., Moriyama, K., Sasaki, Y., Ohashi, K., Sekine-Aizawa, Y., Sehara-Fujisawa, A., Mizuno, K., Goshima, Y. et al. (2001). Phosphorylation of cofilin by LIM-kinase is necessary for semaphorin 3A-induced growth cone collapse. Nat Neurosci 4, 367-73.

Albiges-Rizo, C., Destaing, O., Fourcade, B., Planus, E. and Block, M. R. (2009). Actin machinery and mechanosensitivity in invadopodia, podosomes and focal adhesions. J Cell Sci 122, 3037-49.

Ang, L. H., Kim, J., Stepensky, V. and Hing, H. (2003). Dock and Pak regulate olfactory axon pathfinding in Drosophila. Development 130, 1307-16.

Arias-Romero, L. E. and Chernoff, J. (2008). A tale of two Paks. Biol Cell 100, 97-108.

Bai, G., Chivatakarn, O., Bonanomi, D., Lettieri, K., Franco, L., Xia, C., Stein, E., Ma, L., Lewcock, J. W. and Pfaff, S. L. (2011). Presenilin-dependent receptor processing is required for axon guidance. Cell 144, 106-18.

Boateng, L. R. and Huttenlocher, A. (2012). Spatiotemporal regulation of Src and its substrates at invadosomes. Eur J Cell Biol 91, 878-88.

Boda, B., Alberi, S., Nikonenko, I., Node-Langlois, R., Jourdain, P., Moosmayer, M., Parisi-Jourdain, L. and Muller, D. (2004). The mental retardation protein PAK3 contributes to synapse formation and plasticity in hippocampus. J Neurosci 24, 10816-25.

Bokoch, G. M. (2003). Biology of the p21-activated kinases. Annu Rev Biochem 72, 743-81.

Brennaman, L. H., Moss, M. L. and Maness, P. F. (2013). EphrinA/EphA-induced ectodomain shedding of neural cell adhesion molecule regulates growth cone repulsion through ADAM10 metalloprotease. J Neurochem.

Browne, K., Wang, W., Liu, R. Q., Piva, M. and O'Connor, T. P. (2012). Transmembrane semaphorin5B is proteolytically processed into a repulsive neural guidance cue. J Neurochem 123, 135-46.

Chen, Y. Y., Hehr, C. L., Atkinson-Leadbeater, K., Hocking, J. C. and McFarlane, S. (2007). Targeting of retinal axons requires the metalloproteinase ADAM10. J Neurosci 27, 8448-56.

Cobos, I., Borello, U. and Rubenstein, J. L. (2007). Dlx transcription factors promote migration through repression of axon and dendrite growth. Neuron 54, 873-88.

Courtneidge, S. A. (2012). Cell migration and invasion in human disease: the Tks adaptor proteins. Biochem Soc Trans 40, 129-32.

Daniels, R. H., Hall, P. S. and Bokoch, G. M. (1998). Membrane targeting of p21-activated kinase 1 (PAK1) induces neurite outgrowth from PC12 cells. EMBO J 17, 754-64.

Deakin, N. O. and Turner, C. E. (2008). Paxillin comes of age. J Cell Sci 121, 2435-44.

Dent, E. W., Gupton, S. L. and Gertler, F. B. (2011). The growth cone cytoskeleton in axon outgrowth and guidance. Cold Spring Harb Perspect Biol 3.

Endo, M., Ohashi, K. and Mizuno, K. (2007). LIM kinase and slingshot are critical for neurite extension. J Biol Chem 282, 13692-702.

Endo, M., Ohashi, K., Sasaki, Y., Goshima, Y., Niwa, R., Uemura, T. and Mizuno, K. (2003). Control of growth cone motility and morphology by LIM kinase and Slingshot via phosphorylation and dephosphorylation of cofilin. J Neurosci 23, 2527-37.

Ethell, I. M. and Ethell, D. W. (2007). Matrix metalloproteinases in brain development and remodeling: synaptic functions and targets. J Neurosci Res 85, 2813-23.

Fambrough, D., Pan, D., Rubin, G. M. and Goodman, C. S. (1996). The cell surface metalloprotease/ disintegrin Kuzbanian is required for axonal extension in Drosophila. Proc Natl Acad Sci U S A 93, 13233-8.

Fan, X., Labrador, J. P., Hing, H. and Bashaw, G. J. (2003). Slit stimulation recruits Dock and Pak to the roundabout receptor and increases Rac activity to regulate axon repulsion at the CNS midline. Neuron 40, 113-27.

Fass, J., Gehler, S., Sarmiere, P., Letourneau, P. and Bamburg, J. R. (2004). Regulating filopodial dynamics through actin-depolymerizing factor/cofilin. Anat Sci Int 79, 173-83.

Galko, M. J. and Tessier-Lavigne, M. (2000). Function of an axonal chemoattractant modulated by metalloprotease activity. Science 289, 1365-7.

Giannelli, G., Falk-Marzillier, J., Schiraldi, O., Stetler-Stevenson, W. G. and Quaranta, V. (1997). Induction of cell migration by matrix metalloprotease-2 cleavage of laminin-5. Science 277, 225-8.

Gomez, T. M., Roche, F. K. and Letourneau, P. C. (1996). Chick sensory neuronal growth cones distinguish fibronectin from laminin by making substratum contacts that resemble focal contacts. J Neurobiol 29, 18-34.

Gutierrez-Fernandez, A., Gingles, N. A., Bai, H., Castellino, F. J., Parmer, R. J. and Miles, L. A. (2009). Plasminogen enhances neuritogenesis on laminin-1. J Neurosci 29, 12393-400.
Hagedorn, E. J., Ziel, J. W., Morrissey, M. A., Linden, L. M., Wang, Z., Chi, Q., Johnson, S. A. and Sherwood, D. R. (2013). The netrin receptor DCC focuses invadopodia-driven basement membrane transmigration in vivo. J Cell Biol 201, 903-13.
Harburger, D. S. and Calderwood, D. A. (2009). Integrin signalling at a glance. J Cell Sci 122, 159-63.
Hattori, M., Osterfield, M. and Flanagan, J. G. (2000). Regulated cleavage of a contact-mediated axon repellent. Science 289, 1360-5.
Hayashi, K., Ohshima, T. and Mikoshiba, K. (2002). Pak1 is involved in dendrite initiation as a downstream effector of Rac1 in cortical neurons. Mol Cell Neurosci 20, 579-94.
Hehr, C. L., Hocking, J. C. and McFarlane, S. (2005). Matrix metalloproteinases are required for retinal ganglion cell axon guidance at select decision points. Development 132, 3371-9.
Hing, H., Xiao, J., Harden, N., Lim, L. and Zipursky, S. L. (1999). Pak functions downstream of Dock to regulate photoreceptor axon guidance in Drosophila. Cell 97, 853-63.
Hu, H., Marton, T. F. and Goodman, C. S. (2001). Plexin B mediates axon guidance in Drosophila by simultaneously inhibiting active Rac and enhancing RhoA signaling. Neuron 32, 39-51.
Huveneers, S. and Danen, E. H. (2009). Adhesion signaling - crosstalk between integrins, Src and Rho. J Cell Sci 122, 1059-69.
Je, H. S., Yang, F., Ji, Y., Nagappan, G., Hempstead, B. L. and Lu, B. (2012). Role of pro-brain-derived neurotrophic factor (proBDNF) to mature BDNF conversion in activity-dependent competition at developing neuromuscular synapses. Proc Natl Acad Sci U S A 109, 15924-9.
Kanning, K. C., Hudson, M., Amieux, P. S., Wiley, J. C., Bothwell, M. and Schecterson, L. C. (2003). Proteolytic processing of the p75 neurotrophin receptor and two homologs generates C-terminal fragments with signaling capability. J Neurosci 23, 5425-36.
Kim, M. D., Kamiyama, D., Kolodziej, P., Hing, H. and Chiba, A. (2003). Isolation of Rho GTPase effector pathways during axon development. Dev Biol 262, 282-93.
Kolodkin, A. L. and Tessier-Lavigne, M. (2011). Mechanisms and molecules of neuronal wiring: a primer. Cold Spring Harb Perspect Biol 3.
Kuzniewska, B., Rejmak, E., Malik, A. R., Jaworski, J., Kaczmarek, L. and Kalita, K. (2013). Brain-derived neurotrophic factor induces matrix metalloproteinase 9 expression in neurons via the serum response factor/c-Fos pathway. Mol Cell Biol 33, 2149-62.
Lee, R., Kermani, P., Teng, K. K. and Hempstead, B. L. (2001). Regulation of cell survival by secreted proneurotrophins. Science 294, 1945-8.
Lin, K. T., Sloniowski, S., Ethell, D. W. and Ethell, I. M. (2008). Ephrin-B2-induced cleavage of EphB2 receptor is mediated by matrix metalloproteinases to trigger cell repulsion. J Biol Chem 283, 28969-79.
Linder, S., Wiesner, C. and Himmel, M. (2011). Degrading devices: invadosomes in proteolytic cell invasion. Annu Rev Cell Dev Biol 27, 185-211.
Lowery, L. A. and Van Vactor, D. (2009). The trip of the tip: understanding the growth cone machinery. Nat Rev Mol Cell Biol 10, 332-43.
Lucanic, M., Kiley, M., Ashcroft, N., L'Etoile, N. and Cheng, H. J. (2006). The Caenorhabditis elegans P21-activated kinases are differentially required for UNC-6/netrin-mediated commissural motor axon guidance. Development 133, 4549-59.
MacGrath, S. M. and Koleske, A. J. (2012). Cortactin in cell migration and cancer at a glance. J Cell Sci 125, 1621-6.
Manser, E., Loo, T. H., Koh, C. G., Zhao, Z. S., Chen, X. Q., Tan, L., Tan, I., Leung, T. and Lim, L. (1998). PAK kinases are directly coupled to the PIX family of nucleotide exchange factors. Mol Cell 1, 183-92.
Marler, K. J., Kozma, R., Ahmed, S., Dong, J. M., Hall, C. and Lim, L. (2005). Outgrowth of neurites from NIE-115 neuroblastoma cells is prevented on repulsive substrates through the action of PAK. Mol Cell Biol 25, 5226-41.
Marsick, B. M., Flynn, K. C., Santiago-Medina, M., Bamburg, J. R. and Letourneau, P. C. (2010). Activation of ADF/cofilin mediates attractive growth cone turning toward nerve growth factor and netrin-1. Dev Neurobiol 70, 565-88.
McFarlane, S. (2003). Metalloproteases: carving out a role in axon guidance. Neuron 37, 559-62.
Miller, C. M., Page-McCaw, A. and Broihier, H. T. (2008). Matrix metalloproteinases promote motor axon fasciculation in the Drosophila embryo. Development 135, 95-109.
Mitchison, T. and Kirschner, M. (1988). Cytoskeletal dynamics and nerve growth. Neuron 1, 761-72.

Mitra, S. K., Hanson, D. A. and Schlaepfer, D. D. (2005). Focal adhesion kinase: in command and control of cell motility. Nat Rev Mol Cell Biol 6, 56-68.
Muir, D. (1994). Metalloproteinase-dependent neurite outgrowth within a synthetic extracellular matrix is induced by nerve growth factor. Exp Cell Res 210, 243-52.
Murphy, D. A. and Courtneidge, S. A. (2011). The 'ins' and 'outs' of podosomes and invadopodia: characteristics, formation and function. Nat Rev Mol Cell Biol 12, 413-26.
Myers, J. P., Santiago-Medina, M. and Gomez, T. M. (2011). Regulation of axonal outgrowth and pathfinding by integrin-ECM interactions. Dev Neurobiol 71, 901-23.
Nakamoto, T., Kain, K. H. and Ginsberg, M. H. (2004). Neurobiology: New connections between integrins and axon guidance. Curr Biol 14, R121-3.
Nayal, A., Webb, D. J., Brown, C. M., Schaefer, E. M., Vicente-Manzanares, M. and Horwitz, A. R. (2006). Paxillin phosphorylation at Ser273 localizes a GIT1-PIX-PAK complex and regulates adhesion and protrusion dynamics. J Cell Biol 173, 587-9.
Obermeier, A., Ahmed, S., Manser, E., Yen, S. C., Hall, C. and Lim, L. (1998). PAK promotes morphological changes by acting upstream of Rac. EMBO J 17, 4328-39.
Oser, M., Dovas, A., Cox, D. and Condeelis, J. (2011). Nck1 and Grb2 localization patterns can distinguish invadopodia from podosomes. Eur J Cell Biol 90, 181-8.
Ould-yahoui, A., Tremblay, E., Sbai, O., Ferhat, L., Bernard, A., Charrat, E., Gueye, Y., Lim, N. H., Brew, K., Risso, J. J. et al. (2009). A new role for TIMP-1 in modulating neurite outgrowth and morphology of cortical neurons. PLoS One 4, e8289.
Renaudin, A., Lehmann, M., Girault, J. and McKerracher, L. (1999). Organization of point contacts in neuronal growth cones. J Neurosci Res 55, 458-71.
Rivera, S., Khrestchatisky, M., Kaczmarek, L., Rosenberg, G. A. and Jaworski, D. M. (2010). Metzincin proteases and their inhibitors: foes or friends in nervous system physiology? J Neurosci 30, 15337-57.
Robles, E. and Gomez, T. M. (2006). Focal adhesion kinase signaling at sites of integrin-mediated adhesion controls axon pathfinding. Nat Neurosci 9, 1274-83.
Robles, E., Woo, S. and Gomez, T. M. (2005). Src-dependent tyrosine phosphorylation at the tips of growth cone filopodia promotes extension. J Neurosci 25, 7669-81.
Santiago-Medina, M., Gregus, K. A. and Gomez, T. M. (2013). PAK-PIX interactions regulate adhesion dynamics and membrane protrusion to control neurite outgrowth. J Cell Sci 126, 1122-33.
Sarig-Nadir, O. and Seliktar, D. (2010). The role of matrix metalloproteinases in regulating neuronal and nonneuronal cell invasion into PEGylated fibrinogen hydrogels. Biomaterials 31, 6411-6.
Saygili, E., Schauerte, P., Pekassa, M., Rackauskas, G., Schwinger, R. H., Weis, J., Weber, C., Marx, N. and Rana, O. R. (2011). Sympathetic neurons express and secrete MMP-2 and MT1-MMP to control nerve sprouting via pro-NGF conversion. Cell Mol Neurobiol 31, 17-25.
Schimmelpfeng, K., Gogel, S. and Klambt, C. (2001). The function of leak and kuzbanian during growth cone and cell migration. Mech Dev 106, 25-36.
Sells, M. A., Pfaff, A. and Chernoff, J. (2000). Temporal and spatial distribution of activated Pak1 in fibroblasts. J Cell Biol 151, 1449-58.
Shamah, S. M., Lin, M. Z., Goldberg, J. L., Estrach, S., Sahin, M., Hu, L., Bazalakova, M., Neve, R. L., Corfas, G., Debant, A. et al. (2001). EphA receptors regulate growth cone dynamics through the novel guanine nucleotide exchange factor ephexin. Cell 105, 233-44.
Shekarabi, M., Moore, S. W., Tritsch, N. X., Morris, S. J., Bouchard, J. F. and Kennedy, T. E. (2005). Deleted in colorectal cancer binding netrin-1 mediates cell substrate adhesion and recruits Cdc42, Rac1, Pak1, and N-WASP into an intracellular signaling complex that promotes growth cone expansion. J Neurosci 25, 3132-41.
Stamenkovic, I. (2003). Extracellular matrix remodelling: the role of matrix metalloproteinases. J Pathol 200, 448-64.
Suter, D. M. and Forscher, P. (2000). Substrate-cytoskeletal coupling as a mechanism for the regulation of growth cone motility and guidance. J Neurobiol 44, 97-113.
ten Klooster, J. P., Jaffer, Z. M., Chernoff, J. and Hordijk, P. L. (2006). Targeting and activation of Rac1 are mediated by the exchange factor beta-Pix. J Cell Biol 172, 759-69.
Vikis, H. G., Li, W. and Guan, K. L. (2002). The plexin-B1/Rac interaction inhibits PAK activation and enhances Sema4D ligand binding. Genes Dev 16, 836-45.
Vitriol, E. A. and Zheng, J. Q. (2012). Growth cone travel in space and time: the cellular ensemble of cytoskeleton, adhesion, and membrane. Neuron 73, 1068-81.

Webber, C. A., Hocking, J. C., Yong, V. W., Stange, C. L. and McFarlane, S. (2002). Metalloproteases and guidance of retinal axons in the developing visual system. J Neurosci 22, 8091-100.

Woo, S. and Gomez, T. M. (2006). Rac1 and RhoA promote neurite outgrowth through formation and stabilization of growth cone point contacts. J Neurosci 26, 1418-28.

Woo, S., Rowan, D. J. and Gomez, T. M. (2009). Retinotopic mapping requires focal adhesion kinase-mediated regulation of growth cone adhesion. J Neurosci 29, 13981-91.

Xu, J., Rodriguez, D., Petitclerc, E., Kim, J. J., Hangai, M., Moon, Y. S., Davis, G. E. and Brooks, P. C. (2001). Proteolytic exposure of a cryptic site within collagen type IV is required for angiogenesis and tumor growth in vivo. J Cell Biol 154, 1069-79.

Yamaguchi, H. and Oikawa, T. (2010). Membrane lipids in invadopodia and podosomes: key structures for cancer invasion and metastasis. Oncotarget 1, 320-8.

Yong, V. W., Power, C., Forsyth, P. and Edwards, D. R. (2001). Metalloproteinases in biology and pathology of the nervous system. Nat Rev Neurosci 2, 502-11.

Zuo, J., Ferguson, T. A., Hernandez, Y. J., Stetler-Stevenson, W. G. and Muir, D. (1998). Neuronal matrix metalloproteinase-2 degrades and inactivates a neurite-inhibiting chondroitin sulfate proteoglycan. J Neurosci 18, 5203-11.

CHAPTER 2

PAK-PIX interactions regulate adhesion dynamics and membrane protrusion to control neurite outgrowth

This chapter was published as the following journal article:

Santiago-Medina M., Gregus K. A. and Gomez T. M. (2013). PAK–PIX interactions regulate adhesion dynamics and membrane protrusion to control neurite outgrowth. J. Cell Sci. 126 1122–1133.

Abstract

The roles of P21-activated kinase (PAK) in the regulation of axon outgrowth downstream of extracellular matrix (ECM) proteins are poorly understood. Here we show that PAKs 1-3 and PIX are expressed in the developing spinal cord and differentially localize to point contacts and filopodial tips within motile growth cones. Using a specific interfering peptide called PAK18, we found that axon outgrowth is robustly stimulated on laminin by partial inhibition of PAK-PIX interactions and PAK function, whereas complete inhibition of PAK function stalls axon outgrowth. Furthermore, modest inhibition of PAK-PIX stimulates the assembly and turnover of growth cone point contacts, whereas strong inhibition over-stabilizes adhesions. Point mutations within PAK confirm the importance of PIX binding. Together our data suggest that regulation of PAK-PIX interactions in growth cones controls neurite outgrowth by influencing the activity of several important mediators of actin filament polymerization and retrograde flow, as well as integrin-dependent adhesion to laminin.

Introduction

During development, complex neuronal circuits assemble through guided extension of billions of axons to their correct synaptic target sites. Growth cones at the tips of developing axons use molecular guidance cues deposited in their immediate environment to guide axons to distant targets (Kolodkin and Tessier-Lavigne, 2011). Growth cones integrate signals generated through receptor interactions with ligands that both promote and inhibit axon outgrowth (Lowery and Van Vactor, 2009). Intracellular signals converge onto the cytoskeleton, which powers the force-generating machinery that controls membrane protrusion and retraction (Dent et al., 2011).

Analogous to migrating cells, the regulation of growth cone motility requires the coordination of leading edge membrane protrusion, adhesion, de-adhesion and retraction (Marin et al., 2010). Although many studies have focused on the molecular basis of filopodial and lamellipodial protrusion/retraction, far less in known about the signals that control adhesion/de-adhesion. The stabilization of new protrusions to the ECM occurs at specialized adhesion sites called point contacts (PCs), which are analogous to focal contacts (FCs) of most crawling cells. Growth cone PCs link integrin receptors to the actin cytoskeleton by recruiting various adaptor and signaling proteins (Myers et al., 2011; Santiago-Medina et al., 2011). By linking F-actin to the underlying substratum, PCs restrain myosin-based retrograde flow of F-actin to support membrane protrusion and forward growth cone translocation.

A number of structural proteins, such as the multi-domain scaffolding protein paxillin (PXN), link F-actin to integrins. Moreover, FCs and PCs contain a myriad of signaling proteins that modulate adhesion assembly and disassembly (adhesion

dynamics) through phosphorylation (Zaidel-Bar and Geiger, 2010). For example, paxillin is phosphorylated at N-terminal tyrosine residues by protein tyrosine kinases and at serine residues by p21-activated kinase (PAK) (Deakin and Turner, 2008; Nayal et al., 2006). Phosphorylation of these sites in response to growth factors and guidance cues regulates adhesion dynamics and coordinates additional downstream signals. Recent evidence suggests that the assembly, distribution and dynamic turnover of growth cone PCs is a fundamental regulator of axon outgrowth and guidance (Carlstrom et al., 2011; Hines et al., 2010; Marsick et al., 2012; Myers and Gomez, 2011).

PAK proteins are a conserved family of serine/threonine kinases involved in signaling pathways downstream of the Rho family GTPases, Rac1 and Cdc42 (Bokoch, 2003). PAKs 1-3 (Group 1) consist of an N-terminal regulatory domain and a C-terminal kinase domain. The N-terminal regulatory domain contains an activating p21 GTPase binding domain (PBD), as well as an auto-inhibitory domain (AID) (Arias-Romero and Chernoff, 2008). Adjacent to the PBD / AID domain is a proline-rich motif that interacts with the guanine nucleotide exchange factor (GEF), PIX (Manser et al., 1998). PAK has been shown to target to FCs through PIX, which links to paxillin through paxillin kinase linker (PKL, also known as GIT2) (Brown et al., 2002; Turner et al., 1999). Therefore, this GIT-PIX-PAK complex may target Rac1 and its effector PAK to adhesion sites (ten Klooster et al., 2006). The binding of this complex to paxillin is regulated by PAK-dependent phosphorylation of S273 of paxillin, which could increase local Rac1 activity (Deakin and Turner, 2008; Nayal et al., 2006; ten Klooster et al., 2006). However, PAK-PIX interactions can also mediate functions independently of activating Rho GTPases.

In non-neuronal cells, PAK controls cell motility by regulating the organization and dynamic assembly of F-actin, microtubules and substratum adhesions (Bokoch, 2003). In neurons, PAK isoforms regulate various aspects of neuronal development, such as neuronal cell fate, migration, polarization, as well as neurite initiation and guidance (Cobos et al., 2007; Daniels et al., 1998; Hayashi et al., 2002; Kreis and Barnier, 2009). We previously demonstrated that one isoform of PAK localizes to the tips of filopodia in a Src dependent manner (Robles et al., 2005). PAK disfunction has also been implicated in neurodegenerative diseases and neuronal development disorders, such as X-linked mental retardation (Kreis and Barnier, 2009; Zhang et al., 2005). Despite a clear role for PAK neuronal development, almost nothing is known about how PAK controls growth cone motility. Understanding how the spatial and temporal activity of distinct PAK isoforms influence growth cone adhesion and motility downstream of axon guidance cues is crucial to understanding neural development.

In this study, we show that PAKs 1-3 are expressed in spinal neurons and that PAK2 and 3 localize to distinct sub-cellular regions within growth cones. xPAK2 localizes to filopodial tips, as well as to paxillin-containing PCs, whereas xPAK3 only localizes to adhesions. We also find that α-PIX localizes with PAK to paxillin-containing PCs. Inhibition of PAK-PIX interactions with PAK18 results in dose-dependent effects on neurite outgrowth and growth cone morphology through its downstream actin effectors ADF/cofilin and myosin-II. Moreover, PAK regulates integrin-based adhesion dynamics to further influence effects on axonal outgrowth. Taken together, our findings suggest that PAK functions on two main determinants of growth cone motility, the actin cytoskeleton and adhesive point contacts, to regulate axon outgrowth on ECM proteins.

Materials and methods

RT-PCR and Primers. PAK primers were designed by inserting the corresponding *Xenopus laevis* genomic sequences, obtained from Xenbase into Primer3 (Rozen and Skaletsky, 2000). The designed PAK primers were synthesized at the Biotechnology Center of the University of Wisconsin - Madison. PAK transcripts were amplified from reverse transcribed RNA isolated from stage 25–26 embryo spinal cords. The total RNA was first isolated from 15-20 spinal cords with TRIzol (Invitrogen) and made into cDNA through RT-PCR using random decamers as primers.

Plasmid Constructs. All expression constructs were subcloned into the *Xenopus*-preferred pCS2+ vector for mRNA synthesis (Dave Turner, University of Michigan, Ann Arbor, MI). Gateway technology (Invitrogen, Carlsbad, CA) was used in some cases to generate pCS2+ constructs. cDNAs for chicken paxillin–GFP and paxillin-S273D/A were provided by A. F. Horwitz (University of Virginia, Charlottesville, VA). *Xenopus* isoforms of wild-type PAK1, PAK2 and PAK3 constructs were provided by Tom Moss (University of Toronto, Ontario, Canada), Nathalie Morin (Centre de Recherche de Biochimie Macromoleculaire, France) and Jacob Souopgui (Université Libre de Bruxelles, Belgium) respectively. All cDNA clones were put into pCS2+ vectors using Gateway technology. The mutant constructs of xPAK2 (PR180,181GA) and xPAK3 (PR208,209GA) in the PIX binding domain were generated using QuikChange Site Directed Mutagenesis (Agilent, Santa Clara CA). Dominant negative Rac1 (DN-Rac1; T17N) was provided by Maureen L. Ruchhoeft and William A. Harris (University of Cambridge, UK).

Embryo injection and cell culture. *Xenopus laevis* embryos were obtained and staged as described previously (Gomez et al., 2003). For direct expression experiments using constructs, two dorsal blastomeres of eight-cell-stage embryos were injected with 0.25–0.5 ng of in vitro-transcribed, capped mRNA (mMessage Machine, Ambion, Austin, TX) or 60-80 pg of DNA for paxillin–GFP. Neural tubes were dissected from 1-d-old embryos and explant cultures containing a heterogeneous population of spinal neurons were prepared as previously described (Gomez et al., 2003). Explants were plated onto acid-washed coverslips coated with 25 µg/ml laminin (LN; Sigma, St. Louis, MO) or 50 µg/ml poly-D-lysine (PDL; Sigma, St. Louis, MO). Cultures were imaged or fixed 16–24 h after plating. All methods were approved by the University of Wisconsin School of Medicine Animal Care and Use Committee.

Reagents. PAK18 (EMD Bioscieces, Calbiochem, La Jolla, CA) was diluted in 1xMR and perfused through cultures as described previously (Gomez et al., 2003). The control PAK18 peptide was synthesized by the University of Wisconsin Peptide Synthesis Facility (Madison, WI). The peptide was synthesized in the reverse order of PAK18, coupled to a TAT internalization sequence and HPLC purified as well as confirmed using mass spectrometry. Antibodies used were as follows: xPAK1 and xPAK2 (kind gift from Nathalie Morin, Universités Montpellier, France), βPAK3 (N-19, Santa Cruz Biotechnology), pS3-ADF/cofilin (pS3-XAC1; kind gift from James Bamburg, Colorado State University), pS19-MLC2 (Cell Signaling Technology, Danvers, MA), pY118-Paxillin (Invitrogen), βI,II-Tubulin (Sigma), Rac1-GTP (NewEast Biosciences, King of Prussia, PA). For monomeric G-actin staining, deoxyribonuclease I (Alexa Fluor

488 DNase I; Invitrogen) was used. To visualize actin retrograde flow, neuronal cultures were incubated in 3 nM kabarimide C conjugated to tetramethylrhodamine (TMR-KabC; kind gift from Gerard Marriott, University of California, Berkeley) for 3 min, then washed with 1xMR.

***Immunoblotting and immunocytochemistry*.** Immunoblotting for PAK proteins was performed as described previously (Robles et al., 2005). Total proteins were extracted from stage 25–26 (Nieuwkoop and Faber, 1994) embryo spinal cords. Five spinal cords were processed for each lane and ran on a Novex NuPAGE SDS-PAGE gel (Invitrogen). Primary PAK1-3 antibodies were used at 1:1000. Horseradish peroxidase (HRP)-conjugated secondary antibodies (Jackson Immuno) were used at 1:5000 and the blots were visualized by enhanced chemiluminescence (Thermo Scientific Pierce ECL).

For immunocytochemistry (ICC), spinal neuron cultures were fixed in 4% paraformaldehyde in Krebs + sucrose fixative (4% PKS) (Dent and Meiri, 1992), permeabilized with 0.1% Triton X-100, and blocked in 1.0% fish gelatin in CMF-PBS for one hr at room temperature. Primary antibodies were used at the following dilutions in blocking solution: 1:300 pS3-XAC (Bamburg), 1:250 pS19-MLC2 (Cell Signaling Technology), 1:500 pY118-Paxillin (Invitrogen), 1:500 Rac1-GTP (NewEast Biosciences), 1:500 βI,II-Tubulin (Sigma). Alexa-Fluor-conjugated secondary antibodies were purchased from Invitrogen and used at 1:250 in blocking solution. Included with secondary antibodies was Alexa-546 phalloidin (1:100; Invitrogen) to label filamentous actin (F-actin) and Alexa-647 carboxylic acid, succinimidyl ester (1:1000; Invitrogen) to label total protein.

Image acquisition and analysis. For both live and fixed fluorescence microscopy, high- magnification images were acquired using either a 60X/1.45 NA objective lens on an Olympus Fluoview 500 laser-scanning confocal system mounted on an AX-70 upright microscope or a 100X/1.5 NA objective lens on a Nikon total internal reflection fluorescence (TIRF) microscope. For confocal microscopy, samples were imaged at 2–2.5X zoom (pixel size = 165–200 nm). Images were captured at 10-20 s intervals. For bright field time-lapse microscopy, low-magnification phase-contrast images were acquired using a 20X objective on a Nikon microscope equipped with an x–y motorized stage for multi-positional imaging. Multi-positional images were capture at 1 min intervals. Live explant cultures were sealed within perfusion chambers as described previously (Gomez et al., 2003) to allow rapid exchange of solutions. Images were analyzed using ImageJ software (W. Rasband, National Institutes of Health, Bethesda, MD). Point contacts were identified as discrete areas containing paxillin–GFP that were at least two times brighter than the surrounding background and remained fixed in place for a minimum of 30 s (Woo and Gomez, 2006). Measurements of p-Cofilin and p-MLCII or Rac1-GTP intensity were made by first selecting the perimeter of growth cones from thresholded F-actin-labeled or total protein-labeled images based on intensity to exclude background using ImageJ. These user-defined regions were then used to measure the average pixel intensity of immunolabeling within non-thresholded growth cones. For display purposes, some images were pseudo-colored using ImageJ look up tables.

Dynamic adhesion maps. Dynamic adhesion map images were prepared from image stacks as detailed previously (Santiago-Medina et al., 2011). Briefly, an image stabilization algorithm was applied if necessary and to improve edge detection an unsharp mask routine was applied, followed by thresholding to highlight the puncta of interest. Next, an 8-bit binary filter was applied to equalize point contact intensities. Image stacks were then converted to 16-bit and user-defined subsets were summed so intensity would encode pixel lifetime. Final images were contrast enhanced and pseudo-colorized.

Results

PAK is expressed in the developing spinal cord and localizes to growth cone point contacts and filopodia tips

Most vertebrates, including *Xenopus laevis*, express six PAK proteins from distinct genes. PAK proteins are divided into two groups, based upon sequence and structural homology: group I PAKs (PAK1-3) and group II PAKs (PAK4-6) (Bisson et al., 2003; Cau et al., 2000; Souopgui et al., 2002). However, group I PAKs are most highly expressed in developing neurons, suggesting important roles in neuronal differentiation and function in early development (Kreis and Barnier, 2009). To begin to study the function of PAK in the control of growth cone motility, we determined the expression pattern of group I PAK transcripts in the developing *Xenopus* spinal cord. Using *Xenopus laevis* specific primers, we amplified PAK1-3 transcripts by RT-PCR from mRNA isolated from pure stage 24 *Xenopus* spinal cord, suggesting all three members are expressed in spinal neurons (Fig. 1A). We also found that transcripts for the PAK binding partners α- and β-PIX were present in spinal cord tissue. Although all three PAK isoforms were present, PAK2 and PAK3 transcripts appeared most abundant, consistent with *in situ* hybridizations of spinal cord of a similar developmental age (Souopgui et al., 2002). Using isoform-specific PAK antibodies, we immunoblotted for PAK1, 2 and 3 proteins from stage 24 pure spinal cord preparations. Consistent with our PCR results, we found that PAK2 and PAK3 proteins are highly expressed in the spinal cord, but PAK1 was not detected at the expected molecular mass (Fig. 1B) using two different PAK1 antibodies. These results suggest that PAK2 and PAK3 are the most prominent isoforms of PAK in the developing *Xenopus* spinal cord.

Previously we showed that dsRed-human PAK1 (hPAK1) localizes to extending filopodial tips of growth cones cultured on poly-D-lysine (PDL) (Robles et al., 2005) and to both filopodial tips and PCs within growth cones cultured on laminin (LN; unpublished observations). As the sub-cellular localization of PAK family members may provide clues into isoform-specific functions, we examined the dynamic localization of GFP-xPAK1-3 (*Xenopus* PAKs) in developing spinal neurons on LN by total internal reflection fluorescence (TIRF) microscopy. Neurons were double-labelled for individual GFP-xPAK isoforms together with Paxillin-mCherry (PXN-mCh), to identify PCs. Unlike hPAK1, we found that GFP-xPAK1 was only cytosolic within migrating growth cones (Fig. 1C). In contrast, GFP-xPAK2 robustly targets to both PCs and the tips of extending filopodia (Fig. 1D, G). Differences in the distribution of human versus *Xenopus* PAK isoforms may be due to sequence differences between species (Bisson et al., 2003). Interestingly, in contrast to xPAK1 and 2, GFP-xPAK3 was present exclusively at growth cone PCs and did not localize to filopodial tips (Fig. 1E, H). As a direct binding partner of PAK, PIX should also localize to paxillin-containing adhesion sites. To test this we expressed GFP-α-PIX together with PXN-mCh. We found that GFP-α-PIX localized with PXN-mCh in growth cone adhesion sites but not at the tips of filopodia (Fig. 1F). Although we have no antibodies that work well by immnocytochemistry (ICC), from our combined western blot and live localization studies we can conclude that the distributions of endogenous PAK and PIX isoforms within motile growth cones are distinct.

To assess whether the distribution of PAK isoforms was similar in mammalian neurons compared to *Xenopus*, we immunolabeled for PAK1-3 in developing mouse

neurons (supplementary material Fig. S1). Dissociated neurons from mouse hippocampus (supplementary material Fig. S1A-C) and cortex (supplementary material Fig. S1D-F) were labeled with antibodies to specific PAK isoforms. Interestingly, we observe activated PAK1 (p-Thr423) at growth cone filopodial tips (supplementary material Fig. S1A,D), whereas PAK2 was present at the leading edge of the lamellipodia (supplementary material Fig. S1B, E) and PAK3 at regions reminiscent of adhesion sites within growth cones (supplementary material Fig. S1C,F). However, it should be noted that without additional adhesion markers, it is difficult to determine with certainty which PAK isoforms localize to PCs.

Acute PAK inhibition has dose-dependent effects on growth cone motility and morphology

To begin to examine how PAK activity may influence growth cone motility, we used PAK18, a cell-permeable peptide inhibitor of PAK function (Maruta et al., 2002; Zhao et al., 2006). PAK18 is composed of the TAT internalization peptide sequence fused to 18 amino acids from the PIX-interacting motif of mouse PAK3. This peptide is believed to inhibit PAK function by disrupting PAK-PIX interactions (Maruta et al., 2002). The amino acid sequence of PAK18 is 72%, 89% and 94% identical to *Xenopus* PAK1-3, respectively and all substitutions are with conserved amino acids in xPAK2 and xPAK3. First we tested the dose-dependent effects of PAK18 on axon outgrowth by time-lapse microscopy. Unexpectedly, a low concentration of PAK18 (1 μM) applied acutely to spinal neurons on LN strongly stimulated lamellipodial and filopodial protrusions (Fig. 2A,E-F), leading to an immediate and robust expansion of growth cone

area (Fig. 2G) and prolonged acceleration in the rate of neurite outgrowth (Fig. 2A,D). Both the area of lamellipodium expansion (Fig. 2G), as well as the total number and length of filopodia increase in the presence of 1 μM PAK18 (Fig. 2H). In contrast, a reversed PAK18 control peptide (see methods), had no effect on neurite outgrowth at any dose (supplementary material Fig. S2).

Higher concentrations of PAK18 (10-50 μM) also resulted in an immediate increase in growth cone area (Fig. 2B,C,G), but only briefly enhanced outgrowth (Fig. 2D). Instead, after 5-10 min in 10-50 μM PAK18, axons typically stalled or retracted (Fig. 2C). This result suggests that a modest inhibition of PAK is optimal for outgrowth, whereas strong inhibition of PAK negatively regulates outgrowth. Although off-target effects of PAK18 are possible, our evidence (below) suggests that 1-50 μM PAK18 results in a dose-dependent inhibition of PAK function. Notably, the rate of neurite outgrowth and growth cone area were inversely correlated, which is consistent with growth cone behavior seen *in vitro* and *in vivo* (Godement et al., 1994; Sretavan and Reichardt, 1993). Interestingly, axon extension was not stimulated by any concentration of PAK18 when neurons were cultured on the non-integrin binding substratum, PDL (Fig. 2D), although we did observe a slight increase in growth cone protrusion at 10 μM PAK18 (Fig. 2E). These results suggest that changes in integrin-dependent adhesion or signaling may contribute to enhanced growth cone motility on LN.

We also tested the effects of chronic PAK inhibition by culturing spinal neurons overnight in PAK18. After 16 hours in culture, spinal explants in control medium generated an average of 6.2±1.1 neurites per explant with an average length of 89.7±5.9 μm (supplementary material Fig. S3A,C,D). In contrast, spinal cord explants

cultured in 1 μM PAK18 for 16 hours generated significantly more neurites per explant (24.8±1.9; P<0.001), which had a significantly longer average length (203.6±5.7 μm; P<0.001; supplementary material Fig. S3B,C-D). Additionally, neurons more often migrated away from explants when cultured in the presence of PAK18 (supplementary material Fig. S3B), suggesting that PAK18 also stimulates neuronal cell motility. Taken together, these results show that partial disruption of the PAK-PIX interaction with PAK18 promotes an immediate and sustained increase in neurite outgrowth.

PAK18 inhibits PAK-dependent targets to regulate actin polymerization and retrograde flow

PAK regulates a number of downstream targets known to modulate the cytoskeleton and influence cell membrane protrusion and motility (Bokoch, 2003). For example, PAK can regulate leading edge protrusions through actomyosin contractility or ADF/cofilin-mediated actin depolymerization. PAK can both increase [via direct phosphorylation of myosin light chain (MLC)] and decrease (by inhibition of MLC kinase) myosin-II driven actin contractility (Bokoch, 2003). In addition, active PAK reduces ADF/cofilin-mediated actin depolymerization by phosphorylating LIM kinase (LIMK). Active LIMK phosphorylates and inactivates ADF/cofilin to reduce its binding to F-actin, thus inhibiting actin severing. Therefore, PAK may control growth cone motility by regulating myosin-II driven F-actin contractility and ADF/cofilin induced F-actin depolymerization.

To determine how disrupting PAK-PIX interactions modulates PAK targets, we first measured the levels of phosphorylated *Xenopus* ADF/cofilin (p-XAC) and myosin light-chain (p-MLC) in response to 1, 10 and 50 μM PAK18 by quantitative ICC (Fig. 3A-

J). We measured the level of p-XAC (a direct target of LIMK) and p-MLC in growth cones after 5 min treatment with PAK18. We found that PAK18 reduces the levels of p-XAC in growth cones in a dose-dependent manner (Fig. 3A-E), further indicating that this peptide inhibits PAK function. To confirm that reduced p-XAC was not the result of increased growth cone area, we also measured total protein content in growth cones treated with PAK18 (supplementary material Fig. S4). Despite the morphological changes that accompany PAK18 stimulation, the growth cone total protein content remained constant at all doses (supplementary material Fig. S4A'-D',F), while the ratio of p-XAC / total protein decreased in a dose-dependent manner (supplementary material Fig. S4A'''-D''',G). It is noteworthy that 1 μM PAK18, which strongly stimulated axon outgrowth, only modestly reduced p-XAC, whereas higher levels of PAK18 strongly reduced p-XAC and inhibited outgrowth (Fig. 3A-E). This is consistent with the notion that balanced ADF/cofilin activity is necessary for optimal axon outgrowth and slight variations across a growth cone can promote attractive or repulsive turning (Marsick et al., 2010). On the other hand, p-MLC levels were strongly reduced at 1 μM PAK18, with modest further loss at higher levels of PAK18 (Fig. 3F-J). As with the p-XAC staining, we measured the total protein content in growth cones after PAK18 stimulation to ensure that the changes occurring after PAK18 stimulation were not due to changes in growth cone morphology (supplementary material Fig. S5).

Since active ADF/cofilin is known to depolymerize F-actin, we examined the relative levels of monomeric actin (G-actin) versus filamentous actin (F-actin) after treatment of 1, 10 and 50 μM PAK18. Neurons treated for 5 min with PAK18 were co-labeled for G-actin using Alexa-Fluor-488-DNase I and F-actin with Alexa-Fluor-546-

phalloidin (Fig. 3K-P). Because DNase I binds actin monomers with high affinity relative to actin filaments (Hitchcock, 1980), whereas phalloidin only binds F-actin, we compared the relative abundance of both labels to assess the state of growth cone actin (Marsick et al., 2010). At 1 μM PAK18, we observed only a modest increase in the G/F actin ratio in growth cones (Fig. 3L,O,P), whereas at higher PAK18 concentrations we observed a significant increase in G-actin labeling and an increase in the G/F-actin ratio (Fig. 3M-P). Together these results suggest that enhanced outgrowth at low concentrations of PAK18 is due to modest changes in G/F actin coupled with strong inhibition of myosin-II, whereas inhibition of outgrowth at high PAK18 is due to ADF/ cofilin-mediated actin depolymerization.

If PAK18 inhibits myosin-II, we expected retrograde actin flow to be reduced. Retrograde actin flow is a process whereby actin filaments are drawn rearward because of the pulling force of myosin motors combined with the pushing force of polymerizing actin filaments against the plasma membrane (Dent et al., 2011; Lowery and Van Vactor, 2009). To examine whether PAK18 modulates retrograde F-actin flow, we labeled live neurons with tetramethylrhodamine-conjugated kabiramide-C (TMR-KabC, (Petchprayoon et al., 2005; Tanaka et al., 2003)). TMR-KabC is a small, cell permeable molecule that binds to the barbed end of polymerizing actin filaments and has been used previously at low doses to track the rearward flow of actin filaments (Keren et al., 2008; Santiago-Medina et al., 2011). To label the plus ends of actin filaments, we treated neurons for 3 min with 3 nM TMR-KabC, which rapidly labels neurons, but does not affect the basal rate of neurite outgrowth or growth cone morphology (not shown). Immediately after TMR-KabC labeling, we imaged growth cones on LN at 2 s intervals

by TIRF microscopy for 5 min before and after PAK18 stimulation (Fig. 4A,C). In control conditions the rate of retrograde flow on LN was ~10.6 μm/min (Fig. 4B,E), which is consistent with previous measurements (Chan and Odde, 2008; Marsick et al., 2010). However, upon treatment with PAK18, we observe an immediate reduction in the rate of retrograde flow (Fig. 4D,E), consistent with the inhibition of PAK-mediated myosin-II activity by PAK18. It is interesting to note that we observed similar rates of retrograde flow after treatment with 1 μM and 10 μM PAK18 (Fig. 4E), which is consistent with similar p-MLC labeling at these doses of PAK18 (Fig. 3G-H,J). These results further suggest that the inhibitory effects of PAK18 on axon outgrowth is due to the strong activation of ADF/cofilin at 10 μM (Fig. 3C,E).

PAK regulates growth cone point contact formation and turnover

PAK regulates focal adhesion formation and turnover in crawling cells through phosphorylation of Serine 273 of paxillin (S273-PXN), which requires binding of the PAK-PIX complex to paxillin through GIT (Brown et al., 2002; Deakin and Turner, 2008; Nayal et al., 2006; Turner et al., 1999). Since growth cone motility is tightly linked to adhesion dynamics (Marsick et al., 2012; Myers and Gomez, 2011; Myers et al., 2011; Robles and Gomez, 2006; Santiago-Medina et al., 2011; Woo and Gomez, 2006; Woo et al., 2009) and modulating PAK function has dose-dependent effects on outgrowth (Fig. 2), we asked whether PAK18 also influences growth cone PCs. To first test the effects of PAK18 on endogenous PCs, we stimulated growth cones with varying concentrations of PAK18 and immunolabeled for phosphorylated Y118-PXN (Fig. 5A-G). pY118-PXN is an excellent marker for mature adhesions (Deakin and Turner, 2008;

Zaidel-Bar et al., 2007), which we have previously demonstrated to label *Xenopus* growth cone PCs (Robles and Gomez, 2006). Using particle analysis of thresholded ICC images, we found a dose-dependent increase in PC number, size and total intensity within growth cones treated with PAK18 (Fig. 5A-G). These results suggest that PAK18 promotes PC assembly and might reduce point contact turnover at high concentrations.

To directly test whether PAK18 regulates adhesion formation and turnover, we performed time-lapse TIRF imaging of paxillin-GFP (PXN-GFP) in living growth cones on LN during stimulation with PAK18 (Fig. 5H-M). Acute treatment with 1 μM PAK18 stimulated the rapid assembly of new PCs and accelerated PC turnover (Fig. 5H-I). As the increase in the number of PCs/growth cone exceeds the expanded growth cone area, there is a greater than 50% increase in PC density (3.9±0.3 adhesions/100 μm^2 pre-PAK18 vs. 6.5±0.3/100 μm^2 post-PAK18), which is also apparent in immunolabeled images (Fig. 5A-D). Moreover, at 1 μM PAK18, new PCs have a shorter adhesion lifetime (Fig. 5L). Other characteristics of point contacts, such as size and shape do not significantly change in presence of 1 μM PAK18. In contrast, while treatment with 10 μM PAK18 also stimulates the assembly of new PCs, these adhesions have a considerably longer lifetime and often cluster into larger aggregates, suggesting they are more mature adhesions (Fig. 5J-K,M). Interestingly, the biphasic effects of PAK18 on adhesion lifetime correlates with the effects we observe on the rate of axon outgrowth and are consistent with previous findings that rapid turnover of PCs is associated with fast axon outgrowth (Myers and Gomez, 2011; Robles and Gomez, 2006; Woo and Gomez, 2006). The dose-dependent effects of PAK18 might be due to

a partial displacement of PAK from PCs, as well as effects on actin polymerization and myosin activity.

To directly assess the effects of PAK18 on PAK localization to PCs, we imaged growth cones expressing both PXN-GFP and mCH-PAK3 during stimulation with 10 μM PAK18 (Fig. 6). Prior to PAK18 treatment, PAK3 translocated to PXN-containing PCs with a short delay and typically dissociates from PCs before PXN is lost (Fig. 6A,C), suggesting that PAK has a transient function at adhesions. However, in the presence of 10 μM PAK18, the amount of PAK3 localizing to PXN-based adhesions was reduced significantly (Fig. 6E) and the time PAK3 associates with PXN is shortened dramatically relative to long PXN adhesion lifetime. Although less PAK3 localized to PCs in the presence of PAK18, low levels of PAK3 remained at PCs longer (Fig. 6F), suggesting that increased paxillin lifetime is sufficient to target PAK3 to adhesions.

Serine 273 Paxillin phosphorylation regulates adhesion dynamics and growth cone motility

PAK regulates focal adhesion formation and turnover in part through phosphorylation of S273-PXN in crawling cells (Nayal et al., 2006). Because of the robust effects of PAK18 on PC dynamics (Fig. 5, 6), we reasoned that phosphorylation of S273-PXN might modulate PC turnover to regulate growth cone motility. To examine the role of S273-PXN phosphorylation by PAK, we imaged adhesion dynamics and motility of growth cones over-expressing either phosphomimetic (S273D-PXN-GFP) or non-phosphorylatable (S273A-PXN-GFP) paxillin (Fig. 7). We first examined the effects of S273D-PXN on baseline adhesion dynamics and growth cone motility. Consistent

with the effects of phosphomimetic paxillin on focal adhesions and fibroblast migration (Nayal et al., 2006), growth cones expressing S273D-PXN-GFP had shorter PC lifetimes (Fig. 7B) and increased motility compared to wild-type neurons (Fig. 7C). This result suggests that increasing adhesion turnover with S273D-PXN is sufficient to modestly accelerate neurite outgrowth. We also tested the effects of the non-phosphorylatable, S273A-PXN, on growth cone PC turnover and neurite outgrowth. Unexpectedly, neither PC turnover, nor rate of neurite outgrowth were significantly different in S273A-PXN expressing neurons (Fig. 7B,C). These results suggest that although paxillin phosphorylation at S273 may promote adhesion turnover and growth cone motility, phosphorylation at this site could be low under basal neurite outgrowth conditions on LN.

Next we examined how neurons expressing S273-paxillin mutants respond to partial PAK inhibition with 1 μM PAK18. Although 1 μM PAK18 normally shortens adhesion lifetime and accelerates neurite outgrowth of wild-type neurons, we found that 1 μM PAK18 significantly increased adhesion lifetime in S273D-PXN-GFP expressing neurons and partially increased lifetime in S273A-PXN-GFP expressing neurons (Fig. 7B; $P<0.001$). However, despite slowing adhesion turnover, PAK18 still stimulated neurite outgrowth in both S273D- and S273A-PXN-GFP expressing neurons. This unexpected result suggests that inhibition of PAK with PAK18 likely promotes neurite extension by modulating multiple downstream cellular processes that are independent of S273-paxillin phosphorylation.

PIX-binding mutants of PAK suppress the effects of PAK18 and inhibit baseline growth cone motility

Our evidence suggests that PAK-PIX interactions have diverse affects on various cellular processes that control growth cone motility. However, PAK18 could have off-target effects, so determining the specificity of this peptide is crucial to conclusions regarding PAK function in growth cones. To address the specific function of PAK-PIX interactions in growth cones, we generated PAK constructs with mutated PIX binding motifs (Fig. 8A) that prevent PIX binding in other systems (Bagrodia et al., 1998; Bisson et al., 2007; Manser et al., 1998). We generated point mutants of xPAK2 (xPAK2-PR180,181GA) and xPAK3 (xPAK3-PR208,209GA), because these isoforms are most homologous to PAK18 (Fig. 8A) and are more highly expressed in spinal neurons (Fig. 1). Consistent with a loss of PIX binding, we found by time-lapse TIRF imaging that GFP-xPAK2-PR180,181GA did not associate with adhesions, but still localized to the tips of extending filopodia (Fig. 8B). A similar PIX-binding mutant of xPAK3 did not target to stable PCs or filopodial tips, but appeared as a cytosolic volume marker in growth cones (not shown).

If PAK18 affects growth cones by disrupting PAK binding to PIX, then expressing in neurons PAK mutants deficient in PIX binding should block the effects of PAK18. Consistent with our previous results, suggesting that PAK-PIX interactions regulate growth cone motility, we find that expressing PIX binding mutants of PAK alters axon outgrowth. Interestingly, the xPAK2 and xPAK3 PIX-binding mutants have distinct effects on the basal motility of growth cones, consistent with differing roles for PAK proteins in the regulation of cell motility (Bright et al., 2009). Neurons expressing GFP-

xPAK2-PR180,181GA had faster rates of outgrowth than wild-type neurons, whereas the xPAK3-PIX mutant had no effect on basal neurite outgrowth (Fig. 8C). In addition, expressing the xPAK2 PIX-binding mutant blocked the stimulatory effects of PAK18, whereas xPAK3-PIX mutant growth cones still accelerated in response to PAK18 (Fig. 8C). Taken together, these results suggest that xPAK2 most strongly influences growth cone motility through its interactions with PIX.

PAK and Rac1 compete for PIX binding

PAK and Rac1 are known to compete for a common binding site on PIX (ten Klooster et al., 2006), and PAK has been shown to act both downstream (Bokoch, 2003) and upstream of Rac1 activation (Obermeier et al., 1998), suggesting that the effects of PAK18 may be Rac1 dependent. To assess the role of Rac1 in response to PAK18, we expressed dominant negative T17NRac1 (DN-Rac1) and stimulated mutant neurons with PAK18 during time lapse imaging. DN-Rac1 inhibits endogenous Rac1 by sequestering the GEFs that normally activate Rac1 (Woo and Gomez, 2006). Consistent with an important role for Rac1, we find that neurite outgrowth by DN-Rac1 expressing neurons was not significantly stimulated in response to PAK18, although a partial acceleration still occurred (supplementary material Fig. S6B). This result suggests that Rac1 activity is suppressed by PIX binding and that PAK18 releases active Rac1 to promote axon outgrowth. Moreover, this result is also consistent with the notion that some PAK remains active, which requires Rac1, at low levels of PAK18. To directly assess changes in Rac1 activity in response to PAK18, we used an antibody that specifically recognizes active, GTP-bound Rac1 (see Methods). Neurons were

fixed after a two min treatment with 1 μM PAK18, during the time when membrane protrusion is enhanced and axon outgrowth has accelerated (Fig. 2). ICC labeling for active GTP-Rac1 showed that Rac1 labeling is increased in growth cones treated with PAK18 (supplementary material Fig. S6C-E). To assess the specificity of this antibody, we repeated this experiment in neurons expressing DN-Rac1. We find that DN-Rac1 expressing neurons have reduced basal active Rac1 labeling relative to control neurons within the same dish (supplementary material Fig. S6F-H) and that Rac1 labeling was not increased by PAK18 in DN-Rac1 expressing neurons. Together these data show that PAK18 rapidly activates Rac1 in neurons, which is necessary for the outgrowth-stimulating effects of this peptide.

Discussion

PAKs are multi-target serine/threonine kinases that regulate cell motility through several distinct molecular mechanisms. Here we provide the first detailed study of PAK function in developing neuronal growth cones. We show that PAK1 is weakly expressed, while PAK2 and PAK3 are highly expressed in developing spinal neurons and localize to distinct regions within motile growth cones. Both PAK2 and PAK3 colocalize with the adaptor protein PIX at paxillin-containing point contacts, whereas only PAK2 targets to filopodial tips independent of PIX. The acute disruption of the PAK-PIX interactions with the cell-permeable peptide, PAK18, has robust, dose-dependent effects on growth cone morphology and motility. A low dose of PAK18 strongly stimulated neurite outgrowth by partially activating ADF/cofilin and inhibiting myosin-II, which promotes membrane protrusion and dynamic point contact assembly. In contrast, a high dose of PAK18 strongly inhibited growth cone motility, likely though full activation of ADF/cofilin leading to actin filament depolymerization. Expressing specific PAK mutants in neurons confirmed the specificity of the PAK18 peptide and demonstrates a role for PAK phosphorylation of S273-paxillin in the regulation of adhesion dynamics. Lastly, our evidence suggests that Rac1 activity is controlled in part through PAK and PIX interactions in growth cones.

PAK distribution in growth cones

The distribution of PAK proteins is dynamic and varied within growth cones. The distinct localizations of PAK isoforms may target PAK activity to specific downstream effectors. For example, xPAK2 localized to both paxillin adhesions and to the tips of

extending filopodia (Fig. 1) suggesting a role in adhesion function and actin polymerization at filopodial tips. Functional evidence suggests that xPAK2 promotes filopodial extension, as low dose PAK18 stimulated filopodial production (Fig. 2H), possibly by displacing active PAK away from point contacts to filopodial tips. This is consistent with previous studies implicating PAK signaling in the regulation of both axonal and dendritic filopodial extension (Heckman et al., 2009b; Kayser et al., 2008; Robles et al., 2005). These results suggest that PAK2 regulates actin filament polymerization, but the relevant targets of PAK at filopodial tips remain unknown. Alternatively, xPAK3 was restricted to point contacts, suggesting an overlapping function with xPAK2 in the regulation of adhesion dynamics (see below), but not with actin polymerization at filopodial tips. Interestingly, xPAK1 does not concentrate at either point contacts or filopodial tips, suggesting this family member is missing key targeting sequences contained in PAK2/3.

PAK regulation of the growth cone cytoskeleton

Two of the best known downstream targets of PAK function are ADF/cofilin and myosin-II (supplementary material Fig. S7A). Active PAK inhibits ADF/cofilin through LIM kinase, which phosphorylates cofilin at Serine 3 (Sarmiere and Bamburg, 2004). Interestingly, we observed a robust stimulation of axon outgrowth after partial activation (dephosphorylation) of ADF/cofilin with 1 μM PAK18, but complete inhibition of outgrowth after strong ADF/cofilin activation with 50 μM PAK18 (Fig. 3A-E; supplementary material Fig. S7C,F). Consistent with actin depolymerization by ADF/cofilin, we observed a corresponding loss of F-actin with increasing PAK18

concentration (Fig. 3K-P). Stimulation of axon outgrowth at low PAK18 could be due to partial severing of actin filaments to generate new free barbed ends, together with increased globular actin that promotes polymerization at the leading edge (Ichetovkin et al., 2002). PAK18 also reduced myosin-II activity (Fig. 3F-J), which could stimulate growth cone motility by slowing retrograde actin flow (Fig. 4; supplementary material Fig. S7C,F). However, the inhibitory effects of high PAK18 are unlikely due to stronger myosin inhibition, as we observed only a modest further decrease in both myosin-II dephosphorylation (Fig. 3J) and retrograde flow of actin (Fig. 4) at higher PAK18. Recent evidence also suggests that active ADF/cofilin directly inhibits myosin-II binding to F-actin (Wiggan et al., 2012), which could further account for the decrease in myosin-II activity downstream of high PAK18. It remains to be determined whether the sub-cellular targeting of different PAK isoforms in growth cones controls the activation of specific effector pathways. Interestingly, our results are consistent with the effects of inhibiting RhoA-kinase (ROCK) on neurite outgrowth. ROCK regulates ADF/cofilin and myosin-II similar to PAK and stimulates filopodial and lamellipodial extension in growth cones when inhibited (Loudon et al., 2006). ROCK inhibition has also been reported to potentiate both the size and motility of growth cones (Bito et al., 2000), suggesting that partial inhibition of PAK may effect common targets to ROCK in neuronal growth cones.

PAK regulation of growth cone point contacts

One critical determinant of the speed and direction of cell motility is the assembly and dynamic turnover of substratum adhesion sites (Myers and Gomez, 2011; Myers et al., 2012; Myers et al., 2011; Wu et al., 2012). Although the role of PAK in adhesion-

dependent motility of non-neuronal cells has been extensively studied (Bokoch, 2003; Rosenberger and Kutsche, 2006), almost nothing is known about PAK function in adhesion dynamics in growth cone motility and axon pathfinding. Interestingly, we find that the acute disruption of PAK-PIX interactions with PAK18 leads to dose-dependent, biphasic changes in growth cone point contact turnover that closely mirror motility (supplementary material Fig. S7E). Low PAK18 stimulates the assembly of many new point contacts that have shorter lifetimes (Fig. 6H-I,L) and neurite outgrowth accelerates. Alternatively, high PAK18 causes point contacts to become over-stabilized and neurite outgrowth stalls (supplementary material Fig. S7E). There are several possible explanations for the effects we see on adhesion turnover. At low PAK18, a partial inhibition of myosin may promote growth cone motility by accelerating adhesion turnover, as myosin activity is necessary for focal adhesion maturation (Kuo et al.; Woo and Gomez, 2006). In addition, PAK association with PIX has been shown to stabilize adhesions in breast cancer cells (Stofega et al., 2004), and PAK phosphorylation of PXN promotes adhesion turnover (Nayal et al., 2006), so partial dissociation of PAK from adhesions may destabilize point contacts, but not prevent adhesion reassembly. Moreover, our data suggests that Rac1 is activated by PAK18 (supplementary material Fig. S6), which is known to promote new adhesion formation within nascent protrusions (ten Klooster et al., 2006; Woo and Gomez, 2006). However, the inhibitory effects of 10 μM PAK18 on adhesion turnover in wild-type cells is more difficult to explain, but is likely due to strong inhibition of PAK function (supplementary material Fig. S7E). Some PAK activity may be necessary for adhesion turnover through PXN phosphorylation at S273, so strong loss of PAK from adhesions at 10 μM PAK18 may stabilize adhesions

because of a lack of PAK-dependent phosphorylation of PXN (supplementary material Fig. S7E). Consistent with this notion, we found that there was increased adhesion turnover of growth cones expressing phosphomemetic S273D-PXN (Fig. 7B) and faster neurite outgrowth (Fig. 7C), suggesting that rapid adhesion turnover is sufficient to potentiate outgrowth. However, although S273D-PXN expressing neurons do not exhibit increased adhesion turnover in response to PAK18, they do accelerate their rate of neurite outgrowth, suggesting that several independent pathways promote neurite outgrowth downstream of PAK18. The effects of non-phosphorylatable S273A-PXN on PC lifetime and neurite outgrowth in response to PAK18 dissociate changes in adhesion turnover from neurite acceleration. These results indicate that PAK18-mediated neurite outgrowth must be working independently of paxillin phosphorylation at S273 and that perhaps adhesion turnover is primarily mediated by the cytoskeletal changes triggered by PAK18. It should also be noted that we do observe modest effects of PAK18 on leading edge protrusion of growth cones on PDL (Fig. 2E), suggesting some PAK-PIX interactions occur without integrin engagement. Given the complex interplay between a number of signaling pathways, clearly the role of PAK in the control of growth cone adhesion dynamics requires further study.

PAK in axon guidance

PAK is implicated in axon guidance downstream of both attractive and repulsive cues (Aizawa et al., 2001; Fan et al., 2003; Lucanic et al., 2006; Shekarabi et al., 2005). For example, Netrin-1 stimulates growth cone expansion through PAK1 (Shekarabi et al., 2005) and inhibition of PAK kinase activity permits axon extension over repulsive

ECM molecules (Marler et al., 2005). The distinct cellular distributions of multiple PAK family members in growth cones and numerous functional targets of PAK proteins may explain how PAK functions downstream of positive and negative guidance cues. Moreover, correct axon targeting requires both PAK kinase activity and association with the adaptor protein Nck (Ang et al., 2003; Hing et al., 1999). The regulation of filopodial extension by PAK may also influence growth cone guidance (Kim et al., 2003; Robles et al., 2005). Because guidance cue receptors cluster at the tips of filopodia (Galbraith et al., 2007; Shafer et al., 2011), they serve as important sensory extensions of growth cones (Chien et al., 1993). By regulating filopodial protrusion, PAK may regulate the exploratory behavior of growth cones. Stimulation of filopodial extensions at low PAK18 may be due to a redistribution of active PAK to filopodial tips (Fig. 2F,H), which is consistent with our previous findings showing that PAK regulates filopodial tip elongation (Robles et al., 2005). In a related cellular specialization, PAK1 and 3 appear pivotal in the development of dendritic spines, as over-activation of PAK1/3 increases spines (and filopodia), whereas PAK loss of function, or expression of mutant PAK proteins prevents spine formation and maturation (Boda et al., 2004; Zhang et al., 2005). It is noteworthy that the signaling complex consisting of GIT1, PIX, Rac and PAK, which our evidence suggests operates to control growth cone motility, also functions in spine morphogenesis (Zhang et al., 2005). Importantly, point mutations in brain-specific PAK family members in humans lead to abnormal spines *in vivo*, which is associated with non-syndromic X-linked mental retardation (MRX) (Boda et al., 2004; Raymond, 2006).

References

Aizawa, H., S. Wakatsuki, A. Ishii, K. Moriyama, Y. Sasaki, K. Ohashi, Y. Sekine-Aizawa, A. Sehara-Fujisawa, K. Mizuno, Y. Goshima, and I. Yahara. 2001. Phosphorylation of cofilin by LIM-kinase is necessary for semaphorin 3A-induced growth cone collapse. *Nat Neurosci*. 4:367-73.

Ang, L.H., J. Kim, V. Stepensky, and H. Hing. 2003. Dock and Pak regulate olfactory axon pathfinding in Drosophila. *Development*. 130:1307-16.

Arias-Romero, L.E., and J. Chernoff. 2008. A tale of two Paks. *Biol Cell*. 100:97-108.

Bagrodia, S., S.J. Taylor, K.A. Jordon, L. Van Aelst, and R.A. Cerione. 1998. A novel regulator of p21-activated kinases. *J Biol Chem*. 273:23633-6.

Bisson, N., N. Islam, L. Poitras, S. Jean, A. Bresnick, and T. Moss. 2003. The catalytic domain of xPAK1 is sufficient to induce myosin II dependent in vivo cell fragmentation independently of other apoptotic events. *Dev Biol*. 263:264-81.

Bisson, N., L. Poitras, A. Mikryukov, M. Tremblay, and T. Moss. 2007. EphA4 signaling regulates blastomere adhesion in the Xenopus embryo by recruiting Pak1 to suppress Cdc42 function. *Mol Biol Cell*. 18:1030-43.

Bito, H., T. Furuyashiki, H. Ishihara, Y. Shibasaki, K. Ohashi, K. Mizuno, M. Maekawa, T. Ishizaki, and S. Narumiya. 2000. A critical role for a Rho-associated kinase, p160ROCK, in determining axon outgrowth in mammalian CNS neurons. *Neuron*. 26:431-41.

Boda, B., S. Alberi, I. Nikonenko, R. Node-Langlois, P. Jourdain, M. Moosmayer, L. Parisi-Jourdain, and D. Muller. 2004. The mental retardation protein PAK3 contributes to synapse formation and plasticity in hippocampus. *J Neurosci*. 24:10816-25.

Bokoch, G.M. 2003. Biology of the p21-activated kinases. *Annu Rev Biochem*. 72:743-81.

Bright, M.D., A.P. Garner, and A.J. Ridley. 2009. PAK1 and PAK2 have different roles in HGF-induced morphological responses. *Cell Signal*. 21:1738-47.

Brown, M.C., K.A. West, and C.E. Turner. 2002. Paxillin-dependent paxillin kinase linker and p21-activated kinase localization to focal adhesions involves a multistep activation pathway. *Mol Biol Cell*. 13:1550-65.

Carlstrom, L.P., J.H. Hines, S.J. Henle, and J.R. Henley. 2011. Bidirectional remodeling of beta1-integrin adhesions during chemotropic regulation of nerve growth. *BMC Biol*. 9:82.

Cau, J., S. Faure, S. Vigneron, J.C. Labbe, C. Delsert, and N. Morin. 2000. Regulation of Xenopus p21-activated kinase (X-PAK2) by Cdc42 and maturation-promoting factor controls Xenopus oocyte maturation. *J Biol Chem*. 275:2367-75.

Chan, C.E., and D.J. Odde. 2008. Traction dynamics of filopodia on compliant substrates. *Science*. 322:1687-91.

Chien, C.B., D.E. Rosenthal, W.A. Harris, and C.E. Holt. 1993. Navigational errors made by growth cones without filopodia in the embryonic Xenopus brain. *Neuron*. 11:237-51.

Cobos, I., U. Borello, and J.L. Rubenstein. 2007. Dlx transcription factors promote migration through repression of axon and dendrite growth. *Neuron*. 54:873-88.

Daniels, R.H., P.S. Hall, and G.M. Bokoch. 1998. Membrane targeting of p21-activated kinase 1 (PAK1) induces neurite outgrowth from PC12 cells. *EMBO J*. 17:754-64.

Deakin, N.O., and C.E. Turner. 2008. Paxillin comes of age. *J Cell Sci*. 121:2435-44.

Dent, E.W., S.L. Gupton, and F.B. Gertler. 2011. The growth cone cytoskeleton in axon outgrowth and guidance. *Cold Spring Harb Perspect Biol*. 3.

Dent, E.W., and K.F. Meiri. 1992. GAP-43 phosphorylation is dynamically regulated in individual growth cones. *J Neurobiol*. 23:1037-53.

Fan, X., J.P. Labrador, H. Hing, and G.J. Bashaw. 2003. Slit stimulation recruits Dock and Pak to the roundabout receptor and increases Rac activity to regulate axon repulsion at the CNS midline. *Neuron*. 40:113-27.

Galbraith, C.G., K.M. Yamada, and J.A. Galbraith. 2007. Polymerizing actin fibers position integrins primed to probe for adhesion sites. *Science*. 315:992-5.

Godement, P., L.C. Wang, and C.A. Mason. 1994. Retinal axon divergence in the optic chiasm: dynamics of growth cone behavior at the midline. *J Neurosci*. 14:7024-39.

Gomez, T.M., D. Harrigan, J. Henley, and E. Robles. 2003. Working with Xenopus spinal neurons in live cell culture. *Methods Cell Biol*. 71:129-56.

Hayashi, K., T. Ohshima, and K. Mikoshiba. 2002. Pak1 is involved in dendrite initiation as a downstream effector of Rac1 in cortical neurons. *Mol Cell Neurosci*. 20:579-94.

Heckman, C.A., J.G. Demuth, D. Deters, S.R. Malwade, M.L. Cayer, C. Monfries, and A. Mamais. 2009. Relationship of p21-activated kinase (PAK) and filopodia to persistence and oncogenic transformation. *J Cell Physiol*. 220:576-85.

Hines, J.H., M. Abu-Rub, and J.R. Henley. 2010. Asymmetric endocytosis and remodeling of beta1-integrin adhesions during growth cone chemorepulsion by MAG. *Nat Neurosci*. 13:829-37.

Hing, H., J. Xiao, N. Harden, L. Lim, and S.L. Zipursky. 1999. Pak functions downstream of Dock to regulate photoreceptor axon guidance in Drosophila. *Cell*. 97:853-63.

Hitchcock, S.E. 1980. Actin deoxyroboncuclease I interaction. Depolymerization and nucleotide exchange. *J Biol Chem*. 255:5668-73.

Ichetovkin, I., W. Grant, and J. Condeelis. 2002. Cofilin produces newly polymerized actin filaments that are preferred for dendritic nucleation by the Arp2/3 complex. *Curr Biol*. 12:79-84.

Kayser, M.S., M.J. Nolt, and M.B. Dalva. 2008. EphB receptors couple dendritic filopodia motility to synapse formation. *Neuron*. 59:56-69.

Keren, K., Z. Pincus, G.M. Allen, E.L. Barnhart, G. Marriott, A. Mogilner, and J.A. Theriot. 2008. Mechanism of shape determination in motile cells. *Nature*. 453:475-80.

Kim, M.D., D. Kamiyama, P. Kolodziej, H. Hing, and A. Chiba. 2003. Isolation of Rho GTPase effector pathways during axon development. *Dev Biol*. 262:282-93.

Kolodkin, A.L., and M. Tessier-Lavigne. 2011. Mechanisms and molecules of neuronal wiring: a primer. *Cold Spring Harb Perspect Biol*. 3.

Kreis, P., and J.V. Barnier. 2009. PAK signalling in neuronal physiology. *Cell Signal*. 21:384-93.

Kuo, J.C., X. Han, C.T. Hsiao, J.R. Yates, 3rd, and C.M. Waterman. Analysis of the myosin-II-responsive focal adhesion proteome reveals a role for beta-Pix in negative regulation of focal adhesion maturation. *Nat Cell Biol*. 13:383-93.

Loudon, R.P., L.D. Silver, H.F. Yee, Jr., and G. Gallo. 2006. RhoA-kinase and myosin II are required for the maintenance of growth cone polarity and guidance by nerve growth factor. *J Neurobiol*. 66:847-67.

Lowery, L.A., and D. Van Vactor. 2009. The trip of the tip: understanding the growth cone machinery. *Nat Rev Mol Cell Biol*. 10:332-43.

Lucanic, M., M. Kiley, N. Ashcroft, N. L'Etoile, and H.J. Cheng. 2006. The Caenorhabditis elegans P21-activated kinases are differentially required for UNC-6/netrin-mediated commissural motor axon guidance. *Development*. 133:4549-59.

Manser, E., T.H. Loo, C.G. Koh, Z.S. Zhao, X.Q. Chen, L. Tan, I. Tan, T. Leung, and L. Lim. 1998. PAK kinases are directly coupled to the PIX family of nucleotide exchange factors. *Mol Cell*. 1:183-92.

Marin, O., M. Valiente, X. Ge, and L.H. Tsai. 2010. Guiding neuronal cell migrations. *Cold Spring Harb Perspect Biol*. 2:a001834.

Marler, K.J., R. Kozma, S. Ahmed, J.M. Dong, C. Hall, and L. Lim. 2005. Outgrowth of neurites from NIE-115 neuroblastoma cells is prevented on repulsive substrates through the action of PAK. *Mol Cell Biol*. 25:5226-41.

Marsick, B.M., K.C. Flynn, M. Santiago-Medina, J.R. Bamburg, and P.C. Letourneau. 2010. Activation of ADF/cofilin mediates attractive growth cone turning toward nerve growth factor and netrin-1. *Dev Neurobiol*. 70:565-88.

Marsick, B.M., J.E. San Miguel-Ruiz, and P.C. Letourneau. 2012. Activation of ezrin/radixin/moesin mediates attractive growth cone guidance through regulation of growth cone actin and adhesion receptors. *J Neurosci*. 32:282-96.

Maruta, H., H. He, and T. Nheu. 2002. Interfering with Ras signaling using membrane-permeable peptides or drugs. *Methods Mol Biol*. 189:75-85.

Myers, J.P., and T.M. Gomez. 2011. Focal adhesion kinase promotes integrin adhesion dynamics necessary for chemotropic turning of nerve growth cones. *J Neurosci*. 31:13585-95.

Myers, J.P., E. Robles, A. Ducharme-Smith, and T.M. Gomez. 2012. Focal adhesion kinase modulates Cdc42 activity downstream of positive and negative axon guidance cues. *J Cell Sci*.

Myers, J.P., M. Santiago-Medina, and T.M. Gomez. 2011. Regulation of axonal outgrowth and pathfinding by integrin-ECM interactions. *Dev Neurobiol*. 71:901-23.

Nayal, A., D.J. Webb, C.M. Brown, E.M. Schaefer, M. Vicente-Manzanares, and A.R. Horwitz. 2006. Paxillin phosphorylation at Ser273 localizes a GIT1-PIX-PAK complex and regulates adhesion and protrusion dynamics. *J Cell Biol*. 173:587-9.

Obermeier, A., S. Ahmed, E. Manser, S.C. Yen, C. Hall, and L. Lim. 1998. PAK promotes morphological changes by acting upstream of Rac. *EMBO J*. 17:4328-39.

Petchprayoon, C., K. Suwanborirux, J. Tanaka, Y. Yan, T. Sakata, and G. Marriott. 2005. Fluorescent kabiramides: new probes to quantify actin in vitro and in vivo. *Bioconjug Chem*. 16:1382-9.

Raymond, F.L. 2006. X linked mental retardation: a clinical guide. *J Med Genet*. 43:193-200.

Robles, E., and T.M. Gomez. 2006. Focal adhesion kinase signaling at sites of integrin-mediated adhesion controls axon pathfinding. *Nat Neurosci*. 9:1274-83.

Robles, E., S. Woo, and T.M. Gomez. 2005. Src-dependent tyrosine phosphorylation at the tips of growth cone filopodia promotes extension. *J Neurosci*. 25:7669-81.

Rosenberger, G., and K. Kutsche. 2006. AlphaPIX and betaPIX and their role in focal adhesion formation. *Eur J Cell Biol*. 85:265-74.

Rozen, S., and H. Skaletsky. 2000. Primer3 on the WWW for general users and for biologist programmers. *Methods Mol Biol*. 132:365-86.

Santiago-Medina, M., J.P. Myers, and T.M. Gomez. 2012. Imaging adhesion and signaling dynamics in Xenopus laevis growth cones. *Dev Neurobiol*. 72:585-99.

Sarmiere, P.D., and J.R. Bamburg. 2004. Regulation of the neuronal actin cytoskeleton by ADF/cofilin. *J Neurobiol*. 58:103-17.

Shafer, B., K. Onishi, C. Lo, G. Colakoglu, and Y. Zou. 2011. Vangl2 promotes Wnt/planar cell polarity-like signaling by antagonizing Dvl1-mediated feedback inhibition in growth cone guidance. *Dev Cell*. 20:177-91.

Shekarabi, M., S.W. Moore, N.X. Tritsch, S.J. Morris, J.F. Bouchard, and T.E. Kennedy. 2005. Deleted in colorectal cancer binding netrin-1 mediates cell substrate adhesion and recruits Cdc42, Rac1, Pak1, and N-WASP into an intracellular signaling complex that promotes growth cone expansion. *J Neurosci*. 25:3132-41.

Souopgui, J., M. Solter, and T. Pieler. 2002. XPak3 promotes cell cycle withdrawal during primary neurogenesis in Xenopus laevis. *EMBO J*. 21:6429-39.

Sretavan, D.W., and L.F. Reichardt. 1993. Time-lapse video analysis of retinal ganglion cell axon pathfinding at the mammalian optic chiasm: growth cone guidance using intrinsic chiasm cues. *Neuron*. 10:761-77.

Stofega, M.R., L.C. Sanders, E.M. Gardiner, and G.M. Bokoch. 2004. Constitutive p21-activated kinase (PAK) activation in breast cancer cells as a result of mislocalization of PAK to focal adhesions. *Mol Biol Cell*. 15:2965-77.

Tanaka, J., Y. Yan, J. Choi, J. Bai, V.A. Klenchin, I. Rayment, and G. Marriott. 2003. Biomolecular mimicry in the actin cytoskeleton: mechanisms underlying the cytotoxicity of kabiramide C and related macrolides. *Proc Natl Acad Sci U S A*. 100:13851-6.

ten Klooster, J.P., Z.M. Jaffer, J. Chernoff, and P.L. Hordijk. 2006. Targeting and activation of Rac1 are mediated by the exchange factor beta-Pix. *J Cell Biol*. 172:759-69.

Turner, C.E., M.C. Brown, J.A. Perrotta, M.C. Riedy, S.N. Nikolopoulos, A.R. McDonald, S. Bagrodia, S. Thomas, and P.S. Leventhal. 1999. Paxillin LD4 motif binds PAK and PIX through a novel 95-kD ankyrin repeat, ARF-GAP protein: A role in cytoskeletal remodeling. *J Cell Biol*. 145:851-63.

Wiggan, O., A.E. Shaw, J.G. Deluca, and J.R. Bamburg. 2012. ADF/Cofilin Regulates Actomyosin Assembly through Competitive Inhibition of Myosin II Binding to F-Actin. *Dev Cell*. 22:530-43.

Woo, S., and T.M. Gomez. 2006. Rac1 and RhoA promote neurite outgrowth through formation and stabilization of growth cone point contacts. *J Neurosci*. 26:1418-28.

Woo, S., D.J. Rowan, and T.M. Gomez. 2009. Retinotopic mapping requires focal adhesion kinase-mediated regulation of growth cone adhesion. *J Neurosci*. 29:13981-91.

Wu, C., S.B. Asokan, M.E. Berginski, E.M. Haynes, N.E. Sharpless, J.D. Griffith, S.M. Gomez, and J.E. Bear. 2012. Arp2/3 is critical for lamellipodia and response to extracellular matrix cues but is dispensable for chemotaxis. *Cell*. 148:973-87.

Zaidel-Bar, R., and B. Geiger. 2010. The switchable integrin adhesome. *J Cell Sci*. 123:1385-8.

Zaidel-Bar, R., R. Milo, Z. Kam, and B. Geiger. 2007. A paxillin tyrosine phosphorylation switch regulates the assembly and form of cell-matrix adhesions. *J Cell Sci*. 120:137-48.

Zhang, H., D.J. Webb, H. Asmussen, S. Niu, and A.F. Horwitz. 2005. A GIT1/PIX/Rac/PAK signaling module regulates spine morphogenesis and synapse formation through MLC. *J Neurosci*. 25:3379-88.

Zhao, L., Q.L. Ma, F. Calon, M.E. Harris-White, F. Yang, G.P. Lim, T. Morihara, O.J. Ubeda, S. Ambegaokar, J.E. Hansen, R.H. Weisbart, B. Teter, S.A. Frautschy, and G.M. Cole. 2006. Role of p21-activated kinase pathway defects in the cognitive deficits of Alzheimer disease. *Nat Neurosci*. 9:234-42.

Figure 1. PAK and PIX isoforms are expressed in the embryonic spinal cord and fusion proteins localize to distinct sites within live growth cones. **A.** RT-PCR amplification of PAK1, 2, 3 and α-, β-PIX from stage 24 *Xenopus* spinal cord shows that PAK2 and PAK3, as well as α-PIX are most highly expressed. **B.** Western blot of PAK1, 2 and 3 from stage 24 *Xenopus* spinal cord confirms that PAK2 and PAK3 are highly expressed. **C-F.** TIRF images of representative live spinal neuron growth cones on LN expressing PXN-GFP or PXN-mCh together with different isoforms of fluorescent PAK (C-E) or α-PIX (F). **C**. xPAK1 does not concentrate at any distinct location within this growth cone and does not colocalize with PXN-containing point contacts (PCs). **D.** xPAK2 localizes to PXN-containing PCs (arrows) and to filopodial tips that contain little or no PXN (arrowheads). **E.** xPAK3 localizes only to PXN-containing PCs (arrows). **F.** α-PIX localizes only to PXN-containing PCs (arrows). **G,H.** Montages of merged images of the growth cones shown in D and E, respectively, expressing mCh-xPAK2 and PXN-GFP (G) or mCh-xPAK3 and PXN-GFP (H); images were taken at 15 sec intervals. Note in (G) that xPAK2 is present at the tips of extending filopodia (arrowheads) and colocalizes with PXN at stable point contacts (dashed box). In (H) xPAK3 is not present in filopodia tips (arrowheads), but does colocalize with PXN at stable point contacts (dashed box). Scale bar: 10 μm.

Figure 1.

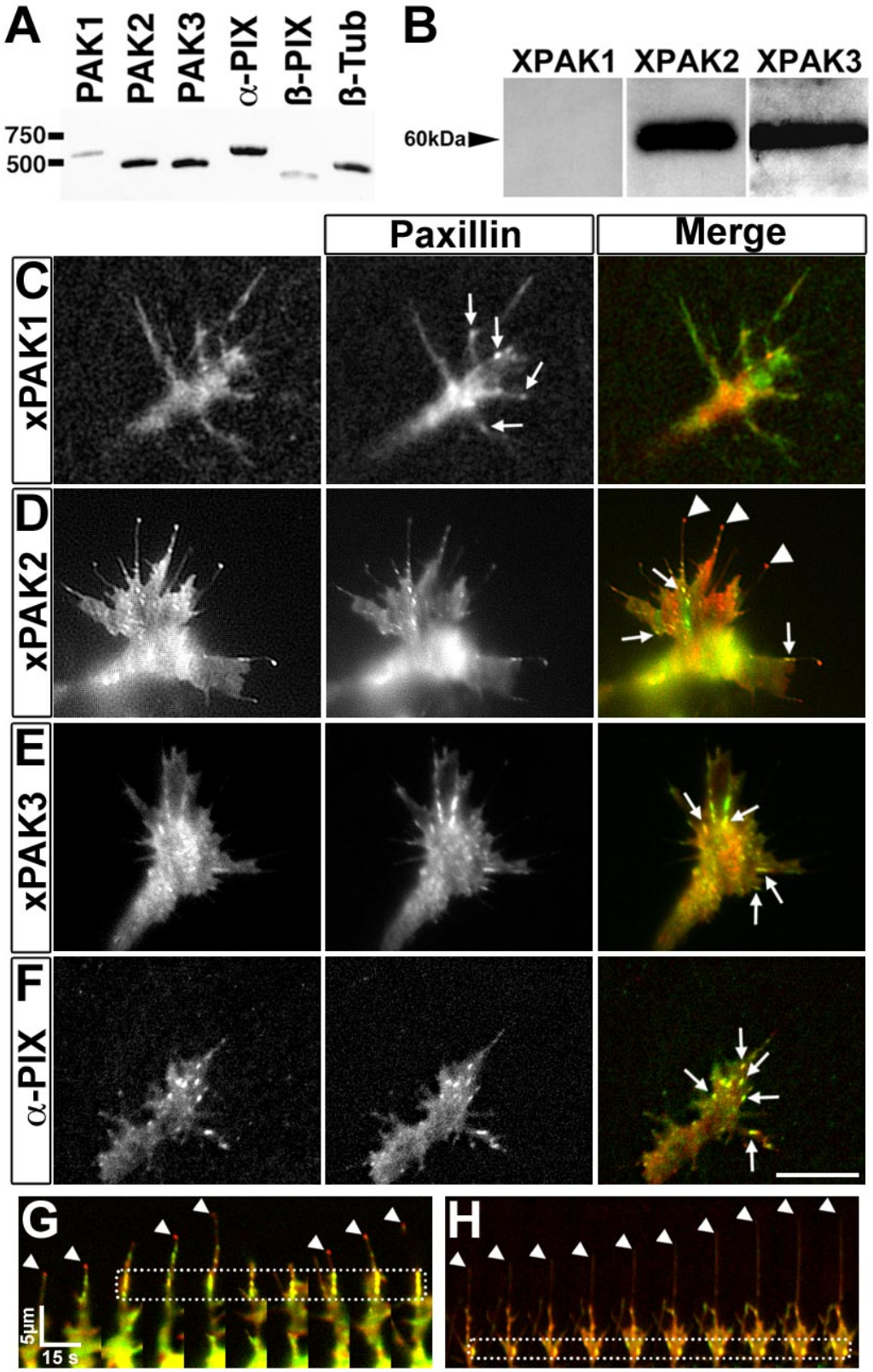
A
PAK1
PAK2
PAK3
α-PIX
β-PIX
β-Tub
750
500
B
XPAK1
XPAK2
XPAK3
60kDa
Paxillin
Merge
C
xPAK1
D
xPAK2
E
xPAK3
F
α-PIX
G
5μm
15 s
H

Figure 2. Dose-dependent effects of acute inhibition of PAK-PIX interactions on growth cone motility and morphology. A-C. Phase contrast images at 5 min intervals of growth cones on LN during stimulation with the indicated concentrations of PAK18 (at 0 min). **D.** The rate of neurite outgrowth of neurons on LN and PDL after stimulation with increasing concentrations of PAK18 normalized to the pretreatment rate of outgrowth. Note that PAK18 maximally stimulates axon outgrowth on LN at 1 μM, but has no effect on neurite outgrowth on PDL at any concentration. Kruskal-Wallis test with Dunn's post-hoc analysis, N ≥ 60. **E.** Kymographs generated from the leading edge of fluorescent growth cones on LN (above) and PDL (below) during stimulation with 1μM PAK18 (at black arrowhead). Note differences in scale bars. **F.** DIC images of a growth cone on LN at 5 min intervals during stimulation with 1μM PAK18. Note an increase in growth cone area, as well as filopodia number and length after PAK18 stimulation. **G.** Growth cone area was measured from fixed neurons after 5 min. stimulation with different concentrations of PAK18. Kruskal-Wallis test with Dunn's post-hoc analysis, N ≥ 148. **H.** Number of filopodia and their length in response to 1μM PAK18. Student's t-test, N ≥ 27. **P < 0.01, ***P < 0.001. Scale: 20 μm (A-C) and 10 μm (F).

Figure 2.

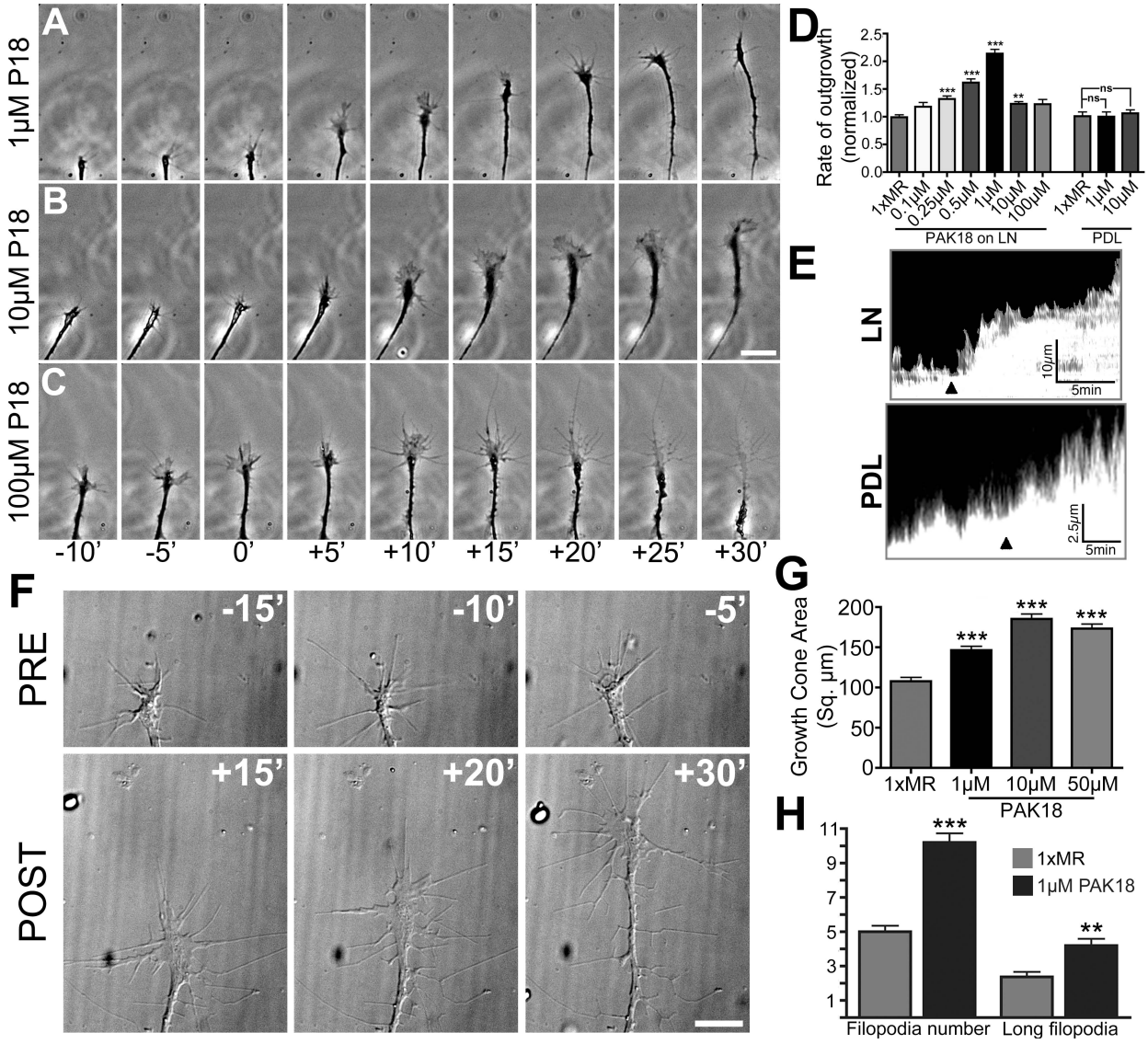
A
1μM P18
B
10μM P18
C
100μM P18
-10'
-5'
0'
+5'
+10'
+15'
+20'
+25'
+30'
D
Rate of outgrowth (normalized)
1xMR
0.1μM
0.25μM
0.5μM
1μM
10μM
100μM
PAK18 on LN
PDL
ns
E
LN
PDL
10μm
5min
2.5μm
F
PRE
POST
-15'
-10'
-5'
+15'
+20'
+30'
G
Growth Cone Area (Sq. μm)
1xMR
1μM
10μM
50μM
PAK18
H
1xMR
1μM PAK18
Filopodia number
Long filopodia

Figure 3. Acute inhibition of PAK with PAK18 has dose dependent effects on PAK targets and regulates actin polymerization. **A-D.** Representative growth cones treated for 5 min. with control medium or increasing concentrations of PAK18 and immunolabeled for p-XAC (Ser3). **A'-D'.** Merged images of p-XAC (green) and F-actin labeling (red). **E.** Fluorescence intensity measurements, normalized to control, of p-XAC labeling of growth cones treated with increasing concentrations of PAK18. **F-I.** Representative growth cones treated for 5 min. with control medium or increasing concentrations of PAK18 and immunolabeled for p-MLC. **F'-I'.** Merged images of p-MLC (green) and F-actin labeling (red). **J.** Normalized fluorescence intensity measurements of p-MLC labeled growth cones. **K-N.** Representative growth cones treated for 5 min. with control media or increasing concentrations of PAK18 and labeled for G-actin (Alexa-488 DNase1). **K'-N'.** Growth cones from (K-N) labeled for F-actin with Alexa-546 phalloidin. **K''-N''.** Merged images of G-actin (green) and F-actin labeling (red). **O.** Fluorescence intensity measurements of G-actin and F-actin labeling in growth cones treated with PAK18. **P.** G-/F-actin ratiometric measurements of growth cones treated with PAK18. **P < 0.01, ***P < 0.001, Kruskal-Wallis test with Dunn's post-hoc analysis, N ≥ 35. Scale, 10 μm.

Figure 3.

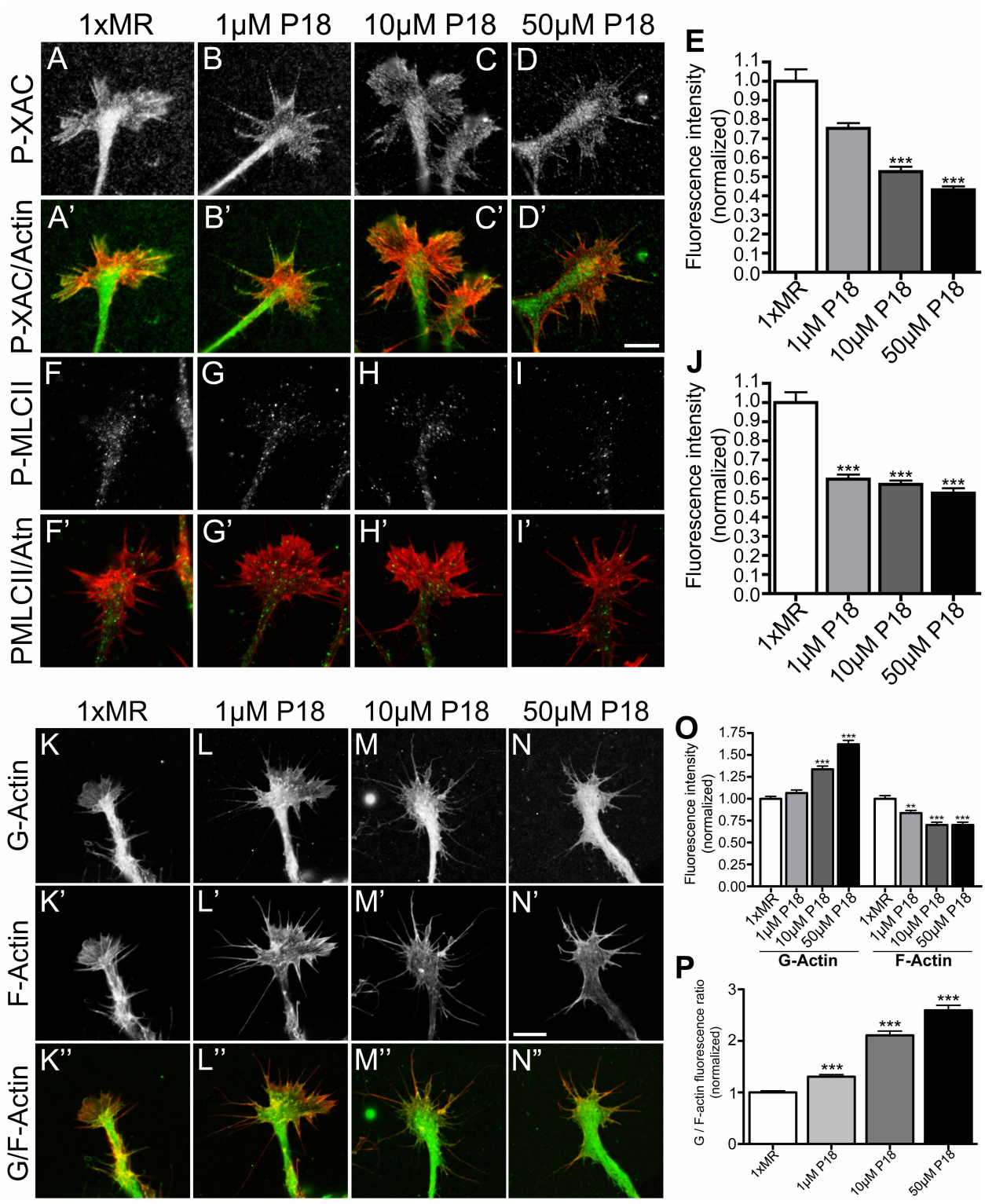
1xMR
1μM P18
10μM P18
50μM P18
P-XAC
P-XAC/Actin
P-MLCII
PMLCII/Atn
G-Actin
F-Actin
G/F-Actin
E
Fluorescence intensity (normalized)
J
O
G-Actin
F-Actin
P
G / F-actin fluorescence ratio (normalized)

Figure 4. Acute inhibition of PAK-PIX interactions decelerates F-actin retrograde flow. **A.** A live growth cone labeled with the F-actin barbed-end binding probe, TMR-KabC. The red box denotes the region used to generate a kymograph (see methods). **B.** Kymograph from the boxed region of the growth cone in (A) indicating the rearward flow of KabC-capped actin filaments (red arrow). Note that the angle of flow lines indicates the rate of retrograde flow. **C.** Growth cone from (A), 5 min after stimulation with 1 μM PAK18. **D.** Kymograph from the boxed region of the growth cone in (C). Note the retrograde flow lines appear more shallow (red arrow), indicating the rate of actin rearward flow is reduced by 1 μM PAK18. **E.** The average rate of retrograde flow is significantly reduced by both 1 and 10 μM PAK18. ***P < 0.001, Kruskal-Wallis test with Dunn's post-hoc analysis, N=10. Scale, 10 μm (A,C).

Figure 4.

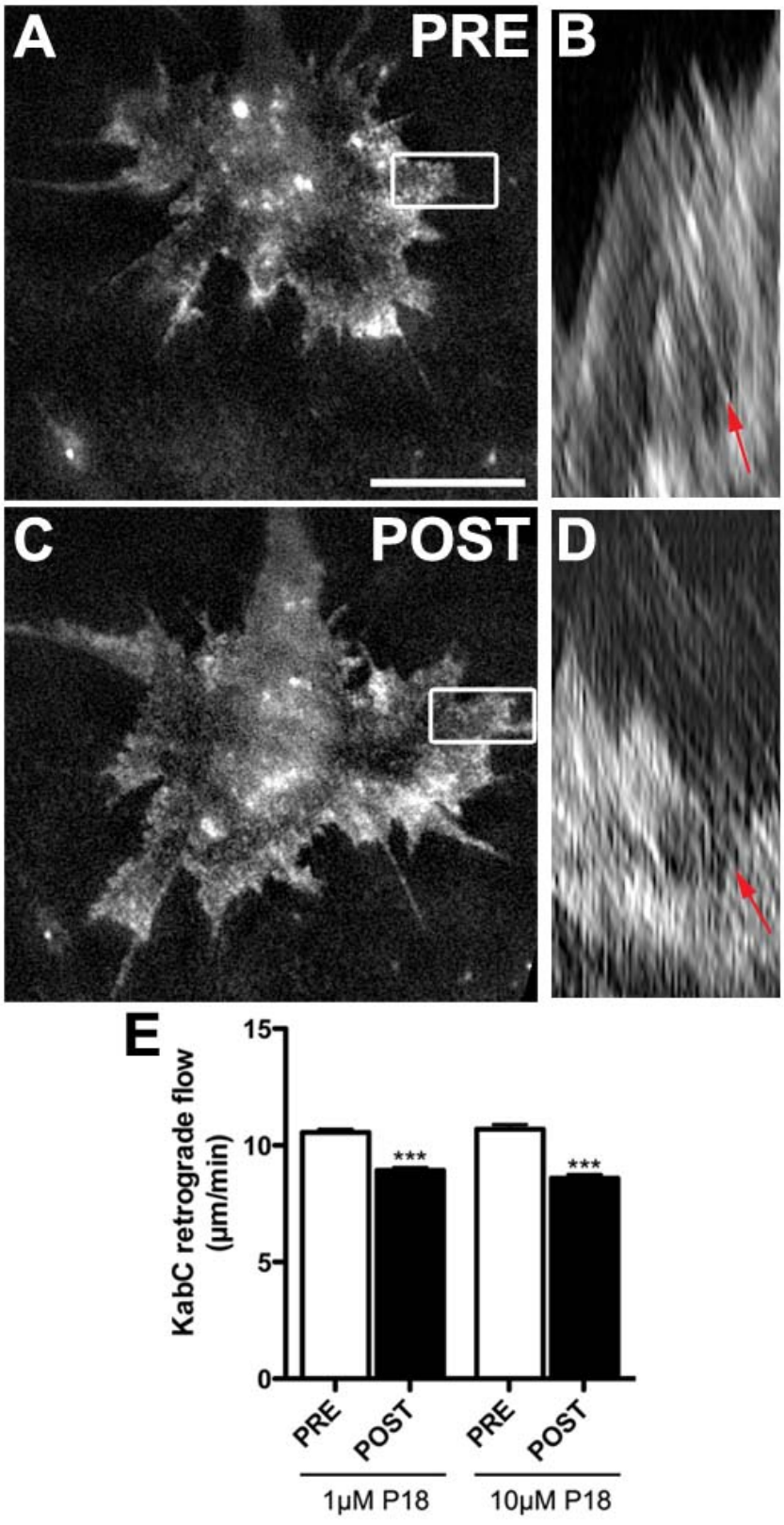
A
PRE
B
C
POST
D
E
KabC retrograde flow (µm/min)
15
10
5
0
***
***
PRE
POST
PRE
POST
1µM P18
10µM P18

Figure 5. Acute inhibition of PAK-PIX interactions regulates point contact formation and turnover. **A-D.** Representative growth cones treated for 5 min with control medium or increasing concentrations of PAK18 and immunolabeled for p-PXN (Tyr118). **A'-D'.** Merged images of p-PXN (green) and F-actin labeling (red). **E-G.** Quantification of adhesions using particle analysis (see methods) of p-PXN labeled growth cones normalized to untreated control growth cones. **P < 0.01, ***P < 0.001, Kruskal-Wallis test with Dunn's post-hoc analysis, N ≥ 29. **H, I.** Time-lapse TIRF images of a live growth cone expressing PXN-GFP shown 10 min before (H) and after (I) stimulation with 1μM PAK18. **H'-I'.** Pseudocolored heat maps (see methods), which illustrate point contact lifetimes over the 15 min periods before and after stimulation with 1 μM PAK18. Note that many adhesions with short lifetimes form after 1 μM PAK18. **J, K.** Time-lapse TIRF images of a live growth cone expressing PXN-GFP shown 10 min before (J) and after (K) stimulation with 10 μM PAK18. **J'-K'.** Pseudocolored heat maps, which illustrate point contact lifetimes over the 15 min periods before and after stimulation with 10 μM PAK18. Note that many adhesions with long lifetimes form after 10 μM PAK18. **L-M.** Point contact adhesion lifetimes measured before and after stimulation with 1 μM PAK18 (L) and 10 μM PAK18 (M). ***P < 0.001, Kruskal-Wallis test with Dunn's post-hoc analysis, N = 10. Scale, 10 μm.

Figure 5.

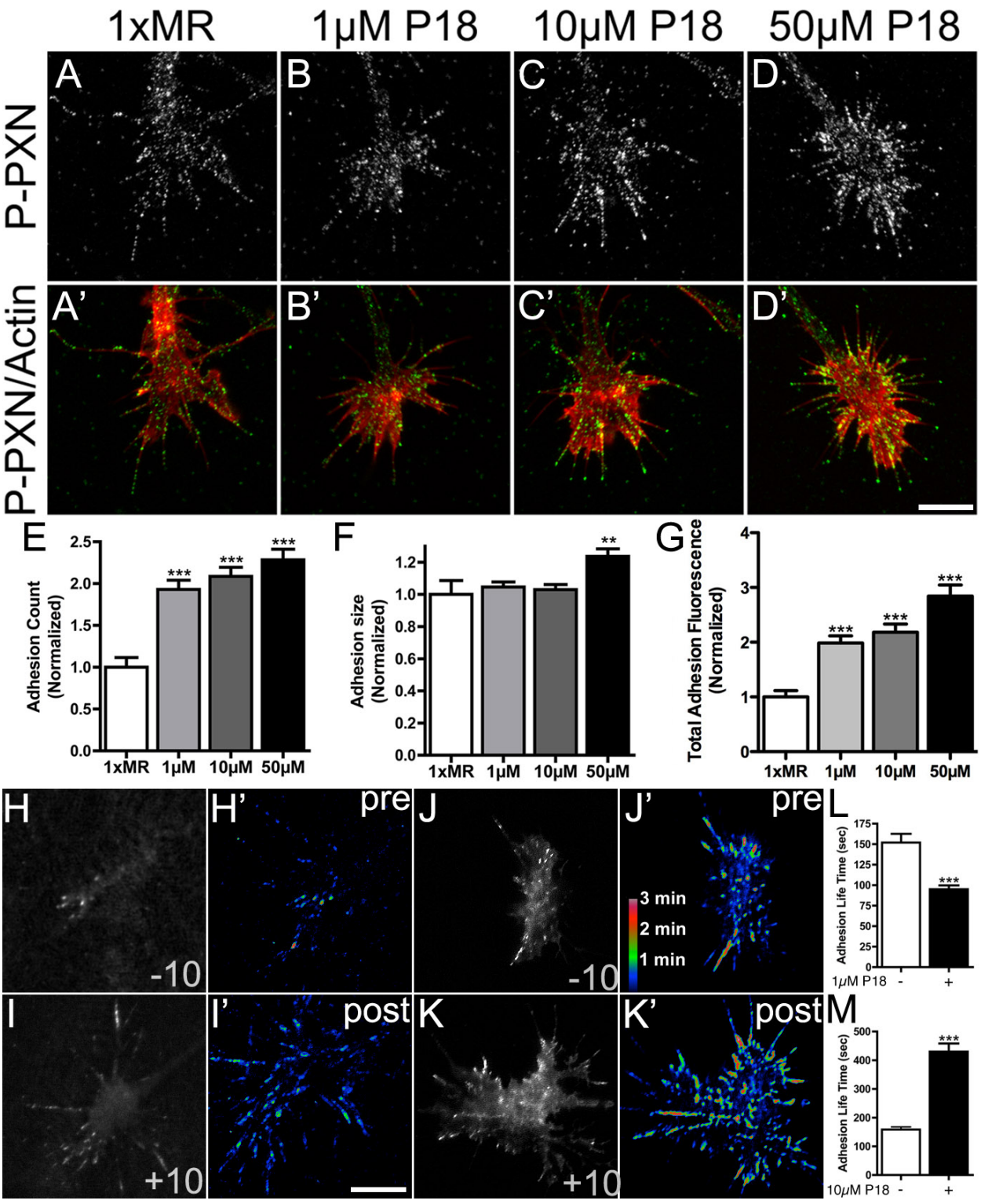
1xMR
1μM P18
10μM P18
50μM P18
P-PXN
P-PXN/Actin
A
B
C
D
A'
B'
C'
D'
E
Adhesion Count (Normalized)
F
Adhesion size (Normalized)
G
Total Adhesion Fluorescence (Normalized)
1xMR
1μM
10μM
50μM
H
H'
pre
J
J'
pre
3 min
2 min
1 min
L
Adhesion Life Time (sec)
1μM P18
I
I'
post
K
K'
post
M
Adhesion Life Time (sec)
10μM P18
-10
+10

Figure 6. Acute inhibition of PAK-PIX interactions displaces PAK from paxillin based adhesions. A, B. TIRF images of a live growth cone expressing both PXN-GFP and mCh-xPAK3 at times before (A) and after (B) stimulation with 10μM PAK18. The white boxes indicate point contacts. **C, D.** TIRF images of point contacts from boxed regions in (A, B) presented at 30 sec intervals. Before PAK18 addition at 0 s, PXN targets to stable point contacts, which colocalize, with some delay, with PAK3 (arrowheads). However, upon addition of PAK18 at 0 s, PAK3 is lost from point contacts. In the continued presence of PAK18 (D), new point contacts recruit little PAK3 and are long lived. **E.** Measurement of mCH-xPAK3 fluorescence at PXN-GFP point contacts shows reduced PAK3 after PAK18 addition. ***P < 0.001, Student t-test, N > 134 point contacts in 7 growth cones. **F.** Measurement of point contact adhesion lifetimes shows that PXN and PAK3 remain within point contacts longer after PAK18. *P < 0.05, ***P < 0.001, Kruskal-Wallis test with Dunn's post-hoc analysis, N = 72 point contacts in 7 growth cones. Scale, 5 μm (A-B) and 2μm (C).

Figure 6.

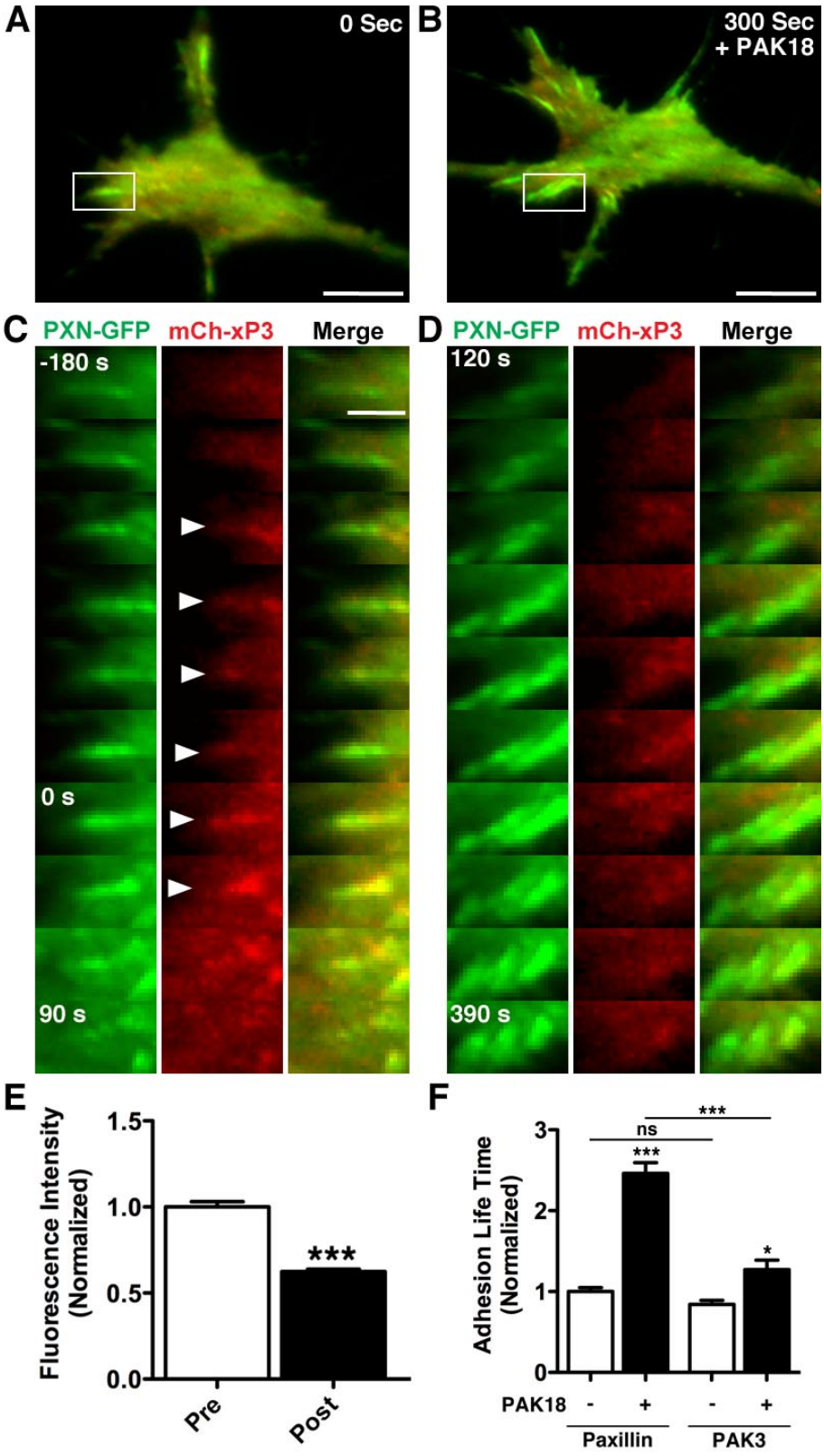
A
0 Sec
B
300 Sec
+ PAK18
C
PXN-GFP
mCh-xP3
Merge
-180 s
0 s
90 s
D
PXN-GFP
mCh-xP3
Merge
120 s
390 s
E
Fluorescence Intensity
(Normalized)
1.5
1.0
0.5
0.0
***
Pre
Post
F
Adhesion Life Time
(Normalized)
3
2
1
0
ns
***
***
*
PAK18
-
+
-
+
Paxillin
PAK3

Figure 7. S273 paxillin regulates point contact adhesion dynamics and growth cone motility. **A.** Schematic diagram of paxillin showing the position of the S273 residue that is phosphorylated by PAK and was mutated to generate phosphomimetic (S273D) and nonphosphorylatable (S273A) variants of paxillin. **B.** From time-lapse TIRF images of S273D/A-PXN-GFP, the lifetime of point contacts was measured before and after stimulation with 1 μM PAK18 in growth cones expressing wild type and mutant variants of PXN. N = 10. **C.** The rate of neurite outgrowth was measured 15 min before and after stimulation with 1 μM PAK18 in growth cones expressing wild type and mutant variants of PXN. N ≥ 38. *P < 0.05, **P < 0.01, ***P < 0.001, Kruskal-Wallis test with Dunn's post-hoc analysis.

Figure 7.

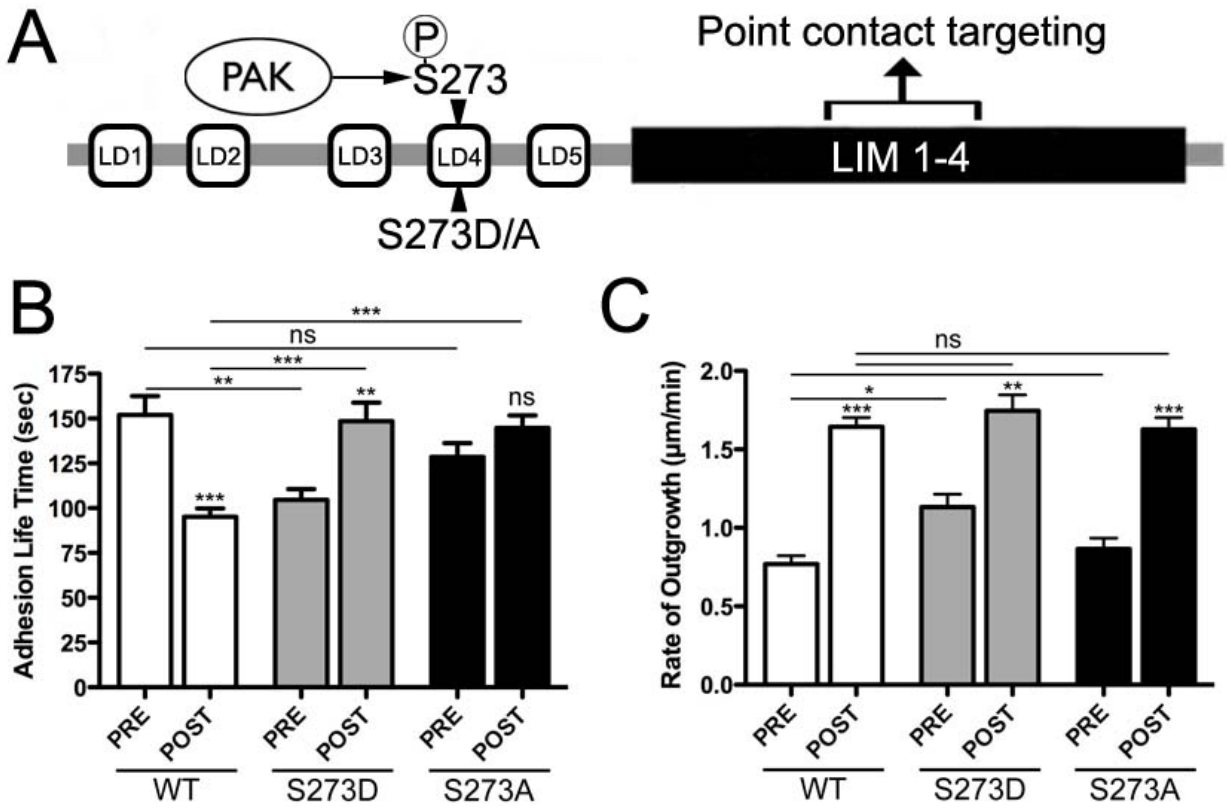
A
PAK
P
S273
Point contact targeting
LD1
LD2
LD3
LD4
LD5
LIM 1-4
S273D/A
B
Adhesion Life Time (sec)
175
150
125
100
75
50
25
0
***
ns
***
**
**
***
ns
PRE
POST
PRE
POST
PRE
POST
WT
S273D
S273A
C
Rate of Outgrowth (µm/min)
2.0
1.5
1.0
0.5
0.0
ns
*
***
**
***
PRE
POST
PRE
POST
PRE
POST
WT
S273D
S273A

Figure 8. A PIX-binding PAK2 mutant blocks the effects of PAK18. A. Schematic diagram of PAK showing the PIX-binding domain and amino acid mutations that disrupt PAK binding to PIX. The PIX-binding domain of all three PAK isoforms is compared to the sequence of PAK18. Note strong sequence homology between PAK18 and xPAK2 and xPAK3, but less homology with xPAK1. Red residues indicate sequence divergence, while blue residues indicate the amino acids necessary for PAK-PIX binding. **B.** Time-lapse TIRF images of a growth cone expressing GFP-xPAK2-PR180,181GA (GFP-xP2-PIXm) shown at 1 min intervals for 5 min before and after stimulation with 1 μM PAK18. Note that GFP-xP2-PIXm does not localize to point contacts, but does localize to filopodia tips (arrows), even after PAK18 treatment (lower panel). Also, note little morphological effect on GFP-xP2-PIXm expressing growth cone after 1 μM PAK18. **C.** Rate of neurite outgrowth measured 15 min before and after stimulation with 1 μM PAK18. ***$P < 0.001$, Kruskal-Wallis test with Dunn's post-hoc analysis, $N \geq 22$. Scale, 10 μm.

Figure 8.

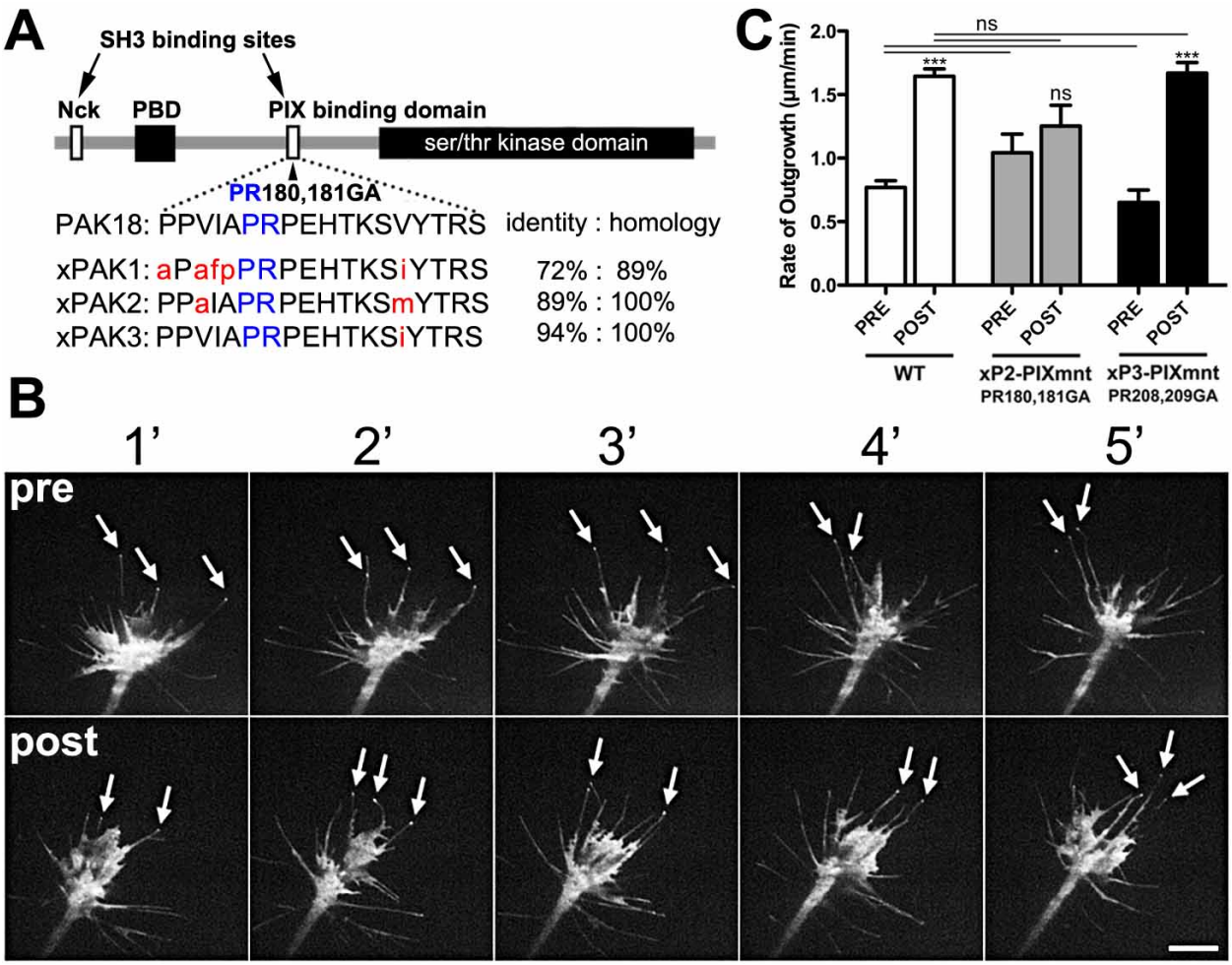
A
SH3 binding sites
Nck
PBD
PIX binding domain
ser/thr kinase domain
PR180,181GA
PAK18: PPVIAPRPEHTKSVYTRS identity : homology
xPAK1: aPafpPRPEHTKSiYTRS 72% : 89%
xPAK2: PPalAPRPEHTKSmYTRS 89% : 100%
xPAK3: PPVIAPRPEHTKSiYTRS 94% : 100%
C
Rate of Outgrowth (µm/min)
2.0
1.5
1.0
0.5
0.0
ns
***
ns
***
PRE
POST
PRE
POST
PRE
POST
WT
xP2-PIXmnt
PR180,181GA
xP3-PIXmnt
PR208,209GA
B
1'
2'
3'
4'
5'
pre
post

Supplementary Materials, Figure S1. Mammalian embryonic neurons express PAK1-3. A-F. Distribution of PAK 1, 2 and 3 in embryonic mouse hippocampal (A,B) and cortical (D,F) neurons cultured for 24 hrs. Neurons were labeled with antibodies to specific PAK isotypes (green) and filamentous actin using fluorescent phalloidin (red). **A, D.** p-Thr423-PAK 1 was labeled to show the distribution of activated PAK1. Note that the punctate distributions of PAK1 and PAK2 (B, E) extend out to the periphery of growth cone lamella and tips of filopodia (arrows), whereas PAK3 (C, F) is more centrally located (arrowheads). Insets illustrate immature neurons that have not yet developed distinct axons and dendrites. Scale: 10 μm.

Supplementary Materials, Figure S1.

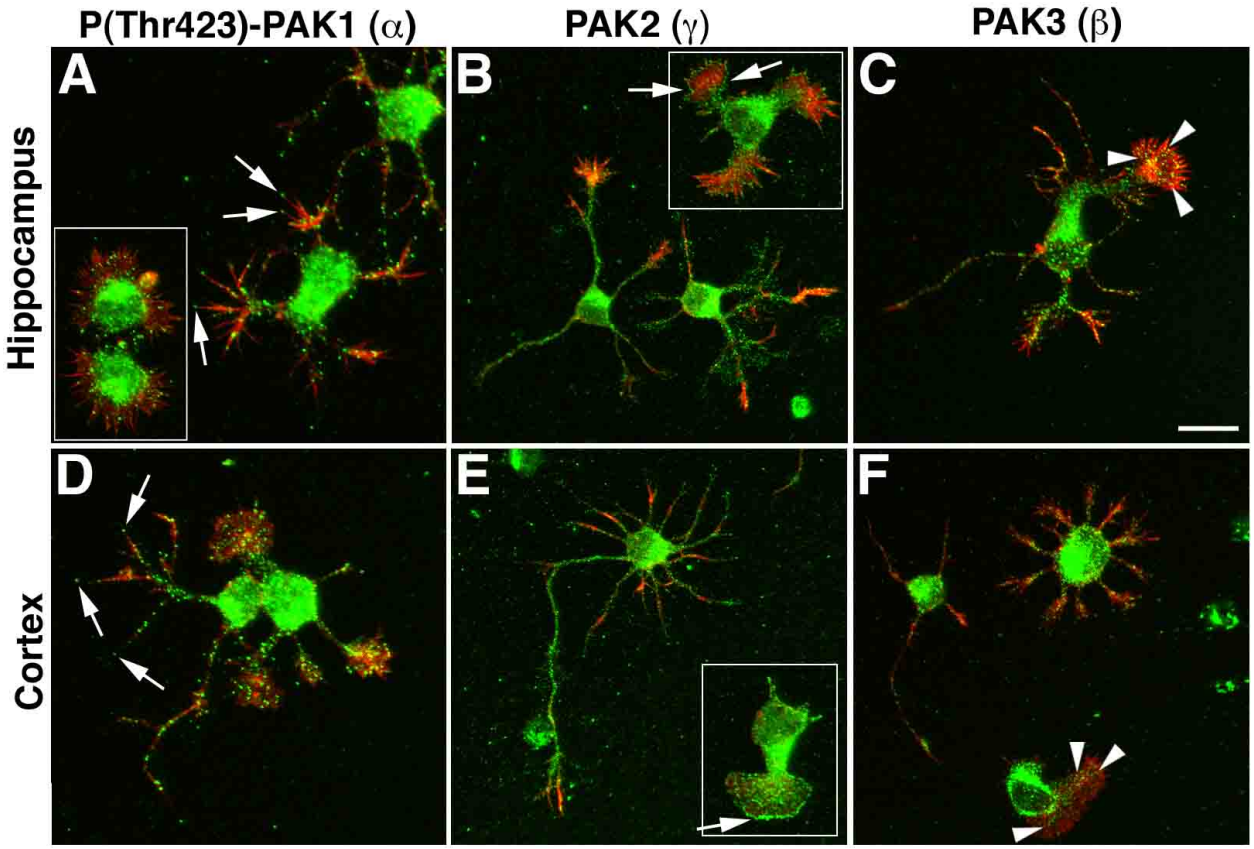

Supplementary Materials, Figure S2. Neurite outgrowth in response to the PAK18 control peptide. The rate of neurite outgrowth of neurons on LN after stimulation with increasing concentrations of Control-PAK18. Note that Control-PAK18 fails to stimulate axon outgrowth on LN at any concentration. Kruskal-Wallis test with Dunn's post-hoc analysis, $N \geq 50$.

Supplementary Materials, Figure S2.

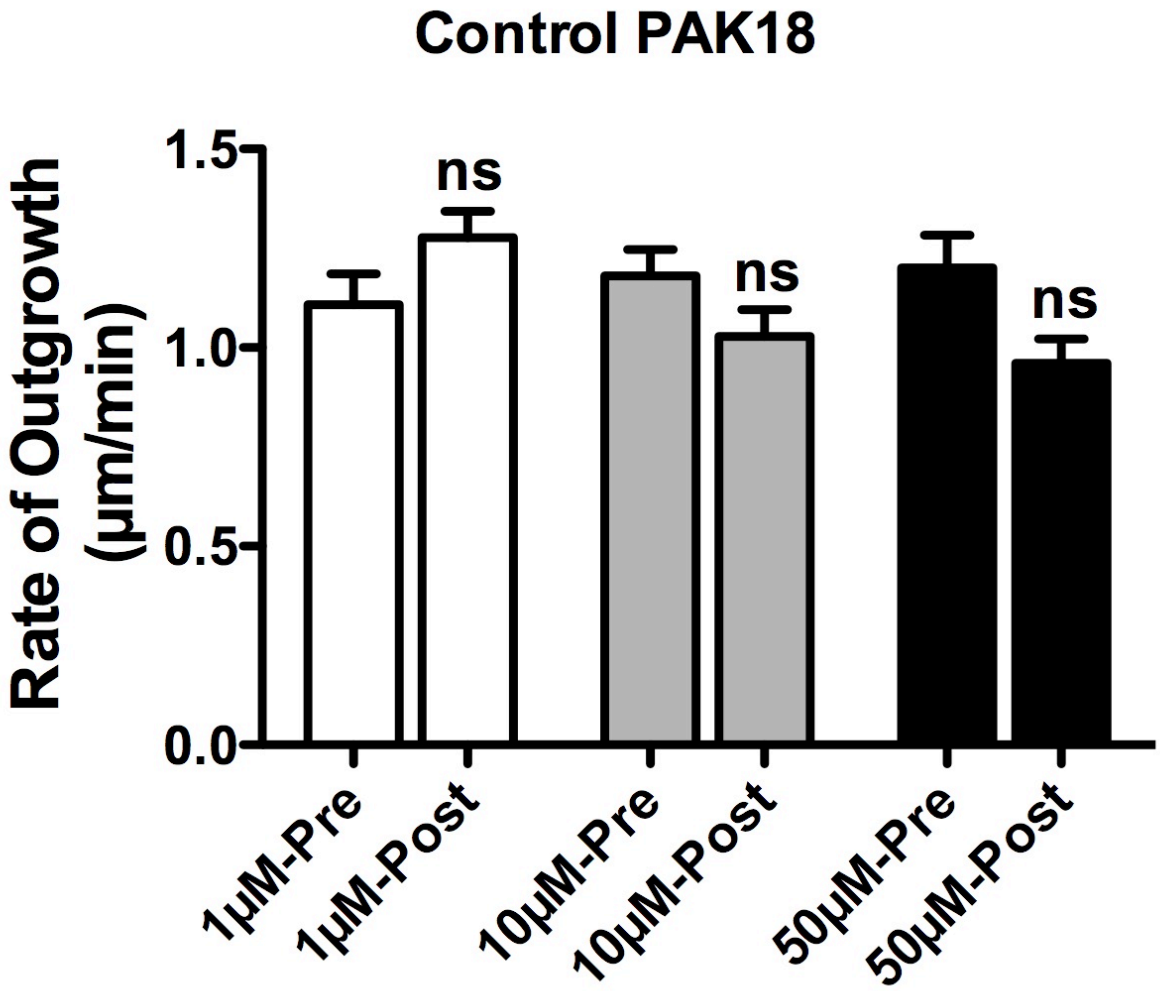

Supplementary Materials, Figure S3. Chronic stimulation of spinal explants with PAK18 promotes increased neurite outgrowth. A-B. Explants were imaged 16 hrs after culturing in the presence of 1xMR (**A**) or 1μM PAK18 (**B**). Note that explants plated in the presence of PAK18 exhibit an increase in both neurites per spinal explant (**C**) and neurite length (**D**). Additionally, in PAK18 stimulated explants, neuronal migration outside of the spinal explant was observed (arrows). ***P < 0.001, Kruskal-Wallis test with Dunn's post-hoc analysis, N ≥ 74 neurites. Scale: 100μm.

Supplementary Materials, Figure S3.

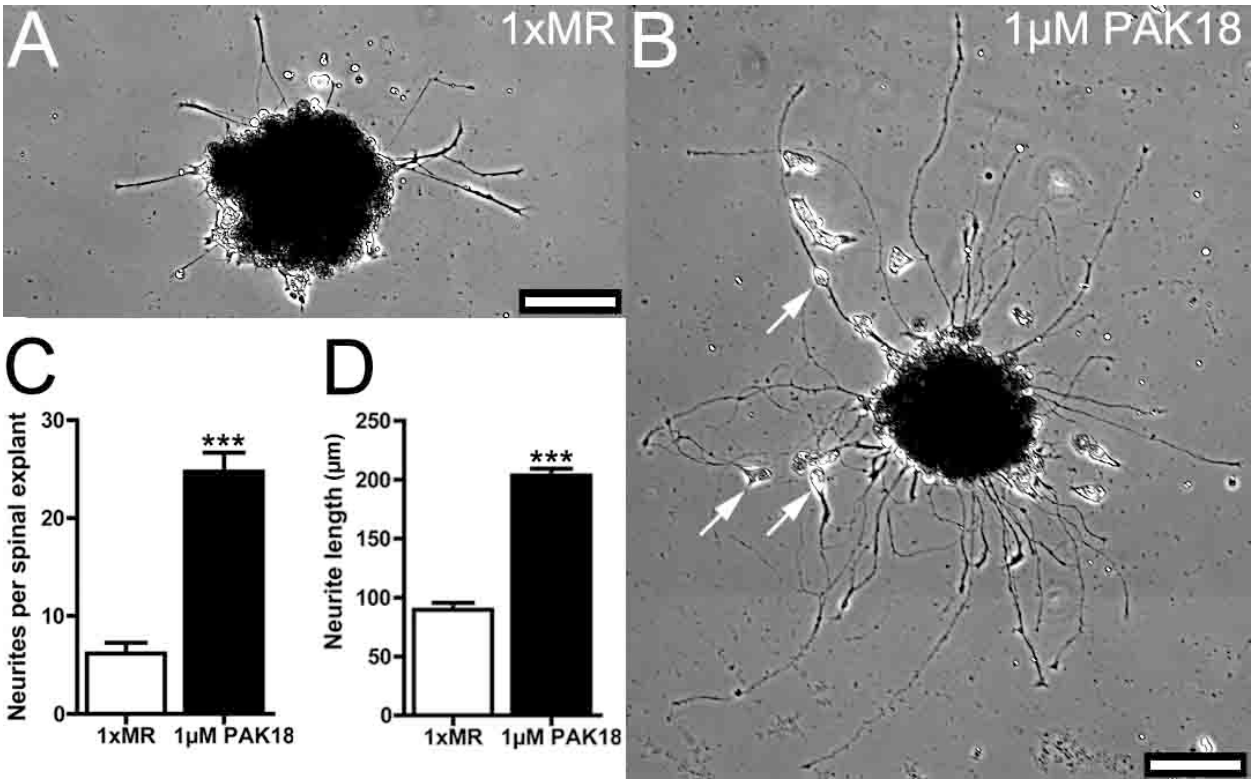

Supplementary Materials, Figure S4. Acute inhibition of PAK with PAK18 decreases P-XAC without affecting total protein content. **A-D.** Representative growth cones treated for 5 min. with control media or increasing concentrations of PAK18 and immunolabeled for p-XAC (Ser3). **A'-D'.** Growth cone total protein was labeled with Alexa Fluor 647 Carboxylic acid, succinimidyl ester. **A"-D".** Merged images of p-XAC (green) and total protein (blue). **A"'-D"'.** Ratio of p-XAC and total protein. **E.** Fluorescence intensity measurements of p-XAC labeling of growth cones treated with increasing concentrations of PAK18 and normalized to control. **F.** Fluorescence intensity measurements of total protein labeling of growth cones treated with increasing concentrations of PAK18 and normalized to control. **G.** Fluorescence ratio measurements of p-XAC/total protein fluorescence intensity measurements. *P < 0.05, ***P < 0.001, Kruskal-Wallis test with Dunn's post-hoc analysis, N ≥ 35 growth cones. Scale: 10μm.

Supplementary Materials, Figure S4.

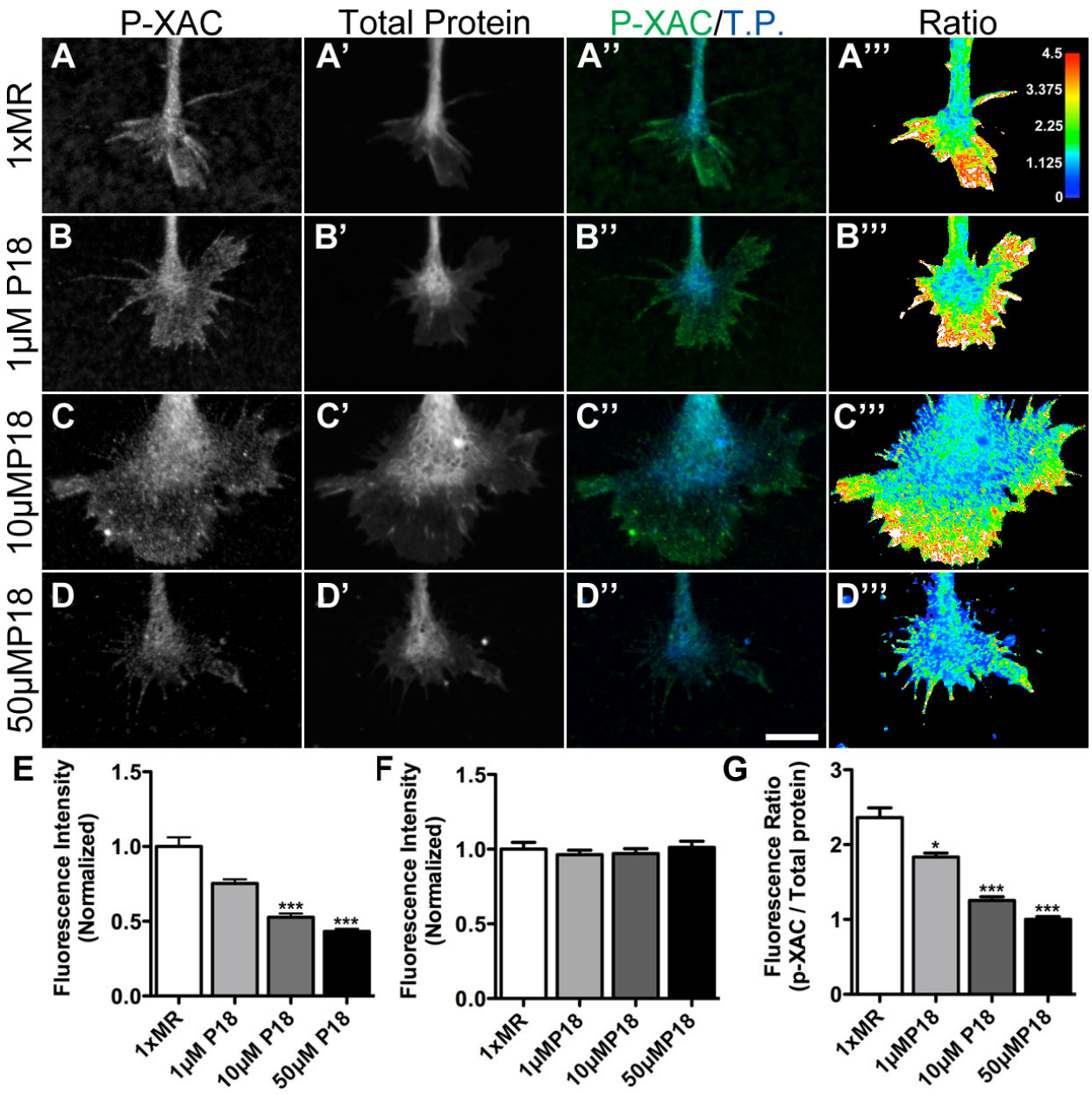

Supplementary Materials, Figure S5. Acute inhibition of PAK with PAK18 decreases P-MLC without affecting total protein content. **A-D.** Representative growth cones treated for 5 min. with control media or increasing concentrations of PAK18 and immunolabeled for p-MLCII (Ser19). **A'-D'.** Growth cone total protein was labeled with Alexa Fluor 647 Carboxylic acid, succinimidyl ester. **A"-D".** Merged images of p-MLCII (green) and total protein (blue). **A"'-D"'.** Ratio of p-MLCII and total protein. **E.** Fluorescence intensity measurements of p-MLC labeling of growth cones treated with increasing concentrations of PAK18 and normalized to control. **F.** Fluorescence intensity measurements of total protein labeling of growth cones treated with increasing concentrations of PAK18 and normalized to control. **G.** Fluorescence ratio measurements of p-MLCII/total protein fluorescence intensity measurements. ***P < 0.001, Kruskal-Wallis test with Dunn's post-hoc analysis, N ≥ 49 growth cones. Scale: 10μm.

Supplementary Materials, Figure S5.

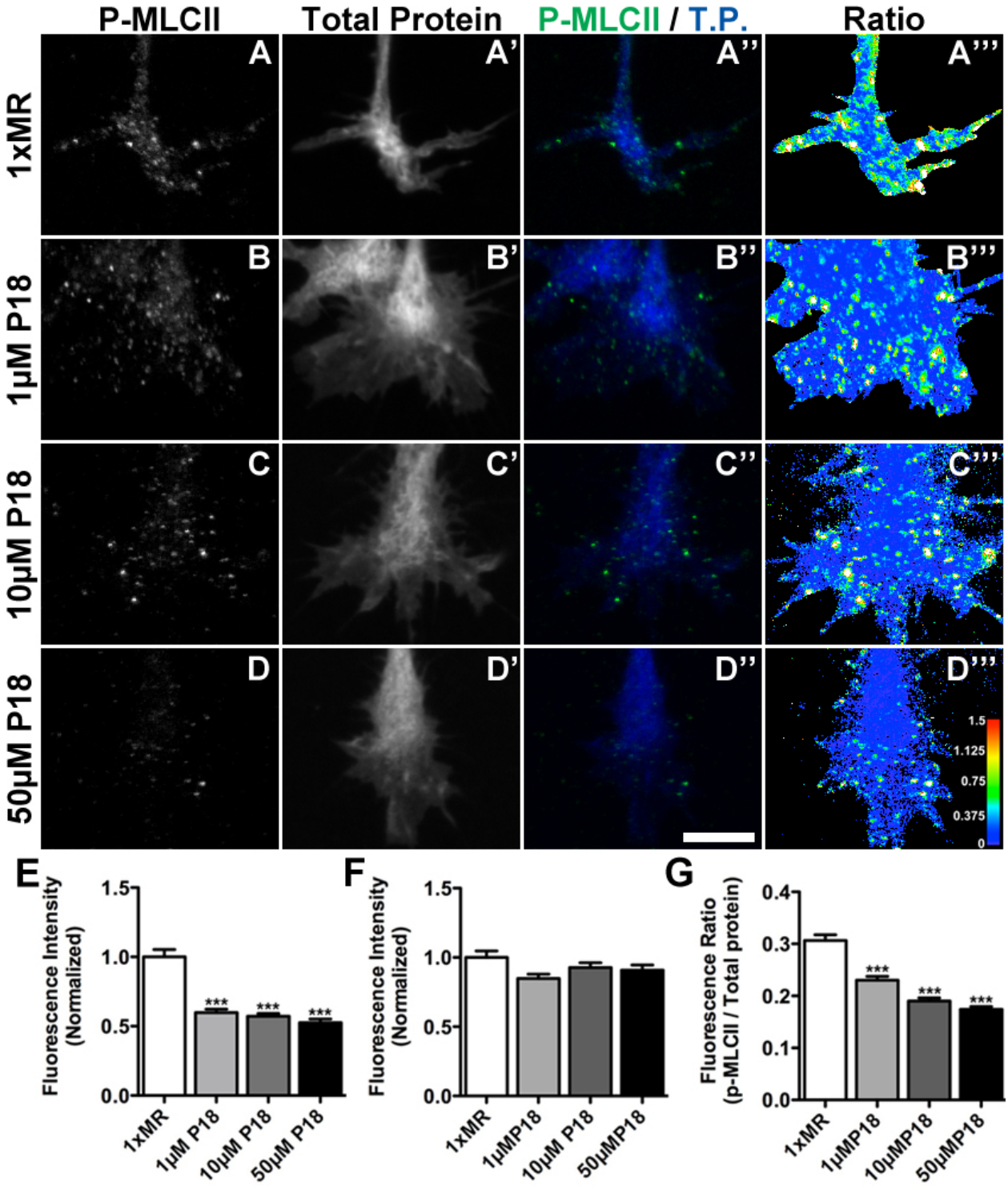

Supplementary Materials, Figure S6. PAK18 may activate Rac1 by disrupting PAK-PIX binding. **A.** Schematic diagram illustrating how Rac1 and PAK compete for PIX binding and how PAK18 induced disruption of PAK from PIX may lead to Rac1 activation. Activated Rac1 may then stimulate cytoskeletal polymerization, possibly through PAK or other downstream effectors, to promote neurite outgrowth. **B.** Rate of neurite outgrowth of wild-type and GFP-DN-Rac1 expressing neurons measured 15 min before and after stimulation with 1 μM PAK18. ***P < 0.001, **P < 0.01, Kruskal-Wallis test with Dunn's post-hoc analysis, N = 17 growth cones. **C-D.** Representative growth cones treated for 2 min with control media or 1μM PAK18 and immunolabeled for active Rac1 (Rac1-GTP). **C'-D'.** F-actin labeling with Alexa546-phalloidin. **C"-D".** Merged images of Rac1-GTP (green) and F-actin labeling (red). **E.** Fluorescence intensity measurements of Rac1-GTP labeling of growth cones treated with PAK18 and normalized to control. **F-G,I.** Representative growth cones expressing GFP-DN-Rac1 (F,I) and a wild-type growth cone (G) treated for 2 min with control media (F,G) or 1μM PAK18 (I) and immunolabeled for active Rac1 (Rac1-GTP). **F'-G', I'.** DN-Rac1 GFP labeling. **F"-G",I".** Merged images of Rac1-GTP (red) and GFP-DN-Rac1 (green). **H-J.** Fluorescence ratio measurements of Rac-GTP / total protein fluorescence intensity measurements of GFP-DN-Rac1 expressing growth cones treated with control media (H) or 1μM PAK18 (J) and normalized to control. *P < 0.05, Student's t-test, N ≥ 9 growth cones for each condition. Scale: 5μm.

Supplementary Materials, Figure S6.

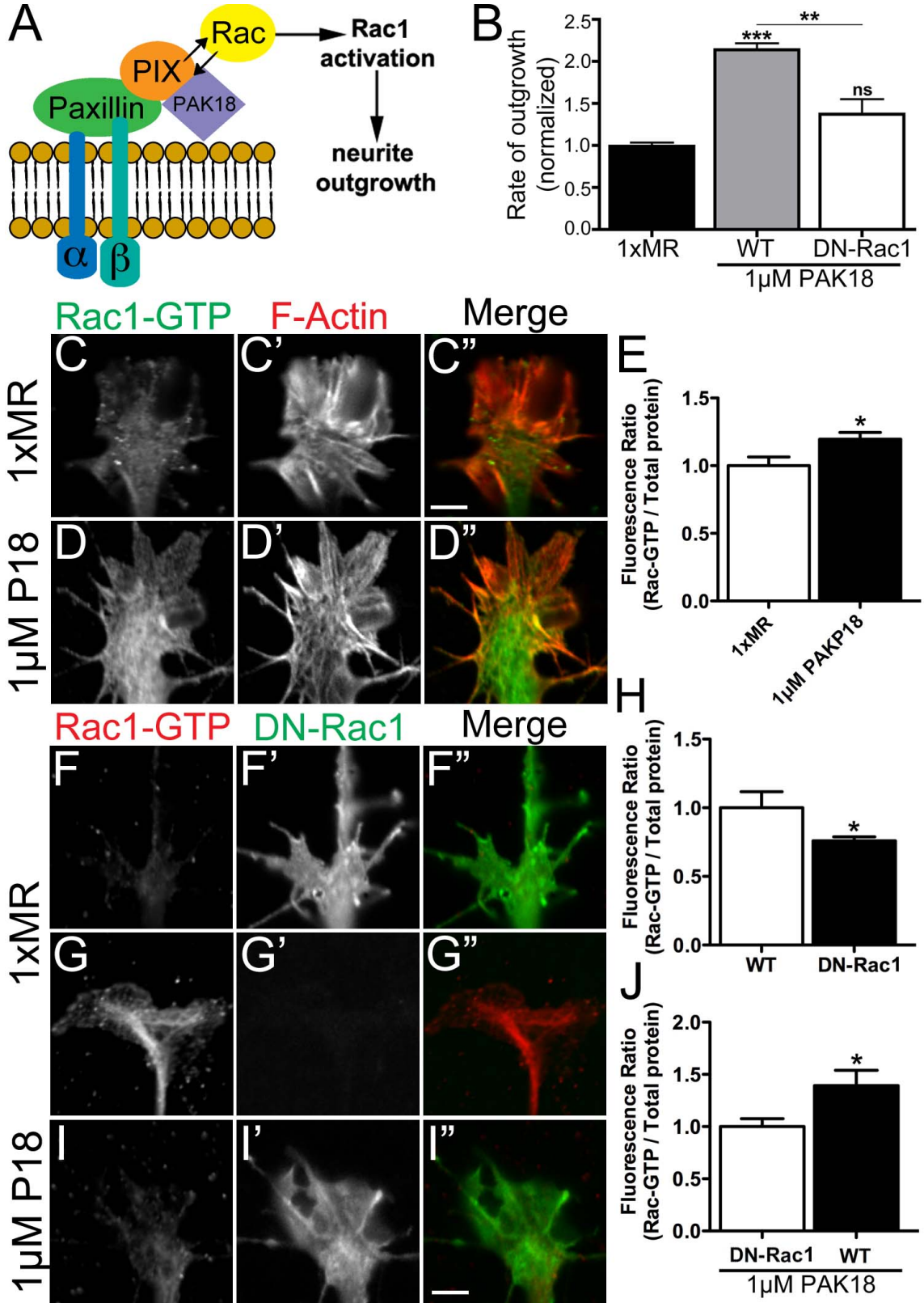

Supplementary Materials, Figure S7. Model illustrating how PAK-PIX interactions may regulate actin dynamics in growth cones to control neurite outgrowth. A. Within growth cone PCs, PAK is bound to PIX, which indirectly associates PAK to paxillin. At point contacts, PAK may regulate the actin modulators myosin-II and ADF/ cofilin, which control retrograde flow and actin depolymerization, respectively. PAK can also regulate point contact dynamics by directly phosphorylating paxillin. In turn, these PAK effectors can lead to changes in point contact turnover and actin polymerization, which regulates the extension of developing neurites. **B.** PAK18 dissociates PAK binding to PIX, which inhibits PAK function. **C.** PAK18 induced inhibition of PAK reduces myosin-II activity, which slows retrograde flow, and increases ADF/cofilin activity, which promotes actin filament severing. Furthermore, at high concentrations of PAK18, further PAK dissociation from adhesions leads to complete PAK inhibition and increased point contact stability. **D.** When PAK binding to PIX is disrupted with PAK18, Rac1 may bind and become activated by PIX. **E.** Graphical representation of the cycling between active and inactive PAK at point contacts and dose-dependent effects of PAK18. Partial displacement of PAK from point contacts at 1 μM PAK18 may promote neurite outgrowth by redistributing PAK throughout the growth cone. However, at high concentrations of PAK18, PAK phosphorylation of paxillin at ser273 is strongly reduced, leading to less adhesion turnover. **F.** Graphical representation of the biphasic, dose-dependent effects of PAK18 on PAK targets and neurite outgrowth. At low concentrations of PAK18, optimal cofilin and myosin activities promote neurite outgrowth. At high concentrations of PAK18, growth cone stalling or retraction result from decreased actin treadmilling and increased actin severing.

Supplementary Materials, Figure S7.

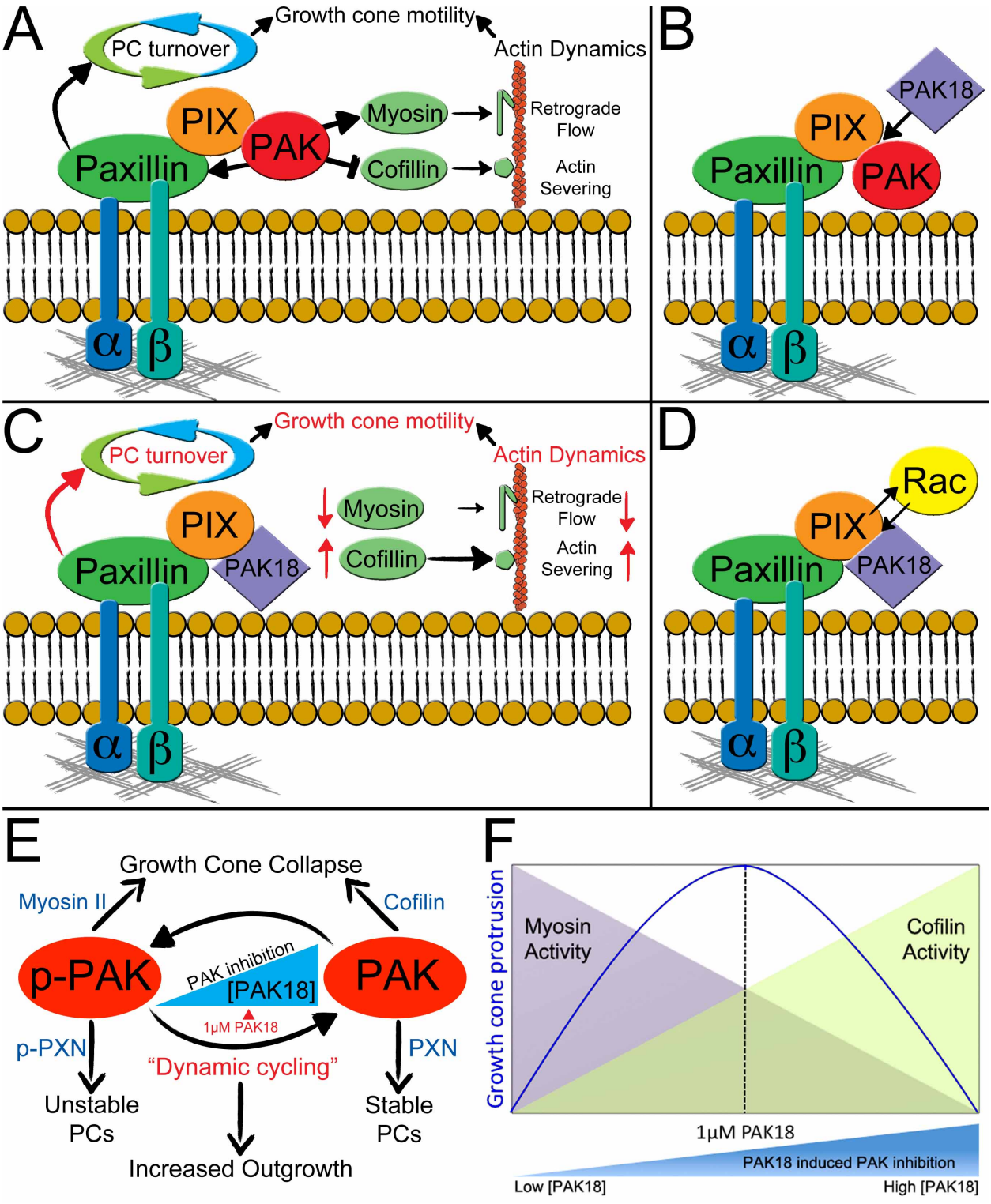

CHAPTER 3

Growth cones form invadosome-like structures in vitro and in vivo

This chapter is in preparation to be published as the following journal article:

Santiago-Medina M., Gregus K. A., Nichol R.H. and Gomez T. M. (2014). Growth cones form invadosome-like structures in vitro and in vivo. In Preparation.

Abstract

During neural development, growth cones at the tips of axons and dendrites sense guidance cues to correctly navigate to their synaptic targets. Extracellular cues guide growth cones by eliciting cytoskeletal changes that regulate the force-generating machinery responsible for membrane dynamics, leading edge protrusion and cell adhesion. While the distribution and function of F-actin at the growth cone periphery is widely studied, the function of F-actin in other regions of the growth cone remains poorly understood. Here, we show that prominent F-actin foci form within the central domain of growth cones and resemble structures analogous to the invadosomes of invasive cells. These actin rich structures appear in a variety of growth cones cultured on a variety of substrata, as well as in the intact spinal cord and skin of the developing embryo. Actin rich foci form as stable structures but exhibit characteristics of a structure with dynamic actin polymerization and contain several known proteins implicated in actin polymerization. Additionally, actin foci colocalize with several markers common to invadosomes, such as cortactin, Src, Tks5 and matrix proteases. When viewed with 3D super resolution microscopy, F-actin foci appear as membrane protrusions perpendicular to the axis of growth in growth cones in vitro and in vivo. In conclusion, our findings identify a previously uncharacterized F-actin rich structure within growth cones that shares a striking resemblance to the invadosomes of cancer cells that may regulate growth cone motility and guidance in the developing nervous system.

Introduction

During development, neuronal growth cones guide neurite extensions to their proper synaptic partners by functioning as highly specialized molecular sensors. Receptors on the surface of growth cones detect the molecular constitution of the surrounding extracellular matrix (ECM) and subtle chemical gradients of secreted proteins present in the environment (Kolodkin and Tessier-Lavigne, 2011). Receptor engagement promotes both physical adhesion and triggers intracellular signaling cascades that affect the behavior of the motile growth cone (Lowery and Van Vactor, 2009). Integrated cell signals converge onto the actomyosin and microtubule cytoskeletons, which power the force-generating machinery responsible for growth cone motility and axon guidance (Dent et al., 2011).

The growth cone contains many structural projections that rearrange in response to local signals generated by guidance cues. Growth cones are further compartmentalized in specialized regions where the cytoskeleton is differentially organized. Within the peripheral (P) domain, actin filaments are organized into bundles and a dense meshwork array that generate the protrusive filopodia and lamellipodia that are occasionally visited by dynamic MTs. Towards the rear of the growth cone is the central (C) domain where stable, bundled MTs splay from the axon shaft. Many organelles and vesicles traffic along MTs within the C-domain. Lastly, the transition zone exists at the interface between the P- and C-domains, and is a region of strong actomyosin contraction and F-actin depolymerization.

In two-dimensional environments, as is typical of most tissue cultures studies, growth cones use filopodial protrusions to help direct neurite extension upon flat

substrata. However, growth cones in vivo must penetrate and transverse through three dimensional (3D) tissues and detect guidance cues that are secreted from sources deep within the developing embryo. To direct neurite extension through 3D environments, growth cones may form protrusions on their apical and basal surface reminiscent of podosomes or invadopodia of normal non-neuronal and metastatic cancer cells, respectively (Linder et al., 2011; Murphy and Courtneidge, 2011). Podosomes and invadopodia, collectively referred to as invadosomes, are filopodia-like protrusions from the ventral surface of migratory cells associated with ECM adhesion, remodeling and degradation. While growth cones have been shown to secrete metalloproteases, which is necessary for proper axon guidance (McFarlane, 2003; Yong et al., 2001), they have not been shown to form invadosomes.

In this study, we show that growth cones form stable, F-actin rich puncta reminiscent of invadosomes of monocytic, invasive and neural crest cells (Murphy and Courtneidge, 2011; Murphy et al., 2011). F-actin foci form primarily within the C-domain of growth cones and colocalize with numerous markers of invadosomes such as cortactin, active Src and Tks5 (Tyr kinase substrate with five SH3 domains). Growth cones of varied neuronal types across species form invadosomes on all substrata tested, as well as in the intact spinal cord, suggesting that they are a fundamental sub-cellular specialization of developing neurons. Growth cone invadosomes are more stable than point contact adhesions, yet colocalize with several actin polymerization and bundling proteins. Consistently, growth cone invadosomes are sites of rapid F-actin turnover with concentrated free F-actin barbed ends, as well as monomeric actin. Super resolution 3D microscopy shows that the F-actin within invadosomes is oriented

as a vertical column that spans the C-domain in the z-plane and can extend as a 3D-protrusion from the ventral surface of growth cones. Moreover, in 3D collagen gels and in vivo, similar projections occur from the dorsal surfaces of growth cones. Lastly, using fluorescent gelatin, we show that growth cone invadosomes target proteolytic activity. Taken together, we have identified a novel structural component of growth cones analogous to the invadosomes of monocytic cells and invasive cancer cells, which may be crucial in guiding axons throughout tissues of the developing nervous system.

Materials and methods

RT-PCR and Primers. The Tks5 and MMP2, 9 and 14 primers were designed by inserting the corresponding Xenopus laevis genomic sequences, obtained from Xenbase (Bowes et al., 2010) into Primer3 (Rozen and Skaletsky, 2000). The designed primers were synthesized at the Biotechnology Center of the University of Wisconsin - Madison. Tks5 and MMP transcripts were amplified from reverse transcribed RNA isolated from stage 24–26 embryo spinal cords. Messenger RNA was isolated from 15-20 spinal cords with TRIzol (Invitrogen) and made into cDNA with the RT-PCR kit RETROscript (Invitrogen) using random decamers as primers.

Plasmid Constructs. Some expression constructs were subcloned into the Xenopus-preferred pCS2+ vector for mRNA synthesis (Dave Turner, University of Michigan, Ann Arbor, MI). Gateway technology (Invitrogen, Carlsbad, CA) was used in some cases to generate pCS2+ constructs. The GFP conjugated actin constructs used were of human and rat origin for β-actin and γ-actin respectively. GFP-γ-actin was provided by Andrew Matus (Friedrich Miescher Institute, Basel, Switzerland). The GFP-β-actin and PA-GFP-γ-actin constructs were provided by James Zheng (Emory University, Atlanta, GA). Both the F-actin reporter, Utrophin-CH as well as the wild-type Xenopus cortactin construct were provided by William Bement (University of Wisconsin - Madison). The endosomal constructs mCherry-Rab5A and DsRed-Clathrin light chain were provided by Jon Audhya (University of Wisconsin - Madison). cDNA for chicken paxillin–GFP was provided by A. F. Horwitz (University of Virginia, Charlottesville, VA). The α-actinin-1 construct of human origin was provided by Carol Otey (University of North Carolina,

Chapel Hill, NC). Human Tks5 tagged with GFP was provided by Sara Courtneidge (Sanford-Burnham Medical Research Institute, La Jolla, CA).

Embryo injection and cell culture. Xenopus laevis embryos were obtained and staged as described previously (Gomez et al., 2003). For direct expression experiments using constructs, two dorsal blastomeres of eight-cell-stage embryos were injected with 0.25–0.5 ng of in vitro-transcribed, capped mRNA (mMessage Machine, Ambion, Austin, TX) or 60-70 pg of DNA. Neural tubes were dissected from 1-d-old embryos and explant cultures containing a heterogeneous population of spinal neurons were prepared as previously described (Gomez et al., 2003). For 2D cultures, explants were plated onto acid-washed coverslips coated with 25 µg/ml LN, 25 µg/ml FN or 50 µg/ml poly-D-lysine (Sigma, St. Louis, MO). For 3D cultures, explants were embedded inside solidified 1.5 mg/ml collagen 1 (BD Biosciences, San Jose, CA) gels flooded with culture media. Cultures were imaged or fixed 18–22 h after plating. All methods were approved by the University of Wisconsin School of Medicine Animal Care and Use Committee.

Human neurons derived from iPSCs. Human neurons were differentiated from induced pluripotent stem cells using methods described previously: forebrain (Liu et al., 2013), motor (Hu and Zhang, 2009) and RGC (Gamm et al., 2008; Pankratz et al., 2007). Neurospheres were plated onto glass coverslips coated with PDL and LN (25 µg/ml) and cultured in neural basal media with B27 supplements (Gibco).

Fluorescent-gelatin degradation assay. Fluorescent-gelatin coated coverslips were prepared as previously described (Artym et al., 2009). Briefly, acid washed coverslips were coated with 50 μg/ml poly-D-lysine, washed with PBS, fixed with 0.5% glutaraldehyde and washed with PBS once again. The coverslips were inverted onto a 100 μL drop of Oregon Green 488 gelatin (Invitrogen) for 10 min at RT. After washing with PBS, the residual reactive groups in the gelatin matrix were quenched with sodium borohydride at 5 mg/mL for 15 minutes followed by washing with PBS. Once washed, gelatin coated coverslips were overlaid with Laminin or Fibronectin for 1 hr. Coverslips coated with DQ-collagen IV (Invitrogen) were prepared as previously described (Sloane et al., 2006). Briefly, acid washed coverslips were coated with 100 μL containing 25 μg/ml LN, FN and DQ-collagen IV and incubated for 15min at 37 °C to solidify. Cultures were fixed 18–22 h after plating and imaged with a confocal microscope.

Reagents. PP2 and MβCD were obtained from Calbiochem (La Jolla, CA) and Sigma respectively. To visualize actin retrograde flow, neuronal cultures were loaded with 3 nM kabarimide C conjugated to TMR (TMR-KabC; kind gift from Gerard Marriott, University of California, Berkeley). Antibodies used are as follows: β1-integrin (8C8; Developmental Studies Hybridoma Bank), function-blocking β1-integrin (AB2999; kind gift from Kenneth Yamada, NIH, Bethesda, MD), pY118-Paxillin (Invitrogen), pY397-FAK (Invitrogen), SV2 (Developmental Studies Hybridoma Bank), Cortactin (4F11; Millipore), pY418-Src (Invitrogen), Tks5 (M-300; Santa Cruz Biotechnology), βI,II-Tubulin and acetylated-Tubulin (6-11B-1; Sigma), MMP14 (Millipore), HNK-1 (NCAM; Sigma). The antibodies: Arp3, N-WASP and Mena were kind gifts from Erik Dent (University of

Wisconsin - Madison). For monomeric G-actin staining, deoxyribonuclease I (Alexa Fluor 488 DNase I; Invitrogen) was used.

Immunoblotting and immunocytochemistry. Immunoblotting for cortactin, Tks5 and MMP14 was performed by extracting total proteins from stage 24-26 embryo spinal cords. Five spinal cords were processed for each lane and ran on a Novex NuPAGE SDS-PAGE gel (Invitrogen). Cortactin primary antibody was used at 1:1000, Tks5 at 1:500 and MMP14 at 1:1000. Horseradish peroxidase (HRP)-conjugated secondary antibodies (Jackson Immuno) were used at 1:5000 and the blots were visualized by enhanced chemiluminescence (Thermo Scientific Pierce ECL).

For immunocytochemistry (ICC), 2D spinal neuron cultures were fixed in 4% paraformaldehyde in Krebs + sucrose fixative (4% PKS) (Dent and Meiri, 1992), permeabilized with 0.1% Triton X-100, and blocked in 1.0% fish gelatin in CMF-PBS for 1 hr at room temperature. Three-dimensional cultures were fixed for 1 hr in 4% PKS, and blocked in CMF-PBS containing 0.5% fish gelatin and 0.2% Triton X-100 overnight at 4 °C. Primary antibodies were used at the following dilutions in blocking solution: 1:250 β-Integrin (8C8), 1:500 β-Integrin (AB2999), 1:500 pY118-Paxillin, 1:500 pY397-FAK, 1:100 SV2, 1:500 Cortactin, 1:250 Arp3, 1:250 N-WASP, 1:500 Mena, 1:500 pY418-Src, 1:250 Tks5, 1:500 βI,II-Tubulin, 1:1000 acetylated-Tubulin, 1:500 HNK-1 and 1:500 MMP14. Alexa-Fluor-conjugated secondary antibodies were purchased from Invitrogen and used at 1:250 in blocking solution. Included with secondary antibodies was Alexa-546 phalloidin (1:100; Invitrogen) to label filamentous actin (F-actin) and Alexa-647 carboxylic acid, succinimidyl ester (1:1000; Invitrogen) to label total protein.

Gelatin Zymography. Gelatin zymography was performed using stage 24–26 Xenopus embryo spinal cords. Lysates were ran on a Novex Zymogram Gelatin Gel and processed according to the manufactures instructions (Invitrogen).

Whole Mount embryo dissection and imaging. Two different approaches were used to label and image neurons in vivo. For the in vivo imaging of commissural interneurons, embryos were processed as described previously (Moon and Gomez, 2005). Briefly, stage 23 and 25 embryos expressing mCh-UtrCH were fixed overnight at 4 °C, rinsed, then removed of skin and somites to expose the spinal cord. Embryos were permeabilized with CMF-PBS containing 0.5% fish gelatin and 0.2% Triton X-100 and incubated in Alexa-Fluor phalloidin (Invitrogen). For the in vivo imaging of peripheral Rohon-Beard (RB) neuron growth cones, embryos were processed as described previously (Huang et al., 2007). Briefly stage 25 embryos were fixed overnight at 4 °C, rinsed, then dehydrated in 100% methanol. Rehydrated embryos were permeabilized with CMF-PBS containing 0.5% fish gelatin and 0.2% Triton X-100 and immunolabeled for NCAM and Cttn overnight 4 °C. After immunolabeling, embryos were dehydrated in 100% methanol once more and viewed in Murray's clearing solution (2:1, Benzyl Benzoate:Benzyl alcohol). In both approaches, whole-mount embryos were pinned onto Sylgard-bottom dishes (Corning) with fine dissection pins for imaging.

Confocal and TIRF image acquisition and analysis. For both live and fixed fluorescence microscopy, high-magnification images were acquired using either a 60x/

1.45 NA objective lens on an Olympus Fluoview 500 laser-scanning confocal system mounted on an AX-70 upright microscope or a 100x/1.5 NA objective lens on a Nikon total internal reflection fluorescence (TIRF) microscope. On the confocal, samples were imaged at 2–2.5x zoom (pixel size = 165–200 nm). Images were captured at 10-20 s intervals. For bright field time-lapse microscopy, low-magnification phase-contrast images were acquired using a 20X objective on a Nikon microscope equipped with an x–y motorized stage for multi-positional imaging. Multi-positional images were capture at 1 m intervals. Live explant cultures were sealed within perfusion chambers as described previously (Gomez et al., 2003) to allow rapid exchange of solutions. Images were analyzed using ImageJ software (W. Rasband, National Institutes of Health, Bethesda, MD). Point contacts were identified as discrete areas containing paxillin–GFP that were at least two times brighter than the surrounding background and remained fixed in place for a minimum of 30 s (Woo and Gomez, 2006). Measurements of actin foci quantity were made by counting the amount of circular actin rich accumulations within the central and transition domains of F-actin-labeled growth cones using ImageJ. Measurements of actin foci area were done with ImageJ by thresholding actin foci within F-actin-labeled images without including other structures of the growth cone. For display purposes, some images were pseudo-colored using ImageJ look up tables.

Structured illumination microscopy image acquisition. High-resolution structured illumination (SIM) Z-stacks were captured using either a DeltaVision OMX microscope (Applied Precision) or an ELYRA PS.1 microscope (Carl Zeiss Microscopy). The

DeltaVision OMX V4 3D SIM platform with Blaze technology was used with a 60x/1.42 Plan-Apo N objective (Olympus), excitation wavelengths of 488, 561 and 635 nm and 3 sCMOS cameras. Images were acquired using DeltaVision software and deconvolved using softWoRx image processing software (Applied Precision). The ELYRA was used with either a 63x/1.4 Plan-Apochromat or 100x/1.46 α-Plan-Apochromat objective and excitation wavelengths of 488 and 561 nm. For each 200 nm step in the Z-axis, five rotations of the structured illumination grid were carried out per channel. An iXon 885 EMCCD camera (Andor) was used for acquisition, bearing 8 x 8 μm pixels and a 1004 x 1002 chip resolution. Resulting stacks were processed using default reconstruction parameters in ZEN 2011 software, followed by channel alignment based on measured affine transformation characteristics of the given objective.

Results

F-actin foci are prominent sub-cellular structures within the central domain of growth cones in culture and in the intact spinal cord

Imaging F-actin in fixed growth cones by high resolution total internal reflection fluorescence (TIRF) or confocal microscopy, we observe pronounced F-actin rich foci within the C-domain, which is predominantly devoid of F-actin (Fig. 1). To begin to understand the role actin foci may have in growth cone motility, we first set out to determine whether foci formation depends on the tissue culture substratum. To accomplish this, we cultured neurons isolated from embryonic Xenopus spinal cord on a variety of ECM proteins, cell adhesion molecules and non-biological substrata. We find that foci form within the C-domain of growth cones cultured on all substrata tested (Fig. 1A), including bare glass, suggesting that these specializations can arise independent of the ECM we provide. To determine whether F-actin foci form in growth cones of diverse neuronal types and across species, we cultured a variety of primary neuronal types, as well as human neurons derived from induced pluripotent stem cells (iPSCs). Fluorescent phalloidin labeling shows that F-actin foci form in growth cones of Xenopus retinal ganglion cells (RGCs; Fig. 1B) and human growth cones (forebrain neurons, motor neurons and RGCs) differentiated from iPSCs (supplementary material Fig. S1A-C). The average number of F-actin foci across all Xenopus spinal neuron growth cones is 3.77 ± 0.65, although growth cones with as many as 13 foci were observed (Fig. 1C). The average size of an individual foci is 0.37 ± 0.01 μm^2, although foci as large as 1.3 μm^2 were recorded in growth cones (Fig. 1D).

While labeling of fixed neurons shows endogenous F-actin distribution, it does not provide any information on foci dynamics. To visualize F-actin in live growth cones we labeled neurons with either the F-actin binding probe Utrophin-CH (calponin homology domain) conjugated to mCherry (mCh-UtrCH) or GFP-β-actin. High resolution live cell imaging shows that both mCh-UtrCH and GFP-β-actin concentrate in F-actin bundles at the growth cone leading edge as expected, but also in prominent actin foci within the C-domain of growth cones (Fig. 1E and supplementary material Fig. S2A). It is noteworthy that GFP-γ-actin also targets to actin foci when expressed in growth cones (supplementary material Fig. S2B). Time-lapse imaging shows that actin foci are relatively long-lived, with an average lifetime of 7.76 ± 0.32 min (Fig. 1E), which is notably longer than PC adhesions (Santiago-Medina et al., 2013). In extreme cases, actin foci were observed to form at the leading edge and remained stable until they disassembled at the rear of the growth cone (supplementary material Fig. S2C). While the majority of foci are stable, a small subset were motile, resembling actin comets (supplementary material Fig. S2D).

While growth cones observed in vitro appear similar to those seen in vivo by many criteria, it is possible that the F-actin foci we observe in vitro are simply a tissue culture artifact. Therefore, to determine if F-actin foci also form within growth cones in vivo, we labeled F-actin with mCh-UtrCH in fixed, whole mount spinal cord preparations. Using confocal microscopy, we viewed commissural interneuron (CI) growth cones positioned within the lateral spinal cord (Fig. 1F) and within the ventral midline (Fig. 1G). We find that F-actin foci form within the C-domain of CI growth cones observed at all positions along their trajectory toward the midline within the spinal cord. Taken together,

we conclude that growth cones of distinct neuronal populations and across species assemble F-actin rich foci independent of their cell substratum and environment.

F-actin foci target to the ventral surface of growth cones and colocalize with growth cone point contact proteins

Stable F-actin foci are clearly detectable by TIRF microscopy, suggesting they are near the ventral surface of growth cones and may function as adhesive points to the underlying substrata. To confirm the ventral membrane targeting of foci, we visualized growth cones expressing mCh-UtrCH by dual fluorescence and interference reflection microscopy (IRM). With IRM, areas of the cell in close association to the substratum appear as dark regions. Using IRM, we find that F-actin foci colocalize with regions of close contact between the membrane and substratum, suggesting they may be adhesion sites (supplementary material Fig. S3A,B).

Growth cones are known to form transient PC adhesions predominantly at the leading edge and within filopodia (Robles and Gomez, 2006), but not typically within the C-domain where foci form and remain stable (Fig. 1). Therefore, we hypothesize that foci are not classical PC adhesions, but still may recruit proteins implicated in integrin-dependent adhesion. To begin to test whether F-actin foci function as adhesion sites, we immunolabeled growth cones cultured on LN using two different antibodies against β1 integrin. By fluorescence confocal microscopy, we find that β1-integrin receptors target with F-actin foci, as well as to PC adhesions (Fig. 2A and supplementary material Fig. S3C,D) and filopodia tips (Fig. 2A). Since F-actin foci contain integrin receptors, we tested whether other adhesion proteins associate with these structures. Paxillin (PXN)

and focal adhesion kinase (FAK) both serve essential roles in PC assembly and turnover (Myers and Gomez, 2011; Woo and Gomez, 2006), so we examined their colocalization with F-actin foci in fixed growth cones. Immunolabeling for active pY118-PXN or pY397-FAK, and F-actin shows a subset of these adhesion proteins colocalized with F-actin foci within the C-domain (Fig. 2B-D). Live cell imaging of mCh-UtrCH with PXN-GFP was particularly informative, as it showed PXN colocalizing transiently with F-actin foci over time (Fig. 2E-H), as well as a subset of foci emerging from preexisting PXN PCs (Fig. 2H). This finding suggests that a subset of PXN-containing PC adhesions may mature into longer-lived F-actin foci that persist within the C-domain as growth cones migrate forward. Taken together, these results suggest that F-actin foci may function as novel adhesion sites, since they form in close proximity to the substratum, remain stable and colocalize with integrin receptors and adhesion proteins.

F-actin foci targeting does not overlap with vesicles

A small population of F-actin foci appeared mobile, suggesting that foci may associate with exocytic or endocytic vesicles. To assess if F-actin foci localize with markers of synaptic exocytic vesicles, we immunolabeled growth cones for the synaptic vesicle protein, SV2, which labels all synaptic vesicles. As expected, we saw no association between SV2 labeling and F-actin foci (supplementary material Fig. S4A). As we lack effective antibodies against endocytic proteins, we expressed two well known reporters of endosomes, mCherry-Rab5A and DsRed-Clathrin light chain, together with the F-actin reporter, GFP-UtrCH. As with SV2, F-actin foci did not associate with either endosomal marker (supplementary material Fig. S4B-E). Taken

together, this data suggest that the F-actin foci observed in growth cones are not docked or mobile exocytic or endocytic vesicles.

F-actin foci are sites of rapid actin turnover

By live cell imaging, F-actin foci appear as stable aggregates of F-actin, yet the dynamics of actin polymerization at foci are unclear. Moreover, some F-actin foci resemble actin comets, suggesting that rapid actin polymerization may occur at these structures. Because the process of actin polymerization requires the addition of monomeric actin (G-actin) to the barbed ends of actin filaments, we first tested whether actin monomers concentrate at foci. Similar to other sites of rapid actin polymerization in growth cones (Lee et al., 2013; Marsick et al., 2010), we find monomeric G-actin colocalizes with F-actin labeled foci (Fig. 3A). Next, to resolve whether foci contain uncapped barbed actin filaments, which G-actin adds to during actin polymerization, we used the F-actin barbed-end binding probe, tetramethylrhodamine-conjugated kabiramide-C (TMR-KabC; (Petchprayoon et al., 2005; Tanaka et al., 2003). TMR-KabC is a small, cell permeable molecule that binds to the barbed end of actin filaments with high affinity and has been used previously to track the rearward flow of actin filaments (Keren et al., 2008; Santiago-Medina et al., 2013; Santiago-Medina et al., 2011). Consistent with the notion of actin polymerization at F-actin foci, TMR-KabC rapidly labels foci in live growth cones (Fig. 3B). Note that KabC strongly labels F-actin filaments undergoing retrograde flow at the leading edge, which is distinct from the static labeling of actin at foci (Fig. 3C), suggesting that foci are disconnected from the contractile network of F-actin within the P-domain. Next, to directly measure the rate of

actin polymerization within foci, we bleached or photoactivated fluorescent protein-conjugated actin in live growth cones. Either GFP-β-actin or photoactivatable-GFP-(PA-GFP)-γ-actin together with mCh-UtrCH were bleached or photocativated within foci and the recovery rate or decay was measured, respectively (Fig. 3D-G). In FRAP experiments, the turnover rate of GFP-β-actin at foci was faster compared to regions immediately adjacent to foci (6.56 ± 0.01 s vs 8.53 ± 0.02 s; Fig. 3D,E), but slower than the recovery of actin within the growth cone veil (5.55 ± 0.02 s). The very fast turnover at the growth cone leading edge is likely due to the additive effects of fast actin polymerization and retrograde flow. Similar results were obtained using photoactivatable-GFP at foci (7.11 ± 0.01 s; Fig. 3F,G). Taken together, these data demonstrate that F-actin is highly dynamic within stable F-actin foci.

F-actin foci colocalize with the classic invadosome markers Cortactin, Src and Tks5

In comparison with the F-actin distribution of other cell types, the F-actin foci of growth cones exhibit a striking similarity to the invadosomes formed by monocytic and invasive cells. Invadosomes are long lived, actin based protrusions located on the ventral surface of cells that appear as prominent punctate accumulations of F-actin in vitro (Linder et al., 2011; Murphy and Courtneidge, 2011). Invadosomes regulate cell migration by both adhering to and remodeling the underlying ECM. As sites of cell adhesion, integrin receptors, PXN and FAK are necessary for invadosome function (Chan et al., 2009). Importantly, invadosomes serve as filopodia-like protrusions of invasive cells, but extend from the basal cell surface of cells, perpendicular to the axis

of growth. As growth cone F-actin foci appear similar to invadosomes, we began to explore the hypothesis that foci are invadosome-like protrusions on neuronal growth cones. To begin to test this hypothesis, we immunolabeled growth cones for several key invadosomal markers. Cortactin (Cttn) is a key modulator of F-actin polymerization that is necessary for invadosome formation in invasive cells (Kirkbride et al., 2011; MacGrath and Koleske, 2012). Immunoblotting cell extracts from isolated spinal cords shows that Cttn is highly expressed in the developing spinal cord (supplementary material Fig. S5A). Interestingly, Cttn exists as both a full length 80 kDa protein and as a 45 kDa fragment, which likely represents a calpain cleavage product (Perrin et al., 2006). By immunocytochemistry (ICC), Cttn is present at the leading edge of growth cones (Fig. 4A and supplementary material Fig. S5B-D), as has been previously reported (Decourt et al., 2009; Kurklinsky et al., 2011). However, we also find robust colocalization of Cttn with F-actin foci in the C-domain of growth cones (Fig. 4A and supplementary material Fig. S5B-D) on all substrata tested (LN, FN, PDL and glass). To confirm this distribution in live cells, we expressed GFP-Cttn together with mCH-UtrCH and find that GFP-Cttn also targets to stable F-actin foci. In addition to Cttn, other actin regulatory proteins that are necessary for invadosome formation target to F-actin foci, including the nucleating proteins Arp2/3 and N-WASP, the cross-linking protein α-actinin and the anti-capping factor, Ena (Murphy and Courtneidge, 2011; Philippar et al., 2008) (Fig. 4B-E). Together these results suggest that F-actin foci in the C-domain of growth cones represent previously undescribed growth cone invadosomes.

One classic marker and specific modulator of invadosome formation is the adaptor protein tyrosine kinase substrate with five SH3 domains (Tks5), which is

phosphorylated by Src tyrosine kinases (Courtneidge, 2012). Phosphorylated Tks5 targets through its N-terminal PX domain to phosphatidylinositol containing lipid rafts (Murphy and Courtneidge, 2011). Activated Tks5 recruits additional proteins involved in invadosome formation, such as the actin polymerizing and stabilizing proteins described above. To begin to understand the roles that both Tks5 and Src play in growth cone invadosomes, we examined the localization of these proteins. By both PCR and immunoblotting of cell lysates isolated from developing Xenopus spinal cord tissues, we find that Tks5, along with the related protein Tks4, are expressed during stages of robust axon outgrowth (Fig. 5A,B). Next, ICC labeling of growth cones for Tks5 and active pY418-Src shows that these proteins also localize to F-actin foci, providing strong evidence that these structures represent growth cone invadosomes (Fig. 5C,D). Finally, to visualize Tks5 dynamics in live growth cones, we expressed human Tks5-GFP along with mCh-UtrCH in spinal neurons. As expected, Tks5 colocalized with F-actin foci (Fig. 5E), but a higher percentage of foci were mobile compared to conditions where only actin probes were expressed. Because Tks5 recruits several actin regulatory proteins, it is possible that Tks5 over expression promotes inappropriate stimulation of actin polymerization leading to mobile F-actin foci.

Both the inhibition of Src and the disruption of lipid rafts decreases invadosome number and stability in growth cones

Active Src regulates invadosome formation in non-neuronal cells downstream of growth factors through phosphorylation of both Tks5 and Cttn (Boateng and Huttenlocher, 2012). As active Src also targets to growth cone invadosomes, we tested

the effects of Src inhibitors on invadosome formation in both fixed and live growth cones. As predicted, inhibition of Src with a pharmacological inhibitor, results in fewer and less stable invadosomes assessed in live and fixed growth cones (Fig. 5F,G). A second key regulator of Tks5 function is recruitment to PIP_2 containing lipid rafts via its PX domain. To test whether intact lipid rafts, to which Tks5 binds, are necessary for growth cone invadosome formation and stability, we treated GFP-β-actin expressing growth cones with methyl-β-cyclodextrin (MβCD). MβCD is a cholesterol sequestering agent previously shown to disrupt lipid rafts in growth cones (Guirland et al., 2004). Acute treatment of growth cones with MβCD leads to a slight acceleration in the rate of neurite outgrowth and decreased growth cone size (Fig. 5H). However, growth cones treated with MβCD failed to form new stable invadosomes despite the increase in neurite extension (Fig. 5I-J). Taken together, these results demonstrate that both the activity of Src kinases, as well as intact lipid microdomains are required for the proper formation and maintenance of growth cone invadosomes. These functional similarities between growth cone and non-neuronal cell invadosomes lends further support to the likelihood that F-actin foci in growth cones are analogous to the invadosomes of invasive cells.

3D super resolution microscopy reveals that growth cone invadosomes protrude from the dorsal and ventral surfaces of growth cones in vitro and in vivo

Invadosomes are typically restricted to the ventral surface below the nucleus of non-neuronal cells in 2D culture, but these sites of F-actin polymerization generate ventral protrusions containing unbranched, bundled F-actin in 3D environments (Linder

et al., 2011). To more accurately resolve the cytoskeletal structure within growth cone invadosomes, we used structured illumination microscopy (SIM), which can achieve a spatial resolution in XY of 130 nm and an axial resolution of 250 nm (Toomre and Bewersdorf, 2010). First, neurons cultured from embryonic Xenopus spinal cord, as well as human forebrain neurons derived from iPSCs, were fixed and labeled for F-actin in 2D culture. Consistent with improved resolution by SIM, we observe F-actin bundles with fine interdigitating cross-linked actin meshwork within the peripheral veil by SIM (Fig. 6A-B). Furthermore, growth cone invadosomes, which normally appear as individual large fluorescent puncta by confocal fluorescence microscopy, often appear as clusters of smaller F-actin puncta in super resolution. Most importantly, when viewed as a 3D rendering (Fig. 6D), F-actin foci appeared as longitudinal columns of F-actin that extend from the dorsal membrane of the growth cone as invadosome-like projections. It is important to note that invadosomal protrusions formed on the dorsal surface of growth cones, possibly due to an inability to project ventrally in culture.

Invadopodia that form on invasive cells contain microtubules (MTs) for structural stability and for the delivery of cargo (Murphy and Courtneidge, 2011). To assess if growth cone invadosomes contain MTs, we immunolabeled for β-tubulin together with F-actin and imaged growth cones using SIM. In super resolution, MTs often appear to avoid or wrap around F-actin foci, which was also apparent in confocal images (supplementary material Fig. S6A-B). This displacement of MTs around F-actin foci is consistent with their distribution as columnar structures spanning the growth cone (Fig. 6D). Moreover, in some instances MTs were found alongside bundled F-actin within dorsal invadosomal protrusions (Fig. 6E-E”, F-F”). It is unclear why some invadosomes

form protrusions and contain MTs, while others remain restricted to the ventral and dorsal surface of growth cones, but likely depends on the 3D environment and the maturation state of the invadosome (Linder et al., 2011; Murphy and Courtneidge, 2011).

As invadosomes are likely stabilized by their 3D environment in vivo, we wanted to visualize the 3D morphology of growth cones with super resolution in collagen gels and in vivo. Xenopus explant cultures in collagen I gels extend profuse axons that spread in 3D as detected by low magnification confocal microscopy (supplementary material Fig. S7) and can be labeled with standard ICC protocols for high resolution imaging. Similar to 2D cultures, growth cones in 3D collagen labeled for F-actin or Cttn exhibit punctate distributions when viewed as flattened 2D images (Fig. 7A). However, when viewed orthogonally and as 3D rendered images, F-actin and Cttn puncta are often clearly found to be 3D protrusions (Fig. 7B). Interestingly, similar to the invadosomes in 2D culture, 3D protrusions in collagen gel extend from the apical surface of the growth cone. Finally, we visualized the 3D morphology of peripheral Rohon-Beard (RB) neuron growth cones from Xenopus embryos to determine whether growth cones form invadosome-like protrusions in their natural environment. To specifically label neurons in vivo, we immunolabeled whole mount stage 25 Xenopus embryos using antibodies against NCAM and Cttn and cleared the embryos with Murray's clearing solution. NCAM is a membrane targeted label which can be used to detect fine protrusions of growth cones in 3D. The peripheral growth cones of RB neurons were viewed by high resolution SIM within intact embryos. SIM imaging of RB neurons within the skin reveals extensive invadosome-like protrusions that extend

orthogonally from the C-domain of growth cones (Fig. 7C-E). Although growth cones in vivo remain largely planar with many peripheral filopodial directed along the axis of growth, discrete orthogonal protrusions can extend up to 10 μm perpendicular to the axis of growth (Fig. 7D-E).

Growth cone invadosomes are sites of ECM degradation

A defining characteristic of invadosomes is their ability to degrade and remodel the local matrix (Linder et al., 2011). Proteolysis of ECM components is a critical function of invadosomes, as matrix degradation allows cells to remodel and penetrate tissues. Cell surface and secreted proteases, such as the matrix metalloproteases (MMPs), accumulate and are released at invadosomes (Poincloux et al., 2009). For example, MMP14 (MT1-MMP) targets to the outer membrane of invadosomes and is required for the proteolytic activation of secreted MMP2 and 9. To determine whether growth cone invadosomes also contain MMPs, we first screened for known invadosomal MMP transcripts by PCR from pure spinal cord extracts. We find that MMP2, 9 and 14 are expressed in developing Xenopus spinal tissue (Fig. 8A). MMP14 expression in developing neurons was confirmed by immunoblot, which reveals bands at approximately 130 kDa, 60 kDa, and 30 kDa, likely representing an MMP14 complex, an active form and a proteolytic fragment, respectively (Fig. 8B). To determine if MMPs are active in the embryonic spinal cord, we performed gelatin zymography on spinal cell extracts, which show degradation at molecular weights corresponding to proMMP9, MMP9, proMMP2 and MMP2 (Fig. 8C). Next, to directly examine whether MMPs are present at invadosomes, we immunolabeled growth cones for MMP14 together with F-

actin. While MMP14 was present in a punctate distribution throughout growth cones, we did observe colocalization between MMP14 and F-actin foci (Fig. 8D,E). Finally, to assess whether there is proteolytic activity at F-actin foci, we performed fluorescent gelatin degradation assays. Xenopus spinal neurons were cultured on two variants of fluorescent gelatin that either show a loss or a gain of fluorescence upon proteolytic degradation by MMPs (Artym et al., 2009; Sloane et al., 2006). These approaches allow local sites of matrix degradation to be observed in relation to the position of growth cone invadosomes. Using both the fluorescence degradation and fluorogenic assays, we find that growth cones exhibit sites of proteolytic activity over regions of ECM contact, which occur at F-actin foci (Fig. 8F,G; supplementary material Fig. S8). Together these results suggest that MMPs are present and active within the developing spinal cord and target to growth cones invadosomes where they remodel the local ECM environment.

Discussion

Many studies identify F-actin rich protrusions from the ventral surface of invasive cells as sites of membrane attachment to and degradation of the ECM, but analogous structures have not been reported in developing neuronal growth cones. In this study we show for the first time that growth cones form 3D protrusions, which share many characteristics to invadosomes of invasive cells. We find that distinct F-actin foci form within the C-domain of growth cones from a variety of neuronal types and species in vitro as well as in the spinal cord and skin of intact Xenopus embryos. Growth cone invadosomes contain β1-integrin receptors and recruit PXN and FAK transiently, yet are distinct from leading edge point contact adhesions. Invadosomes appear to be sites of F-actin polymerization, as they contain F-actin barbed ends, as well as actin monomers and undergo rapid actin turnover determined by FRAP and fluorescence decay after photoactivation (FDAP). Consistent with this notion, the actin regulatory proteins Arp3, N-WASP, α-actinin, and Mena localize to invadosomes. Importantly, the classic invadosomal markers, cortactin, pY418-Src and Tks5 robustly concentrate at growth cone invadosomes. Pharmacological manipulations suggest that Src and lipid rafts, well established Tks5 targeting signals, are both necessary for invadosome formation in growth cones. Growth cones viewed by super resolution microscopy shows that F-actin within invadosomes is oriented as an axial column, perpendicular to the direction of axon extension. Moreover, a subset of axial F-actin bundles also contain MTs and form protrusions on the apical cell surface, in 2D and 3D cultures, as well as in vivo. Lastly, growth cone invadosomes express MMP proteins and are capable of remodeling the ECM through proteolytic activity. Together, these findings demonstrate that growth

cones form protrusions analogous to invadosomes of invasive cells, which may promote axon guidance through the 3D environment of the developing nervous system.

Invadopodia and podosomes are collectively referred to as invadosomes, although these protrusions have some notable differences in structure and function (Linder et al., 2011; Murphy and Courtneidge, 2011). Three common functions ascribed to invadosomes are cell adhesion, matrix degradation and mechanosensing. Podosomes have a more obvious adhesive function, as these form only on the ventral surface of cells in contact with the matrix and contain integrin receptors, as well as other adhesion-related proteins. Both invadopodia and podosomes have a clear matrix degradation function, although due to their slower turnover, invadopodia perform more focused degradation that can breach the local matrix to allow for the penetration of protrusions and cell migration across the basement membrane. Invadopodia and podosomes are also mechanosensory protrusions, as they exert traction forces on the matrix and are influenced by the rigidity of the underlying substratum (Alexander et al., 2008; Collin et al., 2008; Juin et al., 2013). Our evidence suggests that neuronal growth cones form invadosomes that likely have similar functions to classic invadopodia and podosomes (model; Fig. 9). For example, growth cone invadosomes appear to be adhesive structures as stable F-actin foci localize to areas that are in close contact to the substratum (supplementary material Fig. S3A-B) and colocalize with adhesion related proteins such as integrin receptors, paxillin and FAK (Fig. 2; supplementary material Fig. S3C-D). However, although invadosomes are likely adhesive contacts, they clearly differ from point contact (PC) adhesions, which typically assemble within filopodia and are short-lived (~2.5 min). Interestingly, a subset of PCs appear to

transition into invadosomes (Fig. 2E-H) and we suspect that these two processes may be linked (Chan et al., 2009; Liu et al., 2010). For example, growth cones may form PC adhesions in association with the basal lamina in vivo, while specific secreted growth factors or guidance cues may convert PCs into invadosomes. Formation of invadosomes on growth cones may subsequently promote matrix penetration and guidance through the basal lamina. This notion is consistent with the guidance of certain populations of developing axons across basement membranes into new tissue environments in embryos. For example, developing MNs must exit the spinal cord to synapse within lateral muscle and developing retinal ganglion cells extend axon branches deep within the developing optic tectum (Bonanomi and Pfaff, 2010; Dingwell et al., 2000; Schneider and Granato, 2003). However, it is important to note that growth cones from all neuronal types observed in vitro formed invadosomes (Fig. 1A-C; supplementary material Fig. S1A-C), suggesting that these cellular specializations may serve other functions outside of matrix remodeling.

Two important open questions are what extracellular cues and intracellular signals instruct invadosome formation versus PC formation in growth cones? In non-neuronal cells, the formation of invadosomes is stimulated by growth factors such as platelet-derived growth factor (PDGF), transforming growth factor-β (TGFβ) and epidermal growth factor (EGF) (Murphy and Courtneidge, 2011). These growth factors activate Src tyrosine kinases, which phosphorylate Tks5, Cttn and several other key regulatory proteins that target to invadosomes. Consistent with a role for Src in growth cone invadosomes, we find that active pY418 Src targets to invadosomes and inhibition of Src reduces invadosome formation (Fig. 5F-G). However, Src also regulates focal

adhesion and growth cone PC formation (Chan et al., 2009; Woo et al., 2009). Other intracellular signals, such as protein kinase C (PKC) and phosphoinositide 3-kinase (PI3K) cooperate with Src in regulating invadosome formation (Hoshino et al., 2012; Yamaguchi et al., 2011). PI3K may initiate the formation of invadosomes through local production of PI(3, 4, 5)P_3 and PI(3, 4)P_2, which recruit Tks5 through association with its amino terminal PX domain (Hoshino et al., 2013; Yamaguchi and Oikawa, 2010). Activated Tks5 subsequently binds proteins important in actin polymerization, such as cortactin and together with phosphorylation of several other actin binding proteins by Src and PKC, invadosomes may mature, stabilize or turnover. Consistent with a role for intact lipid microdomains, we find that disruption of lipid rafts prevents the formation of new invadosomes (Fig. 5H-J). As several growth factors and axon guidance cues, such as brain-derived growth factor (BDNF), Netrin and Ephrins are known to regulate Src, PKC and PI3K function in growth cones (Dent et al., 2011; Hall and Lalli, 2010), we hypothesize that guidance cues in combination with specific ECM proteins control PC-mediated substratum adhesion versus invadosome-mediated basal lamina penetration.

Using SIM we were able to view the cytoskeleton and other invadosomal components in growth cones at super resolution in 3D in vitro and in vivo. When viewed orthogonally and as a 3D rendering, we were surprised to find that F-actin foci often appear as columns of F-actin that span the depth of the growth cone C-domain and occasionally extend as dorsal protrusions into the surrounding space (Fig. 6). Even in 2D cultures, dorsal protrusions were observed to extend up to ~5 μm above the growth cone (Fig. 6F), which is surprising given the absence of any surrounding matrix or tissue to stabilize these protrusions. Invadosomes were also present in growth cones cultured

inside a collagen gel and in vivo (Fig. 7), where dorsal and ventral protrusions are likely supported by adhesions to the surrounding matrix and cells. However, MTs likely stabilize nascent F-actin containing invadosomes as well (Linder et al., 2011). While many F-actin foci appear to be devoid of or avoided by MTs (supplementary material Fig. S6A,B), some growth cone invadosomes contain MTs, which are required for invadosome maturation in non-neuronal cells (Schoumacher et al., 2010). MTs in invadosomes are believed to provide structural support, promote elongation and allow the delivery of protein cargo, such as MMPs, important for invadosome formation and function (Murphy and Courtneidge, 2011). Consistent with the function of growth cone invadosomes in matrix degradation, we find MMP proteins and sites of matrix degradation localized at invadosomes in culture.

A crucial open question is what role growth cone invadosomes have in the guidance of axons and dendrites to their synaptic targets? One possible function of invadosomes is the targeting of MMPs and other proteases such as ADAMs to promote local matrix degradation and extension of axons through tissues. This function is consistent with the role of invadosomes in the migration of cells under normal and pathological conditions. For example, neural crest cells form invadosomes, which are necessary for their proper migration and the development of craniofacial structures and pigmentation in zebrafish embryos (Murphy et al., 2011). Several studies have implicated MMP and ADAM function in axon guidance through ECM-degradation (McFarlane, 2003; Yong et al., 2001). Matrix proteases may regulate axon extension in part by degrading the surrounding matrix to create a passage for axonal outgrowth (Gutierrez-Fernandez et al., 2009; Hayashita-Kinoh et al., 2001; Zuo et al., 1998), but

more recent studies performed both in vitro and in vivo now suggest that proteolytic cleavage is directed toward specific ligands in the environment, as well as receptors on growth cones to activate or terminate motility (Chen et al., 2007; Fambrough et al., 1996; Hehr et al., 2005; Schimmelpfeng et al., 2001; Webber et al., 2002). For example, MMPs are necessary for conversion of pro-neurotrophins into mature neurotrophins (Lee et al., 2001) and in ectodomain shedding of guidance cue receptors (Bai et al., 2011; Browne et al., 2012; Coleman et al., 2010; Galko and Tessier-Lavigne, 2000; Hattori et al., 2000; Kanning et al., 2003; Lin et al., 2008; Miller et al., 2008; Walmsley et al., 2004). Our findings that MT1-MMP target to invadosomes (Fig. 8D-E) and that growth cones can penetrate through collagen in vitro (supplementary material Fig. S7), are consistent with the role of these protrusions in ECM or receptor proteolysis in vivo. We also find that β1-integrin receptors localize to growth cone invadosomes and suspect that other receptors target to the tips of invadosomes. If true, receptors on tips of dorsal and ventral invadosomal protrusions would allow growth cones to detect molecular cues from sources deep to the direction of outgrowth. Moreover, the function of these receptors could be rapidly modulated through MMP- or ADAM-mediated cleavage. For example, DCC and APP receptors may target to invadosomes on crossing CIs (Fig. 1F-G) and bind netrin deep within the floorplate, but receptor activation could be rapidly terminated by protease dependent receptor cleavage. While DCC and APP receptors are known to be cleaved on neurons by cellular proteases, it is unknown how this is regulated on the surface of growth cones. Future studies should test the effects of disrupting invadosome formation at midline crossing by CIs and axon guidance at sites where developing axons cross basal lamina to enter new tissues.

References

Alexander, N.R., K.M. Branch, A. Parekh, E.S. Clark, I.C. Iwueke, S.A. Guelcher, and A.M. Weaver. 2008. Extracellular matrix rigidity promotes invadopodia activity. *Curr Biol*. 18:1295-9.

Artym, V.V., K.M. Yamada, and S.C. Mueller. 2009. ECM degradation assays for analyzing local cell invasion. *Methods Mol Biol*. 522:211-9.

Bai, G., O. Chivatakarn, D. Bonanomi, K. Lettieri, L. Franco, C. Xia, E. Stein, L. Ma, J.W. Lewcock, and S.L. Pfaff. 2011. Presenilin-dependent receptor processing is required for axon guidance. *Cell*. 144:106-18.

Boateng, L.R., and A. Huttenlocher. 2012. Spatiotemporal regulation of Src and its substrates at invadosomes. *Eur J Cell Biol*. 91:878-88.

Bonanomi, D., and S.L. Pfaff. 2010. Motor axon pathfinding. *Cold Spring Harb Perspect Biol*. 2:a001735.

Browne, K., W. Wang, R.Q. Liu, M. Piva, and T.P. O'Connor. 2012. Transmembrane semaphorin5B is proteolytically processed into a repulsive neural guidance cue. *J Neurochem*. 123:135-46.

Chan, K.T., C.L. Cortesio, and A. Huttenlocher. 2009. FAK alters invadopodia and focal adhesion composition and dynamics to regulate breast cancer invasion. *J Cell Biol*. 185:357-70.

Chen, Y.Y., C.L. Hehr, K. Atkinson-Leadbeater, J.C. Hocking, and S. McFarlane. 2007. Targeting of retinal axons requires the metalloproteinase ADAM10. *J Neurosci*. 27:8448-56.

Coleman, H.A., J.P. Labrador, R.K. Chance, and G.J. Bashaw. 2010. The Adam family metalloprotease Kuzbanian regulates the cleavage of the roundabout receptor to control axon repulsion at the midline. *Development*. 137:2417-26.

Collin, O., S. Na, F. Chowdhury, M. Hong, M.E. Shin, F. Wang, and N. Wang. 2008. Self-organized podosomes are dynamic mechanosensors. *Curr Biol*. 18:1288-94.

Courtneidge, S.A. 2012. Cell migration and invasion in human disease: the Tks adaptor proteins. *Biochem Soc Trans*. 40:129-32.

Decourt, B., V. Munnamalai, A.C. Lee, L. Sanchez, and D.M. Suter. 2009. Cortactin colocalizes with filopodial actin and accumulates at IgCAM adhesion sites in Aplysia growth cones. *J Neurosci Res*. 87:1057-68.

Dent, E.W., S.L. Gupton, and F.B. Gertler. 2011. The growth cone cytoskeleton in axon outgrowth and guidance. *Cold Spring Harb Perspect Biol*. 3.

Dingwell, K.S., C.E. Holt, and W.A. Harris. 2000. The multiple decisions made by growth cones of RGCs as they navigate from the retina to the tectum in Xenopus embryos. *J Neurobiol*. 44:246-59.

Fambrough, D., D. Pan, G.M. Rubin, and C.S. Goodman. 1996. The cell surface metalloprotease/ disintegrin Kuzbanian is required for axonal extension in Drosophila. *Proc Natl Acad Sci U S A*. 93:13233-8.

Galko, M.J., and M. Tessier-Lavigne. 2000. Function of an axonal chemoattractant modulated by metalloprotease activity. *Science*. 289:1365-7.

Guirland, C., S. Suzuki, M. Kojima, B. Lu, and J.Q. Zheng. 2004. Lipid rafts mediate chemotropic guidance of nerve growth cones. *Neuron*. 42:51-62.

Gutierrez-Fernandez, A., N.A. Gingles, H. Bai, F.J. Castellino, R.J. Parmer, and L.A. Miles. 2009. Plasminogen enhances neuritogenesis on laminin-1. *J Neurosci*. 29:12393-400.

Hall, A., and G. Lalli. 2010. Rho and Ras GTPases in axon growth, guidance, and branching. *Cold Spring Harb Perspect Biol*. 2:a001818.

Hattori, M., M. Osterfield, and J.G. Flanagan. 2000. Regulated cleavage of a contact-mediated axon repellent. *Science*. 289:1360-5.

Hayashita-Kinoh, H., H. Kinoh, A. Okada, K. Komori, Y. Itoh, T. Chiba, M. Kajita, I. Yana, and M. Seiki. 2001. Membrane-type 5 matrix metalloproteinase is expressed in differentiated neurons and regulates axonal growth. *Cell Growth Differ*. 12:573-80.

Hehr, C.L., J.C. Hocking, and S. McFarlane. 2005. Matrix metalloproteinases are required for retinal ganglion cell axon guidance at select decision points. *Development*. 132:3371-9.

Hoshino, D., K.M. Branch, and A.M. Weaver. 2013. Signaling inputs to invadopodia and podosomes. *J Cell Sci*. 126:2979-89.

Hoshino, D., J. Jourquin, S.W. Emmons, T. Miller, M. Goldgof, K. Costello, D.R. Tyson, B. Brown, Y. Lu, N.K. Prasad, B. Zhang, G.B. Mills, W.G. Yarbrough, V. Quaranta, M. Seiki, and A.M. Weaver. 2012. Network analysis of the focal adhesion to invadopodia transition identifies a PI3K-PKCalpha invasive signaling axis. *Sci Signal*. 5:ra66.

Juin, A., E. Planus, F. Guillemot, P. Horakova, C. Albiges-Rizo, E. Genot, J. Rosenbaum, V. Moreau, and F. Saltel. 2013. Extracellular matrix rigidity controls podosome induction in microvascular endothelial cells. *Biol Cell*. 105:46-57.

Kanning, K.C., M. Hudson, P.S. Amieux, J.C. Wiley, M. Bothwell, and L.C. Schecterson. 2003. Proteolytic processing of the p75 neurotrophin receptor and two homologs generates C-terminal fragments with signaling capability. *J Neurosci*. 23:5425-36.

Keren, K., Z. Pincus, G.M. Allen, E.L. Barnhart, G. Marriott, A. Mogilner, and J.A. Theriot. 2008. Mechanism of shape determination in motile cells. *Nature*. 453:475-80.

Kirkbride, K.C., B.H. Sung, S. Sinha, and A.M. Weaver. 2011. Cortactin: a multifunctional regulator of cellular invasiveness. *Cell Adh Migr*. 5:187-98.

Kolodkin, A.L., and M. Tessier-Lavigne. 2011. Mechanisms and molecules of neuronal wiring: a primer. *Cold Spring Harb Perspect Biol*. 3.

Kurklinsky, S., J. Chen, and M.A. McNiven. 2011. Growth cone morphology and spreading are regulated by a dynamin-cortactin complex at point contacts in hippocampal neurons. *J Neurochem*. 117:48-60.

Lee, C.W., E.A. Vitriol, S. Shim, A.L. Wise, R.P. Velayutham, and J.Q. Zheng. 2013. Dynamic localization of G-actin during membrane protrusion in neuronal motility. *Curr Biol*. 23:1046-56.

Lee, R., P. Kermani, K.K. Teng, and B.L. Hempstead. 2001. Regulation of cell survival by secreted proneurotrophins. *Science*. 294:1945-8.

Lin, K.T., S. Sloniowski, D.W. Ethell, and I.M. Ethell. 2008. Ephrin-B2-induced cleavage of EphB2 receptor is mediated by matrix metalloproteinases to trigger cell repulsion. *J Biol Chem*. 283:28969-79.

Linder, S., C. Wiesner, and M. Himmel. 2011. Degrading devices: invadosomes in proteolytic cell invasion. *Annu Rev Cell Dev Biol*. 27:185-211.

Liu, S., H. Yamashita, B. Weidow, A.M. Weaver, and V. Quaranta. 2010. Laminin-332-beta1 integrin interactions negatively regulate invadopodia. *J Cell Physiol*. 223:134-42.

Lowery, L.A., and D. Van Vactor. 2009. The trip of the tip: understanding the growth cone machinery. *Nat Rev Mol Cell Biol*. 10:332-43.

MacGrath, S.M., and A.J. Koleske. 2012. Cortactin in cell migration and cancer at a glance. *J Cell Sci*. 125:1621-6.

Marsick, B.M., K.C. Flynn, M. Santiago-Medina, J.R. Bamburg, and P.C. Letourneau. 2010. Activation of ADF/cofilin mediates attractive growth cone turning toward nerve growth factor and netrin-1. *Dev Neurobiol*. 70:565-88.

McFarlane, S. 2003. Metalloproteases: carving out a role in axon guidance. *Neuron*. 37:559-62.

Miller, C.M., A. Page-McCaw, and H.T. Broihier. 2008. Matrix metalloproteinases promote motor axon fasciculation in the Drosophila embryo. *Development*. 135:95-109.

Murphy, D.A., and S.A. Courtneidge. 2011. The 'ins' and 'outs' of podosomes and invadopodia: characteristics, formation and function. *Nat Rev Mol Cell Biol*. 12:413-26.

Murphy, D.A., B. Diaz, P.A. Bromann, J.H. Tsai, Y. Kawakami, J. Maurer, R.A. Stewart, J.C. Izpisua-Belmonte, and S.A. Courtneidge. 2011. A Src-Tks5 pathway is required for neural crest cell migration during embryonic development. *PLoS One*. 6:e22499.

Myers, J.P., and T.M. Gomez. 2011. Focal adhesion kinase promotes integrin adhesion dynamics necessary for chemotropic turning of nerve growth cones. *J Neurosci*. 31:13585-95.

Perrin, B.J., K.J. Amann, and A. Huttenlocher. 2006. Proteolysis of cortactin by calpain regulates membrane protrusion during cell migration. *Mol Biol Cell*. 17:239-50.

Petchprayoon, C., K. Suwanborirux, J. Tanaka, Y. Yan, T. Sakata, and G. Marriott. 2005. Fluorescent kabiramides: new probes to quantify actin in vitro and in vivo. *Bioconjug Chem*. 16:1382-9.

Philippar, U., E.T. Roussos, M. Oser, H. Yamaguchi, H.D. Kim, S. Giampieri, Y. Wang, S. Goswami, J.B. Wyckoff, D.A. Lauffenburger, E. Sahai, J.S. Condeelis, and F.B. Gertler. 2008. A Mena invasion isoform potentiates EGF-induced carcinoma cell invasion and metastasis. *Dev Cell*. 15:813-28.

Poincloux, R., F. Lizarraga, and P. Chavrier. 2009. Matrix invasion by tumour cells: a focus on MT1-MMP trafficking to invadopodia. *J Cell Sci*. 122:3015-24.

Robles, E., and T.M. Gomez. 2006. Focal adhesion kinase signaling at sites of integrin-mediated adhesion controls axon pathfinding. *Nat Neurosci*. 9:1274-83.

Santiago-Medina, M., K.A. Gregus, and T.M. Gomez. 2013. PAK-PIX interactions regulate adhesion dynamics and membrane protrusion to control neurite outgrowth. *J Cell Sci*. 126:1122-33.

Santiago-Medina, M., J.P. Myers, and T.M. Gomez. 2012. Imaging adhesion and signaling dynamics in Xenopus laevis growth cones. *Dev Neurobiol*. 72:585-99.

Schimmelpfeng, K., S. Gogel, and C. Klambt. 2001. The function of leak and kuzbanian during growth cone and cell migration. *Mech Dev*. 106:25-36.

Schneider, V.A., and M. Granato. 2003. Motor axon migration: a long way to go. *Dev Biol*. 263:1-11.

Schoumacher, M., R.D. Goldman, D. Louvard, and D.M. Vignjevic. 2010. Actin, microtubules, and vimentin intermediate filaments cooperate for elongation of invadopodia. *J Cell Biol*. 189:541-56.

Sloane, B.F., M. Sameni, I. Podgorski, D. Cavallo-Medved, and K. Moin. 2006. Functional imaging of tumor proteolysis. *Annu Rev Pharmacol Toxicol*. 46:301-15.

Tanaka, J., Y. Yan, J. Choi, J. Bai, V.A. Klenchin, I. Rayment, and G. Marriott. 2003. Biomolecular mimicry in the actin cytoskeleton: mechanisms underlying the cytotoxicity of kabiramide C and related macrolides. *Proc Natl Acad Sci U S A*. 100:13851-6.

Toomre, D., and J. Bewersdorf. 2010. A new wave of cellular imaging. *Annu Rev Cell Dev Biol*. 26:285-314.

Walmsley, A.R., G. McCombie, U. Neumann, D. Marcellin, R. Hillenbrand, A.K. Mir, and S. Frentzel. 2004. Zinc metalloproteinase-mediated cleavage of the human Nogo-66 receptor. *J Cell Sci*. 117:4591-602.

Webber, C.A., J.C. Hocking, V.W. Yong, C.L. Stange, and S. McFarlane. 2002. Metalloproteases and guidance of retinal axons in the developing visual system. *J Neurosci*. 22:8091-100.

Woo, S., and T.M. Gomez. 2006. Rac1 and RhoA promote neurite outgrowth through formation and stabilization of growth cone point contacts. *J Neurosci*. 26:1418-28.

Woo, S., D.J. Rowan, and T.M. Gomez. 2009. Retinotopic mapping requires focal adhesion kinase-mediated regulation of growth cone adhesion. *J Neurosci*. 29:13981-91.

Yamaguchi, H., and T. Oikawa. 2010. Membrane lipids in invadopodia and podosomes: key structures for cancer invasion and metastasis. *Oncotarget*. 1:320-8.

Yamaguchi, H., S. Yoshida, E. Muroi, N. Yoshida, M. Kawamura, Z. Kouchi, Y. Nakamura, R. Sakai, and K. Fukami. 2011. Phosphoinositide 3-kinase signaling pathway mediated by p110alpha regulates invadopodia formation. *J Cell Biol*. 193:1275-88.

Yong, V.W., C. Power, P. Forsyth, and D.R. Edwards. 2001. Metalloproteinases in biology and pathology of the nervous system. *Nat Rev Neurosci*. 2:502-11.

Zuo, J., T.A. Ferguson, Y.J. Hernandez, W.G. Stetler-Stevenson, and D. Muir. 1998. Neuronal matrix metalloproteinase-2 degrades and inactivates a neurite-inhibiting chondroitin sulfate proteoglycan. *J Neurosci*. 18:5203-11.

Figure 1. Growth cones exhibit F-actin rich foci within their central domain in vitro and in vivo. A-B. Confocal images of Alexa-546 phalloidin labeled spinal neuron (A) or retinal ganglion cell (B) growth cones cultured on different substrata depicting F-actin rich accumulations termed actin foci (arrowheads). **C-D.** Quantification of actin foci number (C; N ≥ 26) and area (D; N ≥ 51) in growth cones cultured on different substata. **E.** TIRF images of a live spinal neuron growth cone on LN expressing GFP-β-actin. Note how a subset of actin foci are highly stable (red boxes). **F-G.** Confocal images of a Xenopus spinal cord expressing mCh-UtrCH and fixed at stage 23 (F) and 24 (G). **F.** Lateral view of the spinal cord showing the axons of commissural interneurons (CI) growing away from the dorsal fascicle (top) and towards the floor plate (bottom). **G.** Ventral view of the spinal cord showing the axons of CI crossing (a) or positioned at (b) the midline. Note the presence of actin foci in CI growth cones at all positions examined (arrowheads). Scale, 5 μm (A-B, E, Ga,b), 20 μm (F), 10μm (G).

Figure 1.

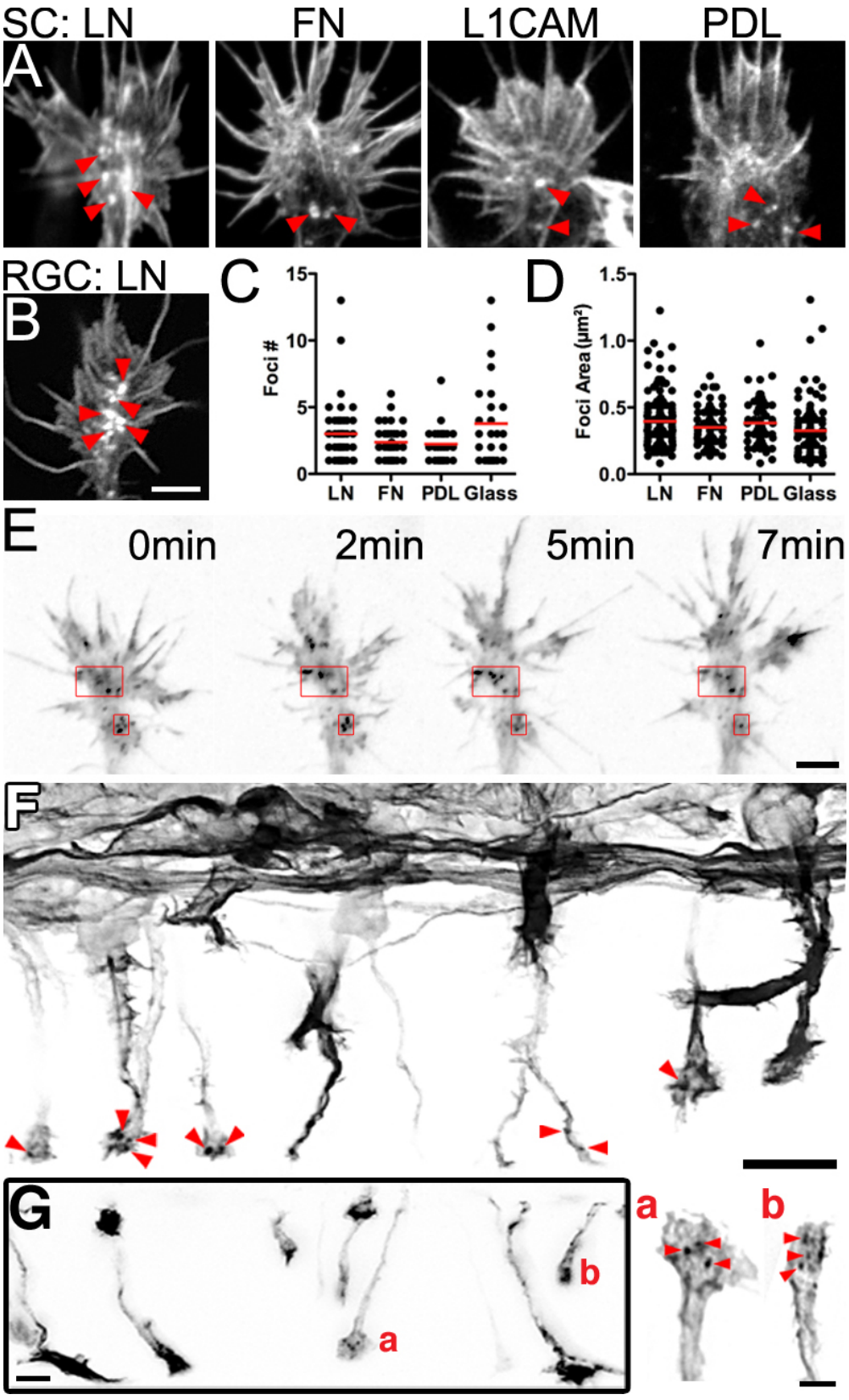
SC: LN
FN
L1CAM
PDL
A
RGC: LN
B
C
Foci #
15
10
5
0
LN
FN
PDL
Glass
D
Foci Area (µm²)
1.5
1.0
0.5
0.0
LN
FN
PDL
Glass
E
0min
2min
5min
7min
F
G
a
b
a
b

Figure 2. F-actin foci colocalize with β1-integrin receptors and the point contact proteins PXN and FAK in growth cones. A-B, D. Confocal images of growth cones on LN, fixed and immunolabeled for β1-integrin (A), pY118-PXN (B), or pY397-FAK (C). **A'-B', D'.** F-actin staining using Alexa-546 phalloidin. **A''-B'', D''.** Merged images of the immunolabels (green) and F-actin staining (red). **A.** Note how β1-integrin targets to the tips of filopodia (solid arrowheads) as well as with actin foci (open arrowheads). **B.** Note the colocalization of pY118-PXN with actin foci (open arrowheads). **C.** Quantification of actin foci and pY118-PXN association in growth cones. **D.** Note how pY397-FAK colocalizes with a small subset of actin foci (open arrowheads) but not with others (solid arrowheads). **E-G.** TIRF images of a live spinal neuron growth cone on LN expressing both mCh-UtrCH (E) and GFP-PXN (F). Note in the merge (G), both the association of PXN to actin foci (open arrowheads) as well as solitary foci (solid arrowheads). **H.** Quantification of mCh-UtrCH labeled actin foci and PXN-GFP association in live growth cones. ***P < 0.001, Unpaired t-test, N = 68. Scale, 5 μm (A-B, D-G).

Figure 2.

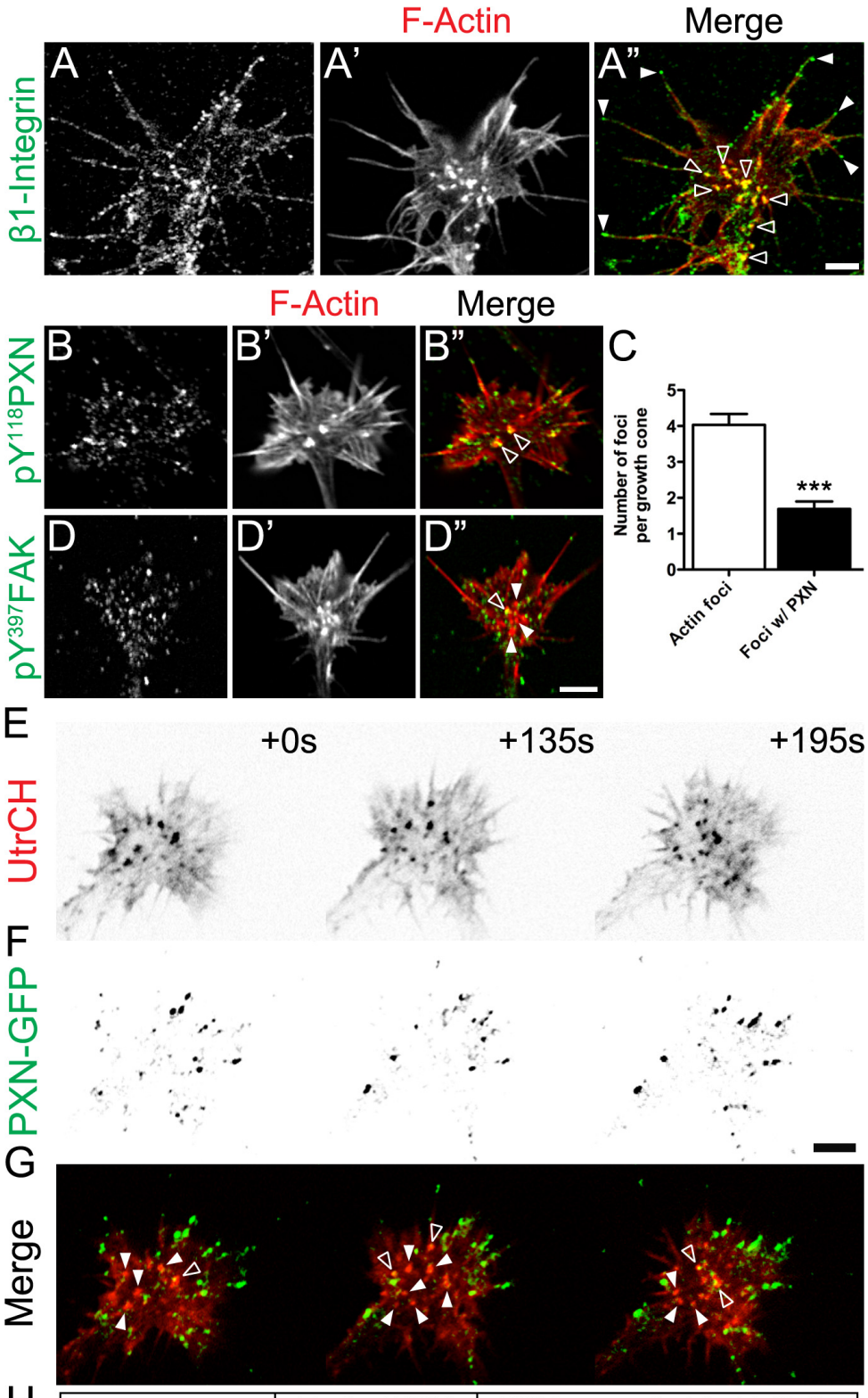

Fraction±SEM	Foci w/ PXN	PXN present at foci initiation
	0.486±0.036	0.657±0.1458

Figure 3. F-actin foci are sites of rapid actin polymerization. A. Confocal images of a growth cone on LN, fixed and stained for G-actin (Alexa-488 DNase1). Note the colocalization of monomeric actin with F-actin foci (solid arrowheads). **B-B".** TIRF images of a live spinal neuron growth cone on LN labeled with the F-actin barbed-end binding probe, TMR-KabC over time. Note the persistence of actin foci (arrowhead) in contrast to the reward tracking puncta of actin in the leading edge. **C.** Kymograph from the boxed region of the growth cone in (B) indicating the rearward flow of KabC-capped actin filaments (angled lines) and the persistence of actin foci (arrowhead). **D,F.** Confocal images of live growth cones expressing GFP-β-actin (D) or PA-GFP-γ-actin (F) together with mCh-UtrCH (D', F') over time. **D.** FRAP experiment depicting the photobleaching (0 s) and recovery of GFP-β-actin at an mCh-UtrCH labeled actin foci (arrowhead). **E.** Normalized quantification of fluorescence recovery over time after photobleaching GFP-β-actin in regions adjacent to actin foci (upper graph) or at actin foci (lower graph). N ≥ 59. **F.** Photoactivation decay experiment depicting the photoactivation (0 s) and decay of PA-GFP-γ-actin at an mCh-UtrCH labeled actin foci (arrowhead). **G.** Normalized quantification of fluorescence decay over time after photoactivating PA-GFP-γ-actin at actin foci (upper graph) and the ratio of PA-GFP-γ-actin by mCh-UtrCH to account for unintentional photobleaching over time. N ≥ 59. Scale, 5 μm (A, D, F).

Figure 3.

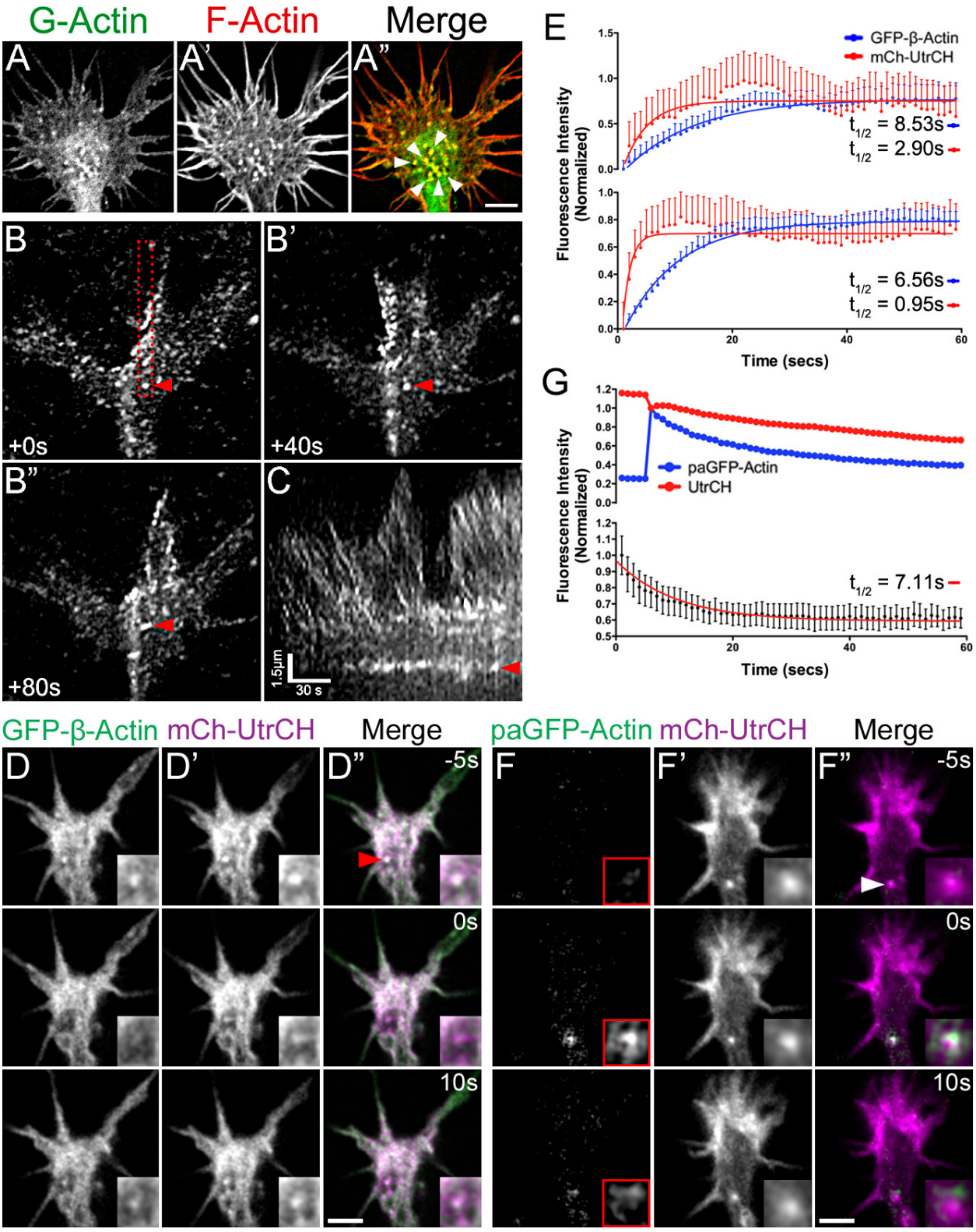
G-Actin
F-Actin
Merge
A
A'
A"
B
B'
+0s
+40s
B"
C
+80s
1.5µm
30 s
E
GFP-β-Actin
mCh-UtrCH
t1/2 = 8.53s
t1/2 = 2.90s
t1/2 = 6.56s
t1/2 = 0.95s
Fluorescence Intensity (Normalized)
Time (secs)
G
paGFP-Actin
UtrCH
t1/2 = 7.11s
Fluorescence Intensity (Normalized)
Time (secs)
GFP-β-Actin mCh-UtrCH
Merge
D
D'
D"
-5s
0s
10s
paGFP-Actin mCh-UtrCH
Merge
F
F'
F"
-5s
0s
10s

Figure 4. F-actin foci colocalize with the invadosome marker Cortactin and other actin modulators within growth cones. A-D. Confocal images of growth cones from spinal neurons cultured on LN and immunolabeled for Cttn (A), Arp3 (B), N-WASP (C) and Mena (E). **A',D'.** Alexa-546 phalloidin labeling of F-actin. **A"-D".** Merged images of the immunolabels (green) and F-actin labeling (red). Note the strong colocalization of actin foci and the proteins immunolabeled (arrowheads). **E.** TIRF images of a live spinal neuron growth cone on LN expressing both GFP-α-actinin (E) and mCh-UtrCH (E'). Note in the merge (E"), the targeting of α-actinin to mCh-UtrCH labeled actin foci (arrowheads). Scale, 5 μm (A-E).

Figure 4.

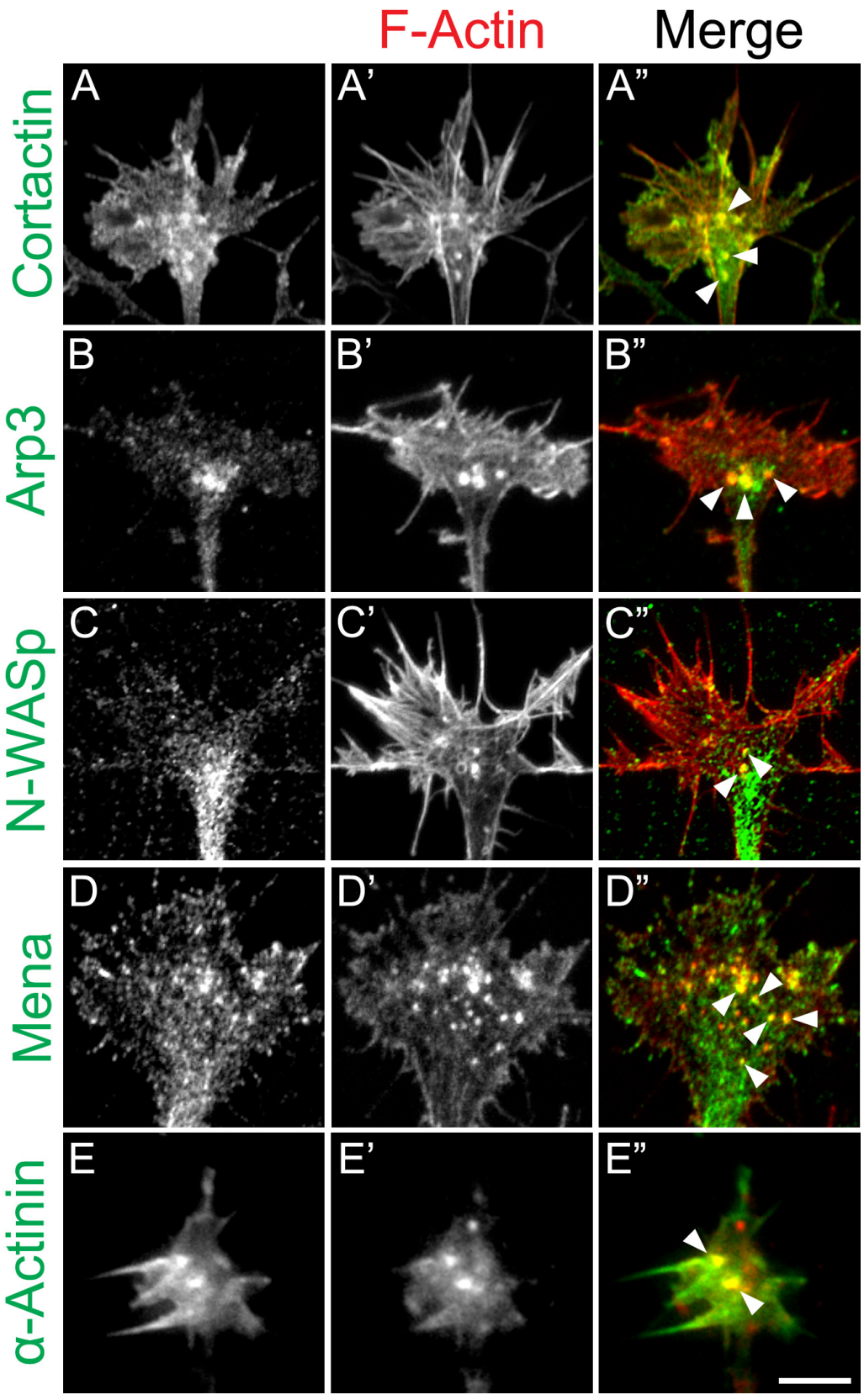
F-Actin
Merge
Cortactin
Arp3
N-WASp
Mena
α-Actinin
A
A'
A"
B
B'
B"
C
C'
C"
D
D'
D"
E
E'
E"

Figure 5. F-actin foci colocalize with the classic invadosome markers Src and Tks5 and require active Src and lipid rafts for their formation in growth cones. A. RT-PCR amplification of Tks4 and Tks5 from stage 22 and stage 25 Xenopus spinal cord. β-Tubulin was used as a positive control. **B.** Western blot of Tks5 from stage 24 Xenopus spinal cord. **C,D.** Confocal images of growth cones from spinal neurons cultured on LN and immunolabeled for Tks5 (C) and pY418-Src (D). **C',D'.** Immunolabel of cortactin. **C'',D''.** Alexa-546 phalloidin labeling of F-actin. **C'''-D'''.** Merged images of Tks5 or Src (blue), Cttn (green) and F-actin (red). Note the presence of Tks5 and active Src with Cttn at growth cone invadosomes (arrows). **E.** TIRF image of a live spinal neuron growth cone on LN expressing both Tks5-GFP (green) and mCh-UtrCH (magenta). Note the targeting of Tks5 to mCh-UtrCH labeled actin foci (arrows). **F.** Quantification of invadosome number in fixed growth cones that were treated with 1 μM PP2 for 5 min. *P < 0.05, Unpaired t-test, N ≥ 101. **G.** Quantification of invadosome lifetime in live, GFP-β-actin expressing growth cones treated with 1 μM PP2 over a 15 min period. ***P < 0.001, Unpaired t-test, N ≥ 99. **H.** TIRF images of a live spinal neuron growth cone on LN expressing GFP-β-actin before (left panel) and after (right panel) treatment with 2.5 μM MβCD. **I.** Quantification of total (left columns) and stable (right columns) invadosomes in live, GFP-β-actin expressing growth cones 15 min before and after treatment with 1 μM MβCD. *P < 0.05, Paired t-test, N = 7. **J.** Quantification of invadosome lifetime in live, GFP-β-actin expressing growth cones 15 min before and after treatment with 1 μM MβCD. ***P < 0.001, Paired t-test, N ≥ 57 Scale, 5 μm (C-E, H).

Figure 5.

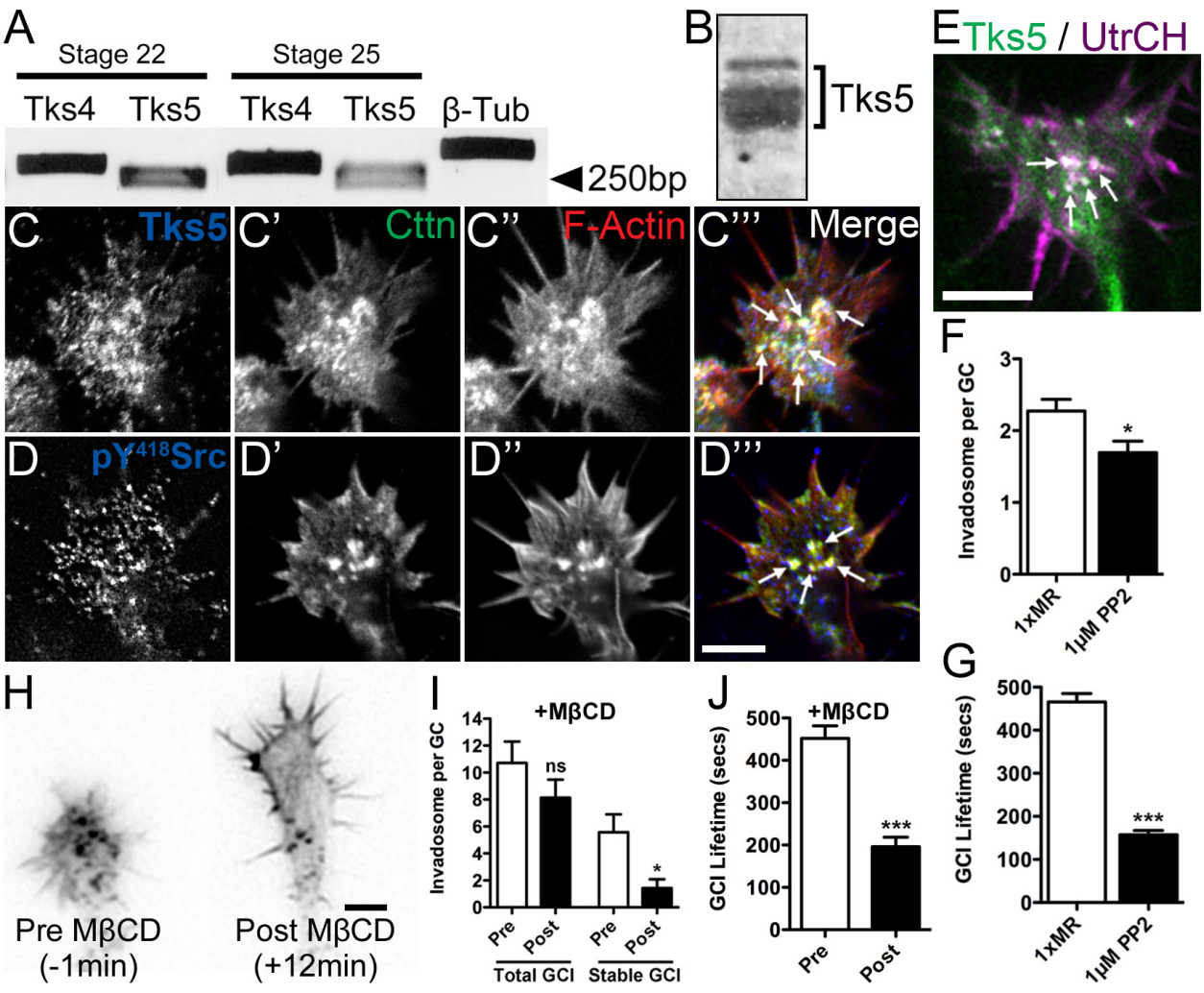
A
Stage 22
Stage 25
Tks4
Tks5
Tks4
Tks5
β-Tub
250bp
B
Tks5
E Tks5 / UtrCH
C Tks5
C' Cttn
C'' F-Actin
C''' Merge
D pY418Src
D'
D''
D'''
F
Invadosome per GC
1xMR
1μM PP2
G
GCI Lifetime (secs)
1xMR
1μM PP2
H
Pre MβCD
(-1min)
Post MβCD
(+12min)
I
+MβCD
Invadosome per GC
ns
Pre
Post
Pre
Post
Total GCI
Stable GCI
J
+MβCD
GCI Lifetime (secs)
Pre
Post

Figure 6. 3D SIM resolves invadosomes as actin rich columns that can protrude from the dorsal or ventral surfaces of growth cones in vitro. A,B. SIM images of Xenopus spinal neuron growth cones on LN (A) or gelatin (B), fixed and stained for F-actin with Alexa-568 phalloidin. Note the interdigitating cross-linked actin meshwork within the peripheral veil and the F-actin rich foci within the growth cone central domain (arrowhead in (A) and red box in (B)). **C.** Magnification of the boxed region in (B). **D.** Lateral-view image obtained by rotating the F-actin rich foci shown in (C) 90 degrees clockwise in the z-plane. Note how the F-actin foci spans from the ventral (V) to the dorsal (D) membrane of the thin growth cone and exhibits a small protrusion on the dorsal membrane (arrowhead). **E-E'.** SIM images of a human forebrain neuron derived from an iPSC on LN, fixed and stained for F-actin with Alexa-568 phalloidin (E) and immunolabeled for βIII-tubulin (E'). Note the F-actin rich foci located within the growth cone central domain (arrowhead). **E".** Merged image of the F-actin label (magenta) and βIII-tubulin immunolabel (green). **F-F".** Lateral-view images obtained by rotating the growth cone shown in (E-E") 90 degrees clockwise in the z-plane. Note how MTs tract along F-actin within the dorsal protrusion (E-E"). Scale, 5 μm (A-B, E), 1 μm (C-D), 2 μm (F).

Figure 6.

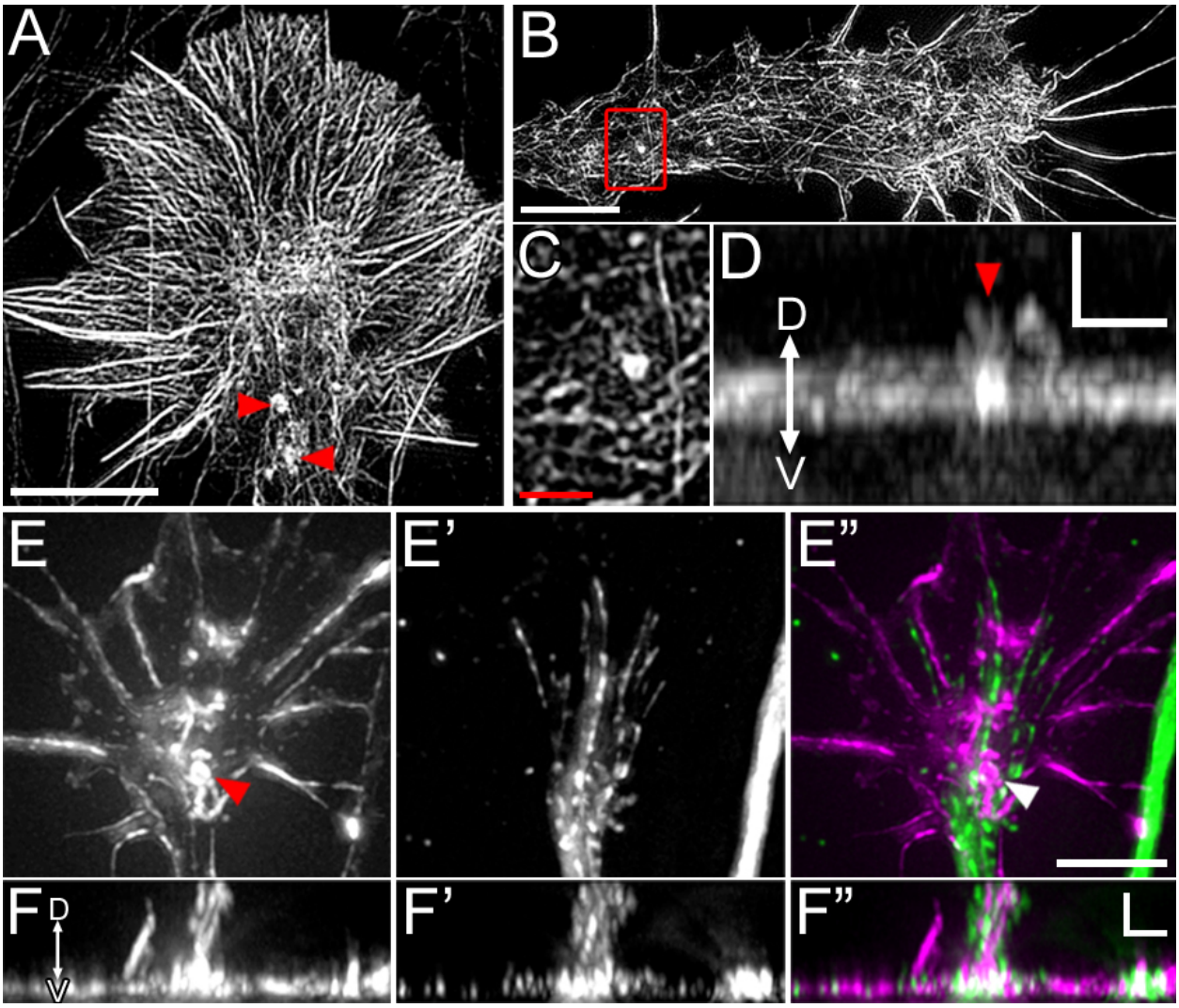

Figure 7. 3D SIM reveals that invadosomes protrude from the surface of growth cones in collagen gels and in vivo. A-A". SIM images of a growth cone from a Xenopus spinal explant cultured in a 3D collagen-1 gel. Growth cones in collagen were fixed and stained for F-actin (A) with Alexa-568 phalloidin and immunolabeled for Cttn (A'). Note the Cttn positive F-actin rich foci within the growth cone (arrowhead in (A")). **B.** A 90 degree rotation in the z-plane providing a side view through the growth cone and F-actin foci shown in (A"). Note the dorsal protrusions emanating into the collagen gel from the F-actin foci (arrowhead). **C-E.** SIM images of a Rohon-Beard peripheral process growth cone in the skin of an intact Xenopus stage 25 embryo fixed and immunolabeled for NCAM (green) and Cttn (red). **C.** Note the presence of an F-actin foci (solid arrowhead) and an apical projecting filopodia (open arrowhead). **D.** Lateral-view image obtained by rotating (C) 90 degrees counterclockwise and 90 degrees clockwise in the z-plane. Note the apical protrusions emanating into the skin from the F-actin foci and filopodia (arrowhead and open arrowhead respectively). **E.** Anterior/ posterior-view image obtained by rotating (C) 90 degrees clockwise in the z-plane. Note the apical protrusions emanating into the skin from the F-actin foci and filopodia (arrowhead and open arrowhead respectively). Scale, 5 μm (A, C-E), 1 μm (B).

Figure 7.

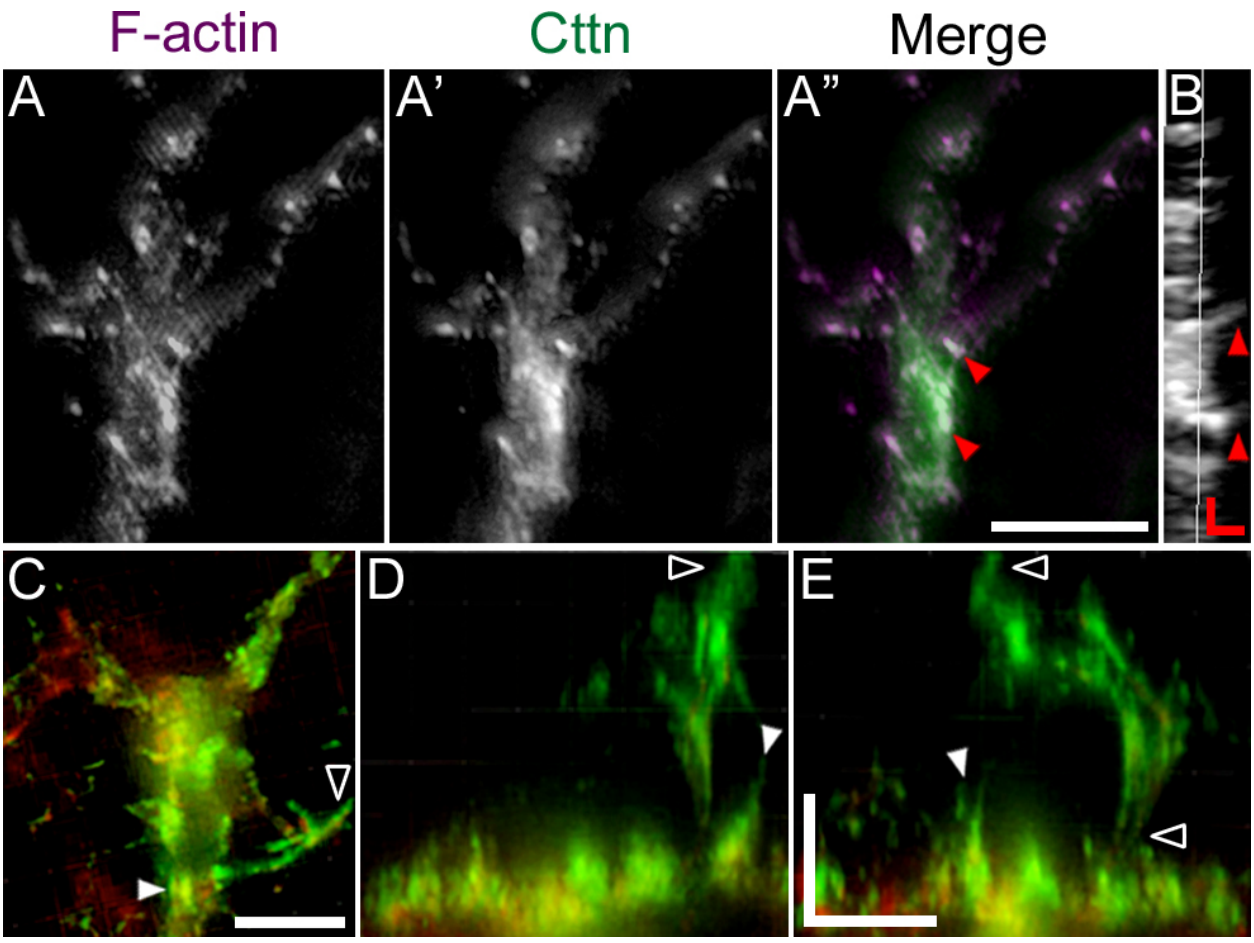

Figure 8. Spinal neurons along with their growth cones express MMP14 and exhibit protease activity. **A.** RT-PCR amplification of MMP2, 9 and 14 from stage 24 Xenopus spinal cord. β-Tubulin was used as a positive control. **B.** Western blot of MMP14 from stage 24 Xenopus spinal cord. **C.** Gelatin zymogram of MMP9 (~90 kDa) and 2 (70 kDa) along with their pro-forms (~110 kDa and ~75 kDa respectively) from stage 24 Xenopus spinal cord. **D-E.** Confocal images of growth cones from spinal neurons cultured on LN and immunolabeled for MMP14 (MT1-MMP). **D'-E'.** Alexa-546 phalloidin labeling of F-actin. **D'"-E'".** Merged images of MMP14 (green) and F-actin (magenta). Note the presence of MMP14 at growth cone invadosomes (arrows). **F-F".** Confocal images of a spinal neuron growth cone subjected to a gelatin degradation assay. **F.** Fluorescently (Oregon Green) labeled gelatin used as the growth cone substratum. **F'.** Alexa-546 phalloidin labeled F-actin. **F".** Merged image of the gelatin (green) and F-actin (magenta) label. Note the colocalization of growth cone invadosomes with areas of gelatin degradation (arrows). **G.** Quantification of gelatin degradation for the total growth cone (Tot. GC) and at growth cone invadosomes (GCIs) compared to background Oregon Green fluorescence. *$P < 0.05$, One-way ANOVA, $N \geq 15$. Scale, 5 μm (D-F).

Figure 8.

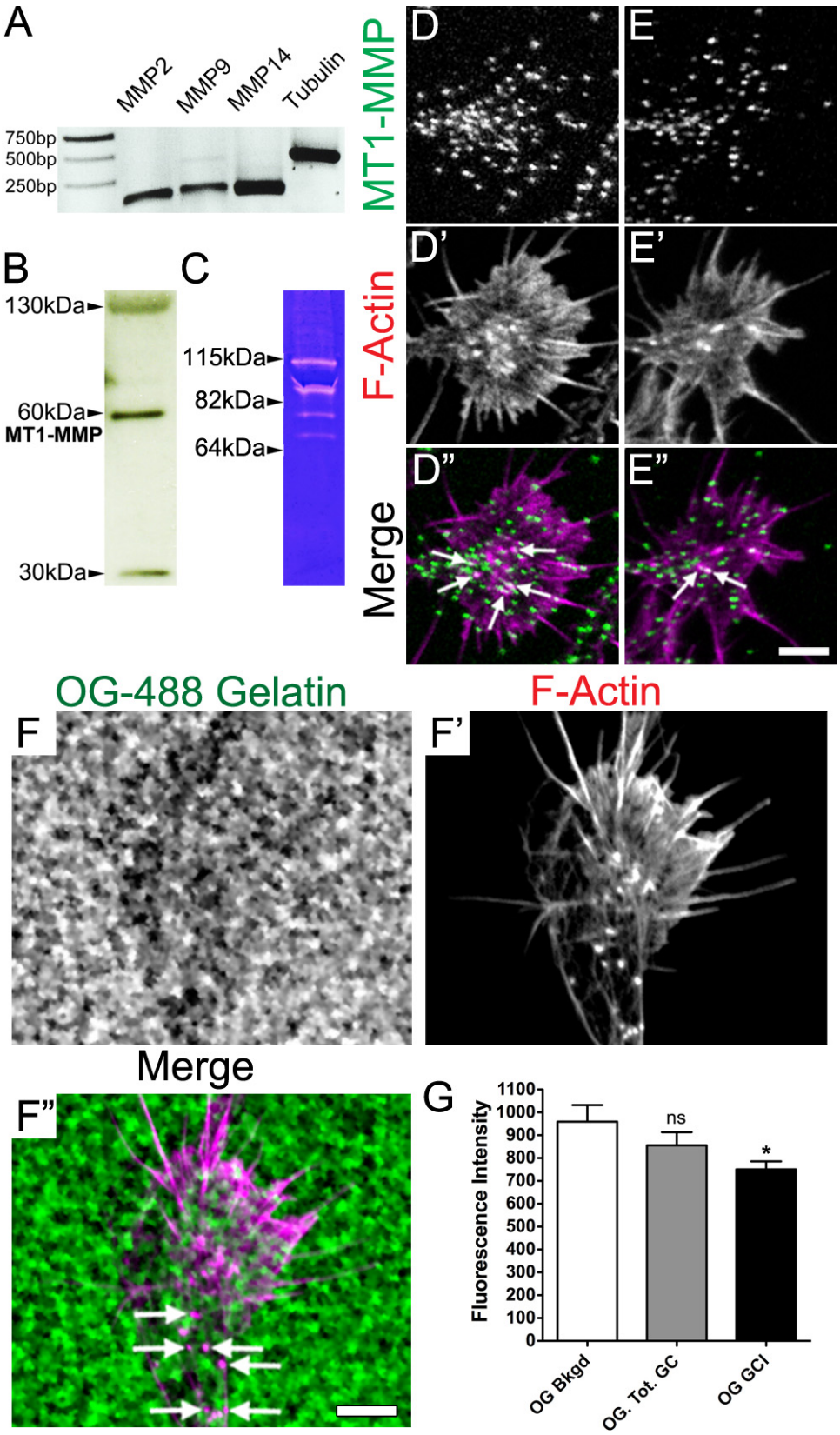
A
MMP2
MMP9
MMP14
Tubulin
750bp
500bp
250bp
B
130kDa
60kDa
MT1-MMP
30kDa
C
115kDa
82kDa
64kDa
MT1-MMP
F-Actin
Merge
D
E
D'
E'
D"
E"
OG-488 Gelatin
F-Actin
F
F'
Merge
F"
G
Fluorescence Intensity
1100
1000
900
800
700
600
500
400
300
200
100
0
ns
*
OG Bkgd
OG. Tot. GC
OG GCI

Figure 9. Model illustrating F-actin rich foci as growth cones invadosomes. A. SIM image of a Xenopus spinal neuron growth cone on LN, fixed and stained for F-actin (green) with Alexa-568 phalloidin and immunolabeled for βIII-tubulin (magenta). Note the F-actin rich foci within the growth cone central domain (arrows). **B.** Illustration of a cross-sectioned growth cone responding to environmental cues by remodeling the ECM with F-actin foci that become protruding invadosomes. Note how invadosomal F-actin lies perpendicular to the actin network within the growth cone. **C.** Magnification of a single cross-sectioned growth cone invadosome. Growth cones establish adhesions with the ECM through the interaction of integrins, SRC and adhesion proteins such as paxillin and FAK. Once localized to adhesion sites, SRC may phosphorylate Tks5 as well as proteins implicated in lipid raft formation. Phosphorylated Tks5 then localizes to lipid rafts and initiates actin polymerization. Polymerizing actin present at adhesion sites is directed perpendicularly through the activation of actin modulators such as cortactin, N-WASP, the Arp2/3 complex and Ena/Vasp. This network of branched actin pushes onto the membrane forming F-actin rich columns that span the width of the growth cone. Membrane bound and secreted proteases begin to degrade the ECM, allowing the actin column to transition into a 3-dimensional membrane protrusion. The protrusion, formed of both branched and unbranched actin filaments is stabilized by proteins such as α-actinin. In mature invadosomes, MTs polymerize into the protrusion providing increased stability and the delivery of vesicular cargo such as proteases and guidance cue receptors. Growth cone invadosome dependent axon guidance may represent a novel mechanism in which growth cones respond to environmental cues by remodeling surrounding tissues with 3-dimensional projections.

Figure 9.

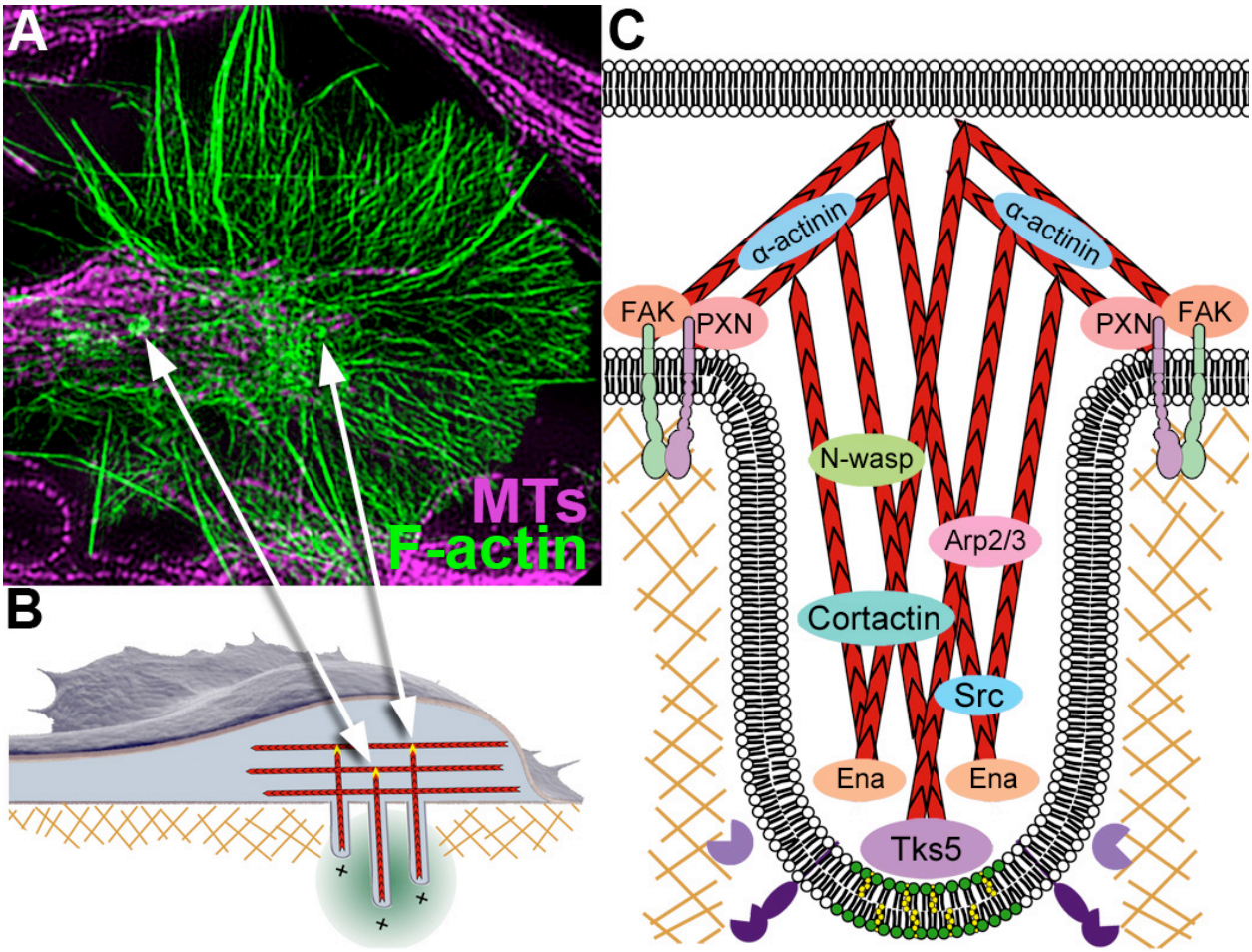
A
MTs
F-actin
B
C
α-actinin
α-actinin
FAK
PXN
PXN
FAK
N-wasp
Arp2/3
Cortactin
Src
Ena
Ena
Tks5

Supplementary Materials, Figure S1. Human iPSC growth cones exhibit F-actin rich foci. A-C. Confocal images of a human forebrain neuron (A), motor neuron (B) and RGC growth cone derived from iPSCs on LN, fixed and stained for F-actin with Alexa-546 phalloidin. Note the F-actin rich foci located within the growth cone central domain (arrowheads). Scale: 5 μm (A-C).

Supplementary Materials, Figure S1.

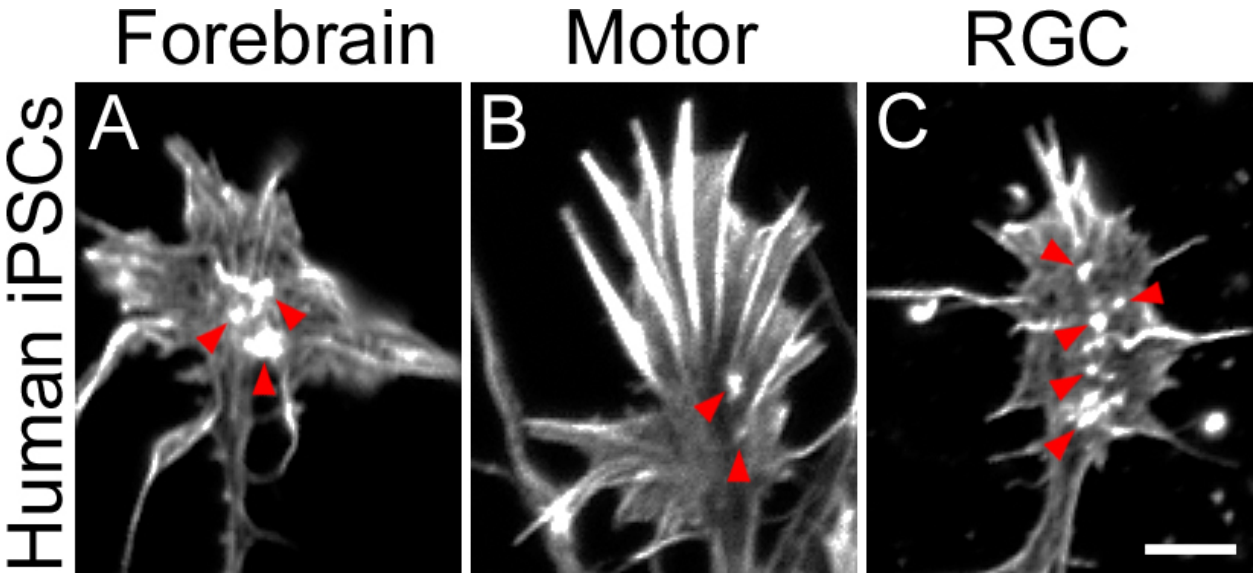

Supplementary Materials, Figure S2. Exogenously expressed actin constructs target to F-actin rich foci within the central domain of growth cones. A,B. TIRF images of a live growth cone on LN expressing mCh-UtrCH together with GFP-β-actin (A) or GFP-γ-actin. Note the colocalization of both β-actin and γ-actin with mCh-UtrCH labeled foci (A", B"; arrowheads). **C.** TIRF images of a live growth cone on LN expressing mCh-UtrCH to label F-actin. Note how a subset of actin foci are highly stable (red and blue boxes). **D**. TIRF images of a portion of veil of a live growth cone expressing mCh-UtrCH. Note how some actin foci are motile over time (arrowheads). Scale: 5 μm (A-B), 10 μm (C), 2.5 μm (D).

Supplementary Materials, Figure S2.

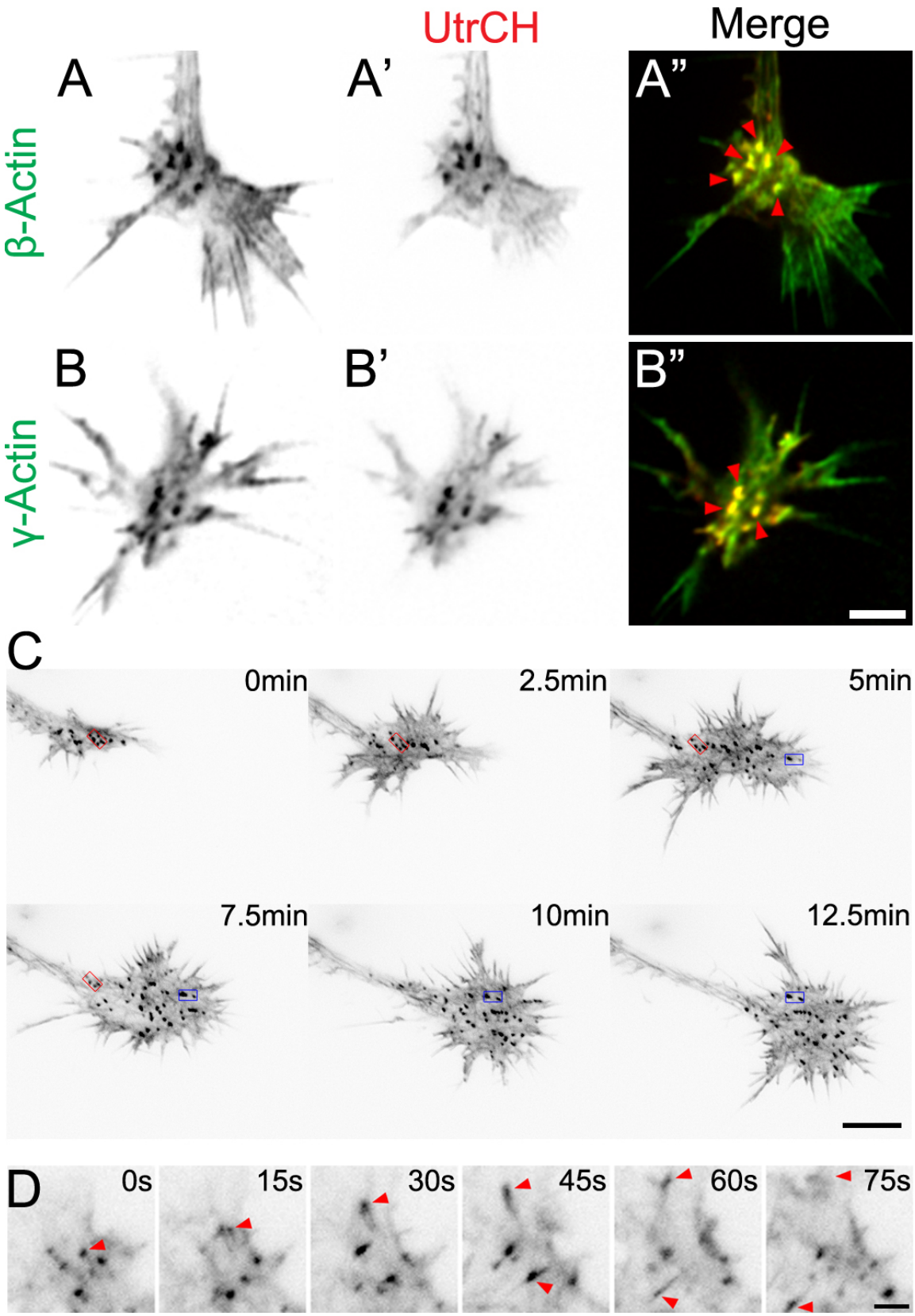

Supplementary Materials, Figure S3. F-Actin foci are in close contact with the substratum and colocalize with β1-integrin receptors. A, B. Confocal images of a live growth cone on LN expressing mCh-UtrCH and imaged using an IRM objective. **A, B.** IRM images. **A', B'.** mCh-UtrCH images. **A", B".** Merged images of the image obtained using the IRM objective (green) and mCh-UtrCH label (magenta). Note the colocalization of F-actin foci with IRM dark spots (sites of light interference created by the close contact of the membrane with the coverslip; solid arrowheads). Also note the interference created by point contacts in growth cone filopodia (open arrowheads). **C, D.** Confocal images of growth cones on LN, fixed and immunolabeled for β1-integrin receptors using the function blocking antibody Ab2999. **C', D'.** Alexa-546 phalloidin labeling of F-actin. **C", D".** Merged images of β1-integrin (green) and F-actin labeling (magenta). Note the colocalization of β1-integrin receptors with F-actin foci (solid arrowheads) as well as F-actin foci surrounded or in close proximity to β1-integrin clusters (open arrowheads). Scale: 5 μm (A-D).

Supplementary Materials, Figure S3.

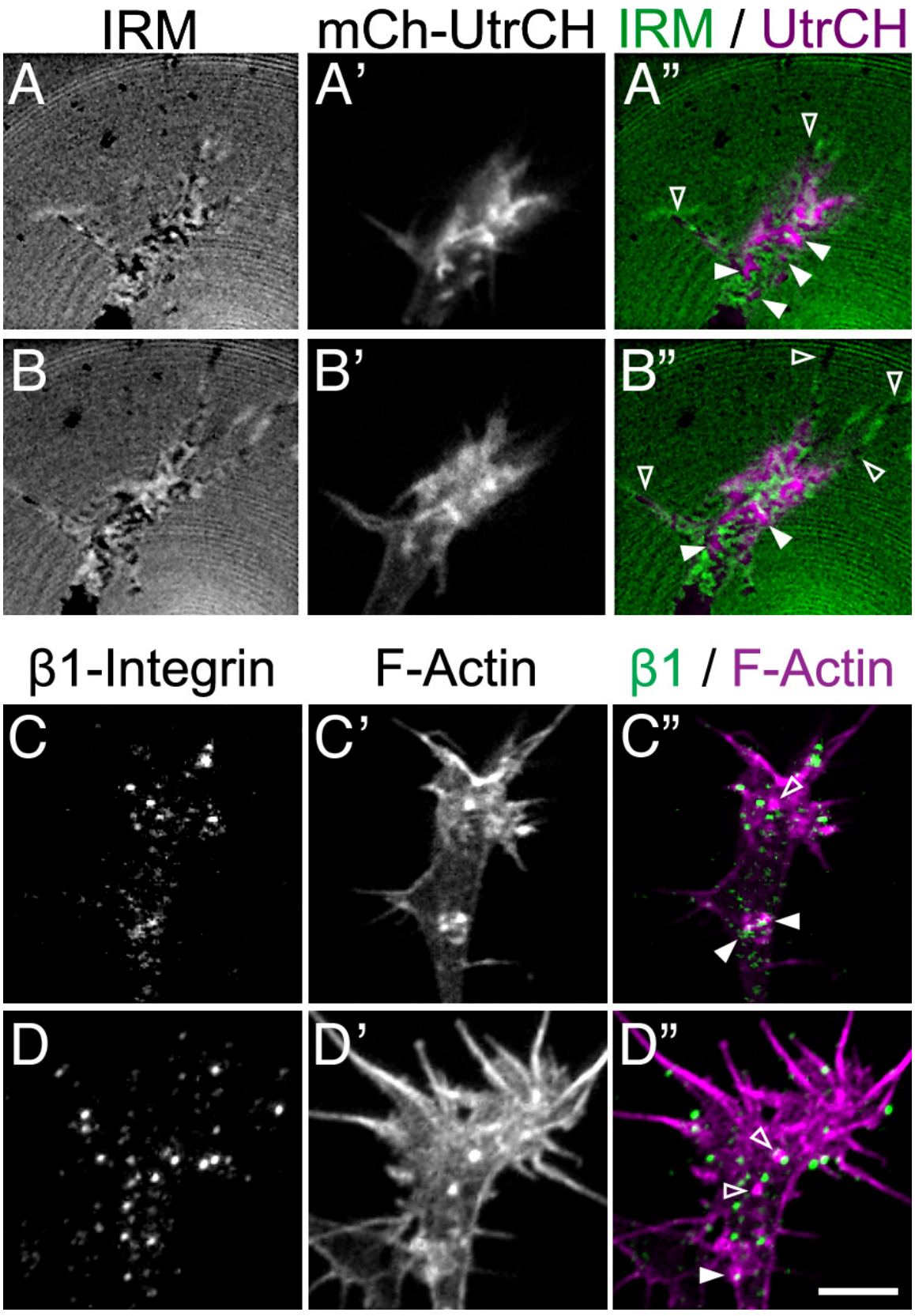

Supplementary Materials, Figure S4. Actin foci do not colocalize with exocytotic synaptic vesicles or endocytic vesicles. A. Confocal images of a growth cone on LN, fixed and stained for synaptic vesicle protein 2 (SV2; A) and F-actin using Alexa-546 phalloidin (A'). Note the distinct labeling of synaptic vesicles (open arrowheads) and actin foci (solid arrowheads) in the merge (A"). **B-E.** TIRF images of live growth cones on LN expressing either mCh-Rab5A (B, C) or DsRed-Clathrin light chain (D, E) and GFP-UtrCH to label F-actin (B'-E'). Note in the merge the lack of association between F-actin foci (solid arrowheads) and Rab5 or Clathrin (open arrowheads). Scale: 5 μm (A-E).

Supplementary Materials, Figure S4.

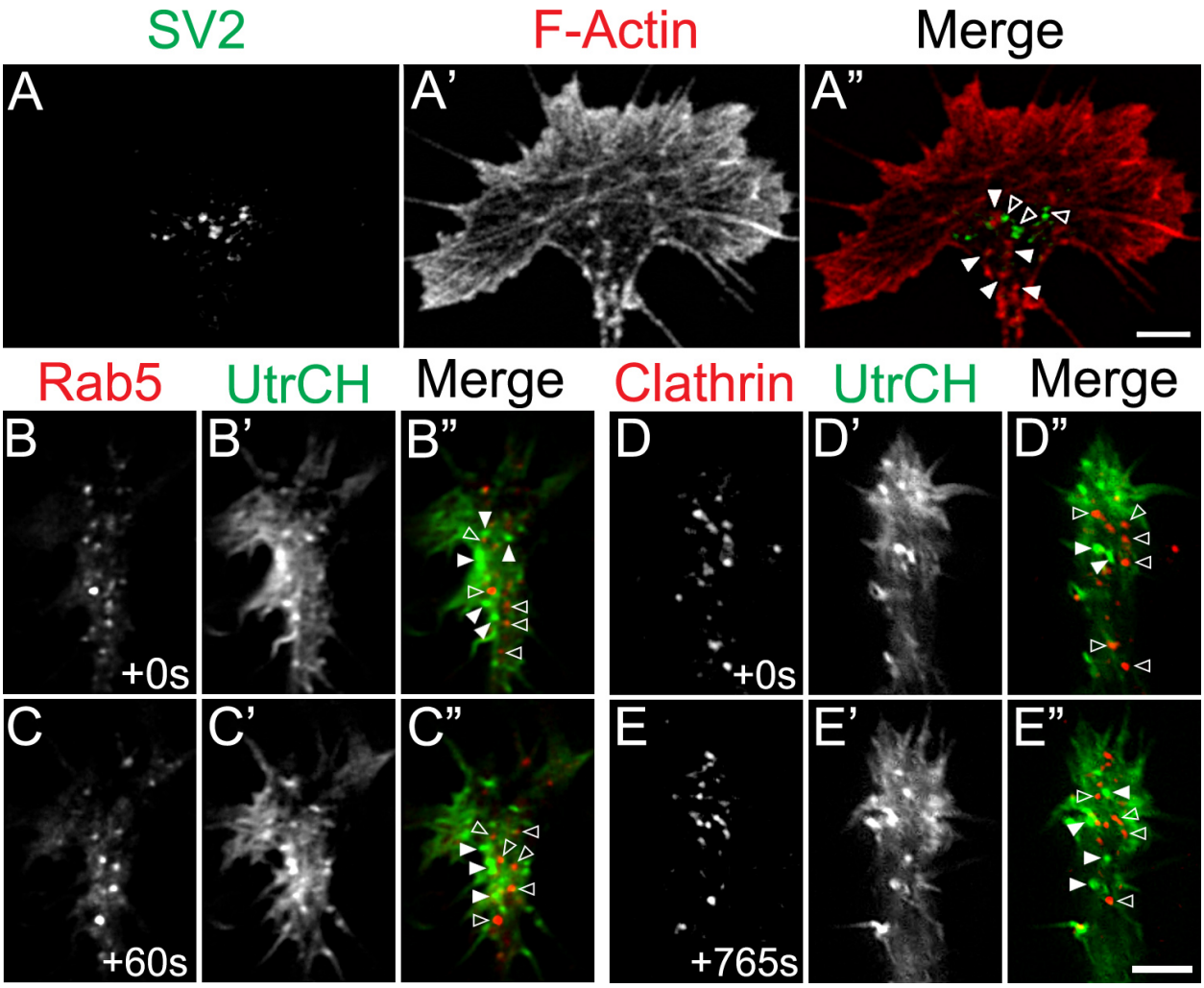

Supplementary Materials, Figure S5. F-actin foci colocalize with the actin modulator Cortactin within growth cones cultured on integrin engaging and independent substrata. A. Western blot from stage 24 Xenopus spinal cord illustrating the presence of Cttn in spinal neurons. Note the presence of both the full length protein (80 kDa) as well as the calpain proteolytic product of Cttn (45 kDa). **B-D.** Confocal images of growth cones from neurons cultured on fibronectin (FN; B), poly-D-lysine (PDL; C) or bare glass (D) and immunolabeled for Cttn. **B', C'.** Alexa-546 phalloidin labeling of F-actin. **B"-C".** Merged images of Cttn (green) and F-actin labeling (red). Note the strong colocalization of F-actin foci and cortactin despite the substrata provided for the growth cone (arrowheads). Scale: 5 μm (B-D).

Supplementary Materials, Figure S5.

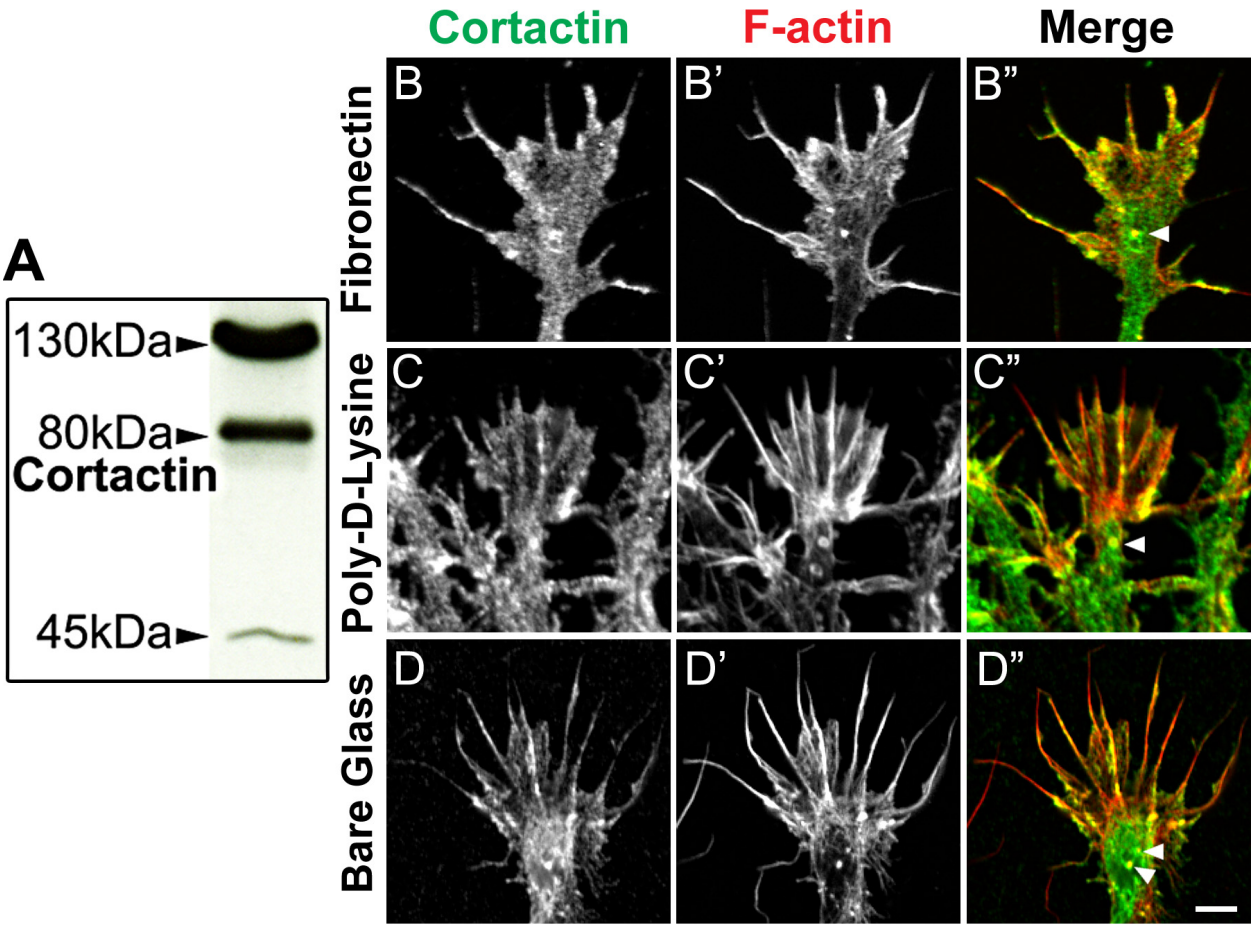

Supplementary Materials, Figure S6. Microtubules avoid or wrap around growth cone invadosomes. A-B. Confocal images of growth cones on LN, fixed and stained for βI,II-tubulin (A, B) and F-actin using Alexa-546 phalloidin (A', B'). Note how MTs avoid (A"; open arrowhead) or wrap around F-actin foci (B"; solid arrowheads). Scale: 5 μm (A-B).

Supplementary Materials, Figure S6.

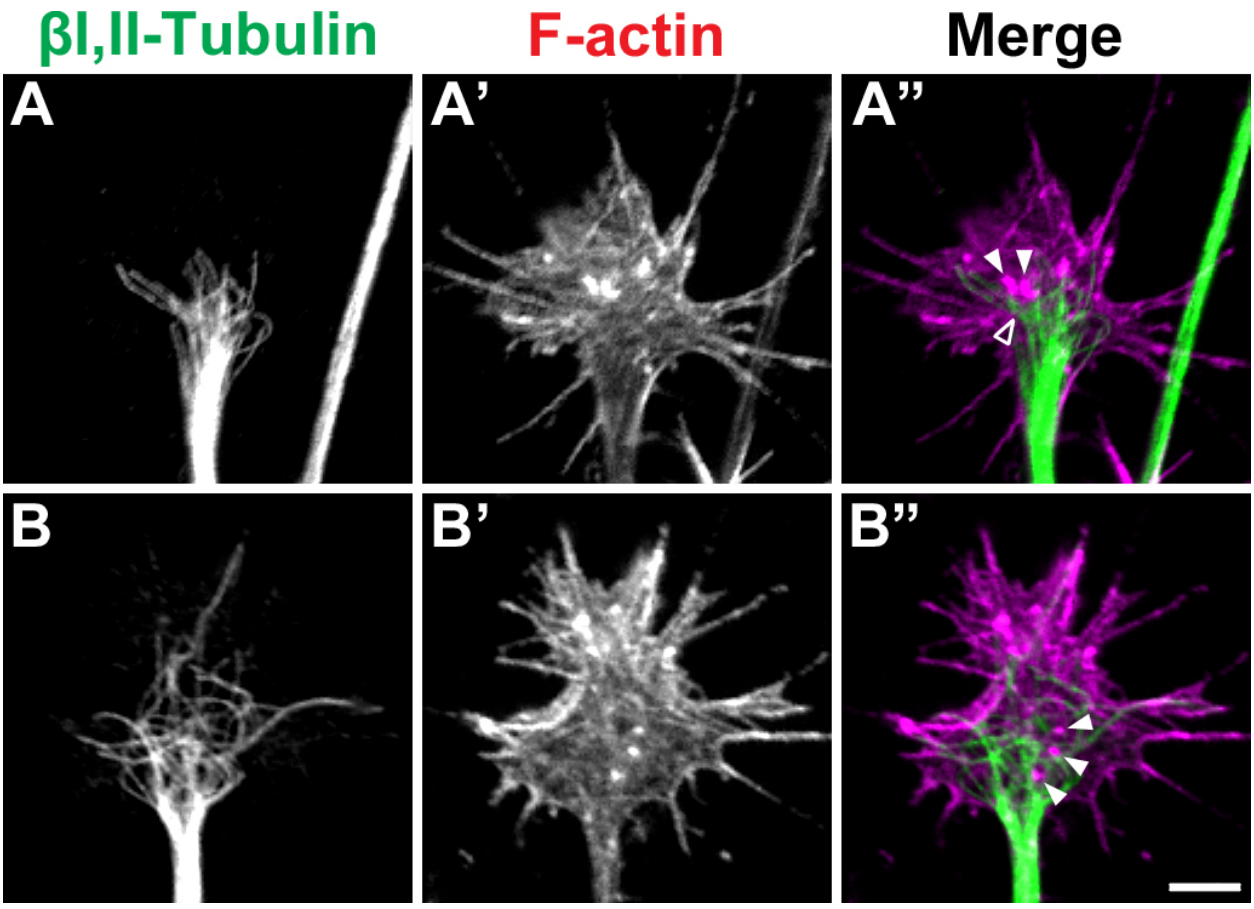

Supplementary Materials, Figure S7. Xenopus spinal axons extend in a 3-dimensional manner throughout a collagen gel. A-A". Confocal images of a Xenopus spinal explant cultured within a 3-dimensional collagen-1 gel. The gel embedded explant was fixed and stained for F-actin with Alexa-546 phalloidin (red) and immuolabeled for Cttn (green). **A.** Image of slice 1 of a 30 slice stack through the z-plane. **A'.** Image of slice 15 of 30. **A".** Image of slice 30 of 30. Note how axons are present throughout different focal planes (slices). Scale: 100 μm (A-A").

Supplementary Materials, Figure S7.

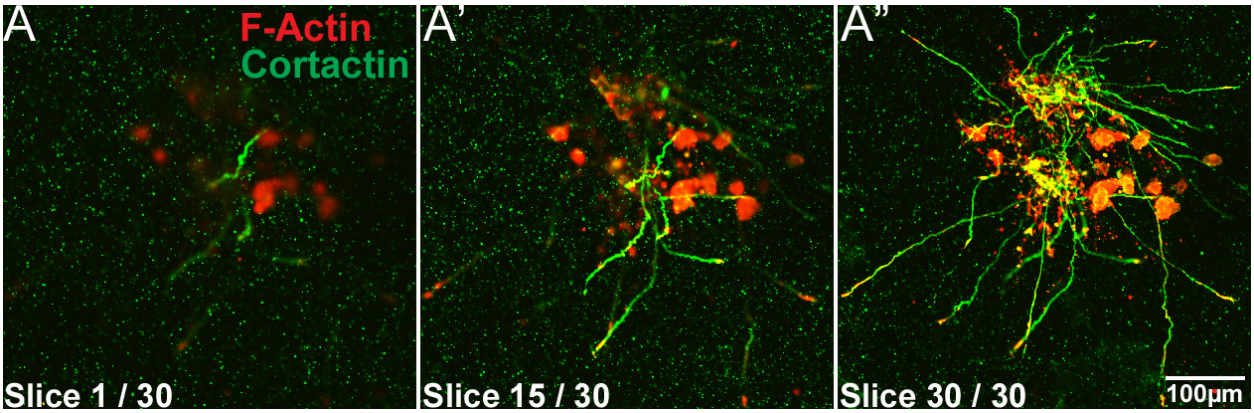

Supplementary Materials, Figure S8. Growth cone invadosomes are sites of ECM degradation. A, B. Confocal images of spinal neuron growth cones cultured on DQ-collagen IV. **A', B'.** Alexa-546 phalloidin labeling of F-actin. **A", B".** Merged images of the DQ-collagen IV (green) and F-actin label (magenta). Note the colocalization of growth cone invadosomes with areas of collagen degradation visualized as sites of unquenched fluorescence (open arrowheads). Scale: 5 μm (A-B).

Supplementary Materials, Figure S8.

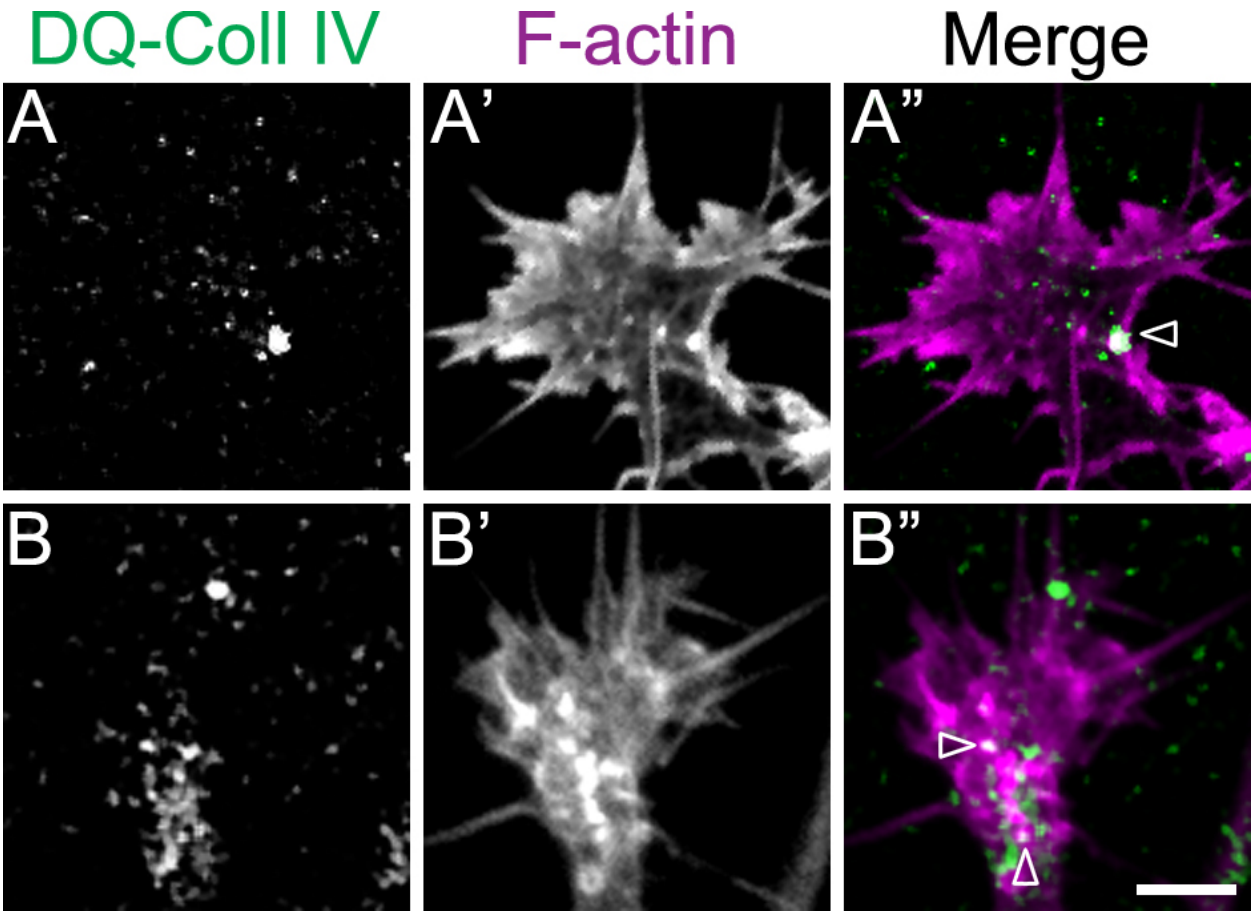

CHAPTER 4

Conclusions and Future Directions

In chapters 2 and 3, I describe two mechanisms important in the regulation of growth cone motility that likely function to guide axons within the developing embryo. Both mechanisms detail how the actin cytoskeleton and adhesions can modulate growth cone protrusion. Chapter 2 focuses on how PAK signaling is mediated in response to the disruption of its interaction with PIX at growth cone adhesions. I show that PAK2 and 3 localize with PIX to paxillin containing PCs. Upon disruption of the PAK-PIX interaction and, thus, removal of PAK from adhesions, I show that growth cones either accelerate or collapse depending on the amount of PAK displaced from PCs. Moreover, the acute removal of PAK from PIX leads to decreased PAK activity as measured by the phosphorylation of cofilin and myosin light chain, which function downstream of PAK. Additionally, I found Rac to also regulate neurite outgrowth by associating to PIX. In summary, I found that the PAK-PIX complex modulates neurite outgrowth.

In chapter 3, I describe a previously uncharacterized structure in growth cones that is analogous to the invadosomes of cancer and immune cells. I observed invadosomes in growth cones from many different cell sources and on many different substrata. Growth cone invadosomes contain many of the same key proteins found in cancer cell invadosomes and exhibit similar behaviors such as high actin turnover, protrusion into 3D space and ECM degradation. Moreover, I found that growth cone invadosomes require active Src function and intact lipid rafts for their stability and formation, respectively. Lastly, through imaging intact embryos with 3D super resolution microscopy, I found that invadosomes can be observed projecting deep into the skin from spinal neuron growth cones. My studies illustrate the importance of both the F-actin cytoskeleton and adhesion-based structures in mediating growth cone protrusion.

PART I: The role of PAK and its adaptor proteins in growth cone motility

PAK distribution in growth cones

In chapter 2, I demonstrate that PAK isoforms localize to different regions throughout spinal growth cones. PAK2 localizes to the tips of extending filopodia and to PCs whereas PAK3 localizes exclusively to point contacts. PAK1, conversely, is absent from spinal neurons and distributes homogeneously when expressed in growth cones. Because PAKs 1-3 all have very similar binding domains, it is unclear what determines their targeting specificity. To address if there are specific sequence differences among PAK members that dictate their differential targeting, the expression of isolated PAK domains and PAK isoform chimeras should be assessed. The expression of isolated PAK1-3 domains along with the use of chimeric proteins consisting of domains from PAK1-3 could narrow down the specific regions in PAK that are responsible for filopodial tip or point contact association in growth cones. This may also provide an understanding of why PAK1 does not localize to specific regions in growth cones despite containing similar binding domains as PAK2 and 3. Additionally, mutant versions of PAK2 and 3, such as catalytically inactive and constitutively active variants can be expressed and visualized to assess whether PAK kinase activity plays a role in its localization in growth cones. Similarly, point mutations in known PAK regulatory sites such as the Src phosphorylation site, Y132 (Renkema et al., 2002), can be studied to determine if posttranslational modifications play a role in PAK targeting.

PAK function in filopodia

The localization profile of PAK2 suggests that this PAK isoform regulates adhesion function and actin polymerization at PCs and filopodial tips in developing spinal growth cones. Functional evidence obtained using PAK18 and PAK2 mutants that can no longer bind PIX further suggest that PAK2 functions in filopodia formation and elongation as well as in neurite outgrowth. Because PAK18 disrupts PAK binding to PIX, and in doing so, displaces PAK from point contacts, it would be interesting to measure PAK2 at filopodia tips pre and post varying concentrations of PAK18. I would expect the increase in filopodia formation and extension to be accompanied by an increase in PAK2 at filopodial tips in response to PAK18. Interestingly, the downstream targets of PAK2 at filopodial tips remain unknown. While paxillin does not localize to the tips of extending filopodia, it can concentrate in filopodia, which may serve a role in the assembly of nascent adhesions (Hoffmann and Schafer, 2010). Therefore, PAK may function at filopodial tips to regulate adhesion dynamics, as well as actin polymerization and growth cone protrusion. However, because PAK2 localizes to filopodia in growth cones cultured on integrin independent substrata, and because the adaptor protein PIX, which links PAK to paxillin, is absent from filopodia, it is likely that PAK has additional functions on actin dynamics at tips independent of adhesion formation. This strongly suggests that PAK2 may regulate filopodia protrusion independent of its association to PCs. Indeed, several other studies have also implicated PAK signaling in the regulation of both axonal and dendritic filopodial extension and dynamics (Heckman et al., 2009a; Kayser et al., 2008). As mentioned above, the downstream targets of PAK2 at filopodial tips remain unknown. Although there are many PAK targets known to regulate actin

polymerization and filopodia elongation, a direct effector and mechanism has yet to be shown. The actin binding proteins mDia2 (Xie et al., 2008) and filamin (Vadlamudi et al., 2002) are two PAK substrates that have been implicated in filopodia formation and maintenance (Eisenmann et al., 2007; Ohta et al., 1999). To test if these proteins play a role in filopodia formation downstream of PAK function, their endogenous expression profiles should be examined followed by the expression of mutant variants in growth cones. It is likely that PAK2 may contain multiple effectors important in filopodial dynamics. To find additional PAK binding partners in developing spinal neurons and growth cones, proteins from isolated spinal cords should be co-immunoprecipitated with each PAK isoform then subjected to mass spectrometry (ten Have et al., 2011). Because the cell population within spinal cords consists of both neuronal and nonneuronal cells, fluorescence activated cell sorting (FACS) can be used to remove contaminants and enrich the cell population of interest within the sample (Schaffner et al., 1987). Phosphorylation screens, such as *in vitro* phosphorylation assays may also assist in the identification of PAK substrates (Johnson and Hunter, 2005). The aforementioned approaches may be useful in discovering previously unidentified PAK targets as well provide a further understanding of the molecular mechanisms of PAK-dependent filopodia extension and growth cone protrusion.

PAK-PIX function in PCs

In chapter 2, I show that PAK2 and 3 along with αPIX localize to PXN containing PCs. However, the role of these proteins in PCs and how these proteins interact with one another to regulate adhesion dynamics remains unclear. It is widely accepted that

PAK association to PXN based adhesions requires PIX binding since PAK mutants that can no longer bind PIX fail to target to adhesions (Manser et al., 1998; Santiago-Medina et al., 2013; Turner et al., 1999). What remains unclear about this interaction is the activation state of PAK while bound to PIX at PXN based adhesions. Some studies suggest that when bound to PIX, PAK is active (Manser et al., 1998; Stofega et al., 2004) whereas other studies put forward the contrary (Mott et al., 2005; ten Klooster et al., 2006). Additionally, some studies suggest that PAK activity is differentially regulated depending on the specific PIX isoform it is engaging. The PIX isoforms, αPIX and βPIX, are encoded by two different genes, and can be expressed as different splice variants, which are thought to regulate PAK function and adhesion dynamics differently (Mayhew et al., 2007). For example, αPIX greatly enhances PAK activity whereas βPIX can have both a permissive effect or an inhibitory effect on PAK activity. This suggests that the PAK-PIX interaction may regulate adhesion dynamics and cell motility in a cell specific manner, depending on the variant of PIX expressed in the cell. From my own results, I observed that *Xenopus* spinal neurons express more αPIX than βPIX and that disruption of the PAK-PIX interaction in neurons results in PAK inhibition (Santiago-Medina et al., 2013), which is in accordance with the notion that αPIX associates with active PAK. However, it would be interesting to determine the expression profile of PIX isoforms and their splice variants in developing neurons over time as well as in different neuronal populations. Biochemical techniques such as RT-PCR and pull-downs can be used to determine which PIX variants are present in specific neuronal populations and the activation status of PAK when bound to a PIX variant, respectively. Interestingly, a number of βPIX splice variants are expressed in the developing CNS and are thought to

function in early neuronal migration (Kim et al., 2000; Kim and Park, 2001).

Another important question to address is whether PAK phosphorylates PIX and if so, what effect does this modification have on the interaction between these proteins. The diverse and highly regulated functions of PIX strongly suggest it is modulated through phosphorylation. Indeed, PAK2-dependent phosphorylation of PIX at S525 and T526, augments Rac1 activation by enhancing PIX GEF function (Shin et al., 2002; Shin et al., 2004). Similarly, phosphorylation of PIX at S516 and T526, results in PIX translocation to adhesions and activation of Cdc42 (Chahdi et al., 2005). These studies place PAK-induced phosphorylation of PIX upstream of Rho-GTPase activity and adhesion targeting, further complicating the conventional mechanism of PAK activation and function. Additional roles for PIX phosphorylation may include enhanced targeting of PAK to PXN-based adhesions or perhaps the binding and sequestering of PAK as a way to control its activity on other targets. More research is needed to assess the role of PIX phosphorylation on adhesions and on Rho-GTPase activation and the role these may play in modulating growth cone motility throughout development. To address the possible functions of phospho-PIX in adhesion dynamics and growth cone motility, phosphomimetic and non-phosphorylatable point mutants can be introduced and examined in spinal neurons. Excitingly, much remains unknown about the function of PIX in nonneuronal cells and even more so, in developing neurons.

PAKs are known to regulate cell motility by affecting both the formation and turnover of cell-substratum adhesions. In certain breast cancer cell lines, PAK is constitutively active and functions to promote both the formation and stability of focal adhesions (Stofega et al., 2004). Disruption of the PAK1-αPIX interaction, in these

cancer cells, leads to a dramatic reduction in both PAK activity and in PIX and PXN localization to adhesions. Conversely, PAK1 activity has been linked to focal adhesion disassembly in HeLa cells (Manser et al., 1997). In CHO cells, PAK activity was found to induce adhesion turnover through PXN phosphorylation of S273 (Nayal et al., 2006). Cell expressing a phosphomimetic version of PXN (S273D-PXN) contain faster adhesion turnover and increased cell motility whereas cells expressing a non-phosphorylatable variant (S273A-PXN) do the opposite. It is important to consider that the differences in PAK-induced adhesion regulation observed across cell types may arise due to specific PAK or PIX isoforms present, as mentioned above as well as other adhesion-implicated mechanisms employed in the cell. For example, Xenopus spinal neuron growth cones that express S273D-PXN exhibit faster rates of adhesion turnover and motility whereas growth cones expressing S273A-PXN are unaffected and behave mostly like WT cells. This suggests, that in spinal growth cones, PAK may serve a role in regulating PXN turnover but that other mechanisms within the cell, such as FAK or Rac induced adhesion turnover, are sufficient to modulate growth cone motility (Myers and Gomez, 2011; Woo and Gomez, 2006). Furthermore, there may also exist other downstream targets of PAK that modulate growth cone adhesion, such as the clutch protein, shootin1 (Toriyama et al., 2013). Additional work is needed to elucidate the mechanisms pertinent to adhesion-based growth cone motility and axon guidance.

Rac1 activity is controlled in part through PAK-PIX interactions

In chapter 2, I demonstrate that disruption of the PAK-PIX interaction with a low dose of PAK18 can potentiate neurite outgrowth. Enhanced growth cone motility in

response to PAK18 was due to the inhibition of PAK and activation of ADF/cofilin, myosin II and, surprisingly, Rac1. This finding was unexpected since the conventional mechanism involving PAK activation places Rac1 upstream of PAK, not downstream as it seems to occur in response to disruption of the PAK-PIX interaction. Other studies confirm that the association of PAK with PIX can regulate Rac1 function, which in turn can further regulate PAK activity in a specialized feedback loop (Obermeier et al., 1998; ten Klooster et al., 2006). These reports state that PAK modulates Rac1 activation by localizing Rac1 to PAK bound PIX, which in turn can execute its function as a GEF on Rac1. The experiments done, both in my study as well as in those done by others, used a dominant negative version of Rac1 (T17N-Rac1), which has a high affinity for GEFs but cannot be activated by them. Since this variant of Rac1 sequesters and inhibits other GEFs from activating other GTPases, there may be nonspecific effects when trying to study the interaction solely between Rac1 and PIX. Furthermore, when using T17N-Rac1 you can no longer study the interaction between PAK and PIX since dominant negative Rac will have presumably sequestered all PIX proteins. Other mutants versions of Rac should be designed such as versions that can no longer bind PIX or PAK, to understand the role Rac has in regard to the PAK-PIX interaction. Moreover, future studies should decipher what the normal levels of PAK and Rac competition for PIX are in growth cones as well as discern the endogenous regulators of competitive PIX binding. It is possible that the competition between PAK and Rac for PIX may be to establish a balance in the activation of these two proteins. Alternatively, a scenario may exist that when at select decision points within the developing spinal cord, navigating axons are exposed to certain guidance cues that can prompt the

dissociation of PAK from PIX to enhance the activation of Rac, which can potentiate neurite outgrowth. Because PIX can also function as a GEF for Cdc42, the role of this Rho-GTPase downstream of the PAK-PIX interaction should also be examined.

The role of PAK in axon guidance

Previous studies have shown that PAKs can induce growth cone changes in response to both attractive and repulsive guidance cues *in vitro* and *in vivo* (Kreis and Barnier, 2009). The data I present in chapter 2 suggest that PAKs may play an important role in the guidance of developing axons by modulating the cytoskeleton and adhesions of growth cones. Specifically, my findings demonstrate that PAKs regulate neurite outgrowth by influencing F-actin polymerization and retrograde flow, as well as integrin-dependent adhesion to laminin (Santiago-Medina et al., 2013). Since PAK function is implicated in adhesion regulation, cytoskeletal rearrangements and membrane protrusion, PAKs may play a crucial role in the guidance of developing axons downstream of guidance factors. Interestingly, both filopodia and adhesion dynamics, which PAK can directly modulate, have been implicated in axon guidance (Gomez and Letourneau, 1994; O'Connor et al., 1990; Zheng et al., 1996). Therefore, it is of extreme importance to examine and understand how PAK dependent changes on the cytoskeleton and PCs can mediate growth cone behavior in response to attractive and repulsive axon guidance cues.

PAK is known to produce cytoskeletal rearrangements in the presence of neurotrophic factors and guidance cues through its association with the adaptor protein Nck (Ang et al., 2003; Fan et al., 2003; Hing et al., 1999). Nck is a PAK binding adaptor

protein that links the N-terminal of PAKs to guidance cue receptors, such as receptor tyrosine kinases (RTKs), DCC, EphB, and Robo (Fan et al., 2003; Galisteo et al., 1996; Shekarabi et al., 2005; Srivastava et al., 2013). Despite the importance of the PAK-Nck complex, the molecular mechanisms controlling Nck function in growth cones remain poorly understood. In nonneuronal cells, Nck localizes to adhesions and functions in regulating filopodia formation and extension (Antoku et al., 2008; Woodring et al., 2004). Because Nck is such an important adaptor protein implicated in PAK-mediated axon guidance, significant research should go into examining the distribution of Nck isoforms in growth cones and assessing how they interact with PAKs in the absence and presence of guidance cues. It would be interesting to determine if Nck binding is important in the redistribution of PAK proteins downstream of different guidance cues and neurotrophic factors. For example, since the PAK-Nck interaction functions downstream of RTK signaling in nonneuronal cells (Galisteo et al., 1996), perhaps it also plays a role in BDNF-TrkB signaling in growth cones. Additionally, because PAK-Nck function is known to act downstream of netrin and slit signaling (Fan et al., 2003; Lucanic et al., 2006; Shekarabi et al., 2005), it would be interesting to determine if PAK proteins play a role in mediating commissural axon midline crossing at the spinal cord floor plate. PAK, Nck and PIX mutants can be introduced into commissural neurons to assess the roles they may have in guiding axons across the spinal cord midline. Turning assays *in vitro* may also be used on growth cones expressing the previously mentioned mutants.

Studies suggest that in response to guidance cues, PCs are asymmetrically regulated during growth cone turning (Hines et al., 2010; Myers and Gomez, 2011;

Myers et al., 2011). In chapter 2, I show that acute disruption of the PAK-PIX interaction can increase the formation of PCs as well as modulate adhesion lifetime. It remains unclear, however, if guidance cues modulate the function of PAK or PIX on PCs to influence growth cone motility and axon guidance. Interestingly, it has been shown that the PAK-Nck signaling complex can recruit the PIX-PXN adhesion complex downstream of integrin and Rho-GTPase signaling (Brown et al., 2005; Turner et al., 1999). This would create an intriguing molecular complex where receptor activation would be linked with adhesion dynamics, through PAK function, to promote growth cone protrusion. Moreover, it would be interesting to determine if the PAK-Nck interaction plays a key role in filopodia dynamics in the presence of guidance cues by acting as an intermediate between growth factor and adhesion signaling to mediate growth cone guidance. Furthermore, the association of Nck with PAK-PIX-PXN and the function of this complex on PC dynamics should also be tested in navigating spinal axons in response to guidance cues.

PART II: The role of invadosomes and metalloproteases in growth cone motility

Invadosome-like structures in growth cones

Metastatic cancer cells, osteoclasts and those of monocytic lineage form actin rich structures known as invadosomes. Invadosomes assist in cell migration by functioning as adhesion sites and invasive modules through adhesion to the ECM and localization of extracellular protease activity, respectively. The role of invadosomes in the cell types mentioned above are not only well documented but are continually studied. Their existence and possible role in neuronal cells, however, remains mostly unexplored. To date, neural crest cells are the only other neuronal cell type that has been documented to form invadosomes (Murphy et al., 2011). In chapter 3, I demonstrate that growth cones from different neuronal populations and across species form actin rich structures highly reminiscent of invadosomes. Using ICC, pharmacological perturbations and super resolution microscopy, I was able to determine that growth cones form invadosome-like structures both *in vitro* and *in vivo*. This finding initially came as a surprise since no other study has ever mentioned the presence of invadosomes in growth cones. However, the role for invadosomes in growth cone motility and axon guidance seems highly plausible. In the developing embryo, axon extension through 3D tissues likely requires growth cones to interact with ligands presented to both their ventral (apical) and dorsal (basal) surfaces. Moreover, guidance along pathways or entry into tissues likely requires local proteolytic cleavage of ECM molecules and other ligands or receptors by pericellular proteases expressed and secreted by growth cones and their invadosomes.

Many of the proteins localized to invadosomes are ones that are functional else where in the cell. For example, two well known regulatory proteins for invadosome function are cortactin and Src (Boateng and Huttenlocher, 2012). In growth cones, both these proteins have roles in lamellipodia and filopodia formation (Decourt et al., 2009; Robles et al., 2005). Furthermore, I show that cortactin and Src do target to growth cone invadosomes as well as to the leading edge and tips of filopodia, respectively. Because many of the proteins implicated in invadosome formation are broadly expressed throughout the cell, it is hard to perturb their activity and selectively study their role in invadosomes. Two proteins said to be unique in invadosomes are Tks4 and Tks5 (Courtneidge, 2012). In chapter 3, I show that both isoforms are expressed in spinal neurons and that Tks5 localizes to actin rich foci in fixed and live growth cones. Interestingly, although exogenously expressed Tks5 did localize to F-actin foci, its expression caused foci, which are usually stable, to become motile. This observation was obtained using human Tks5, which is 70% homologous to *Xenopus* Tks5. Because of the sequence differences between human and *Xenopus* Tks5, it is possible that human Tks5 may be altering the endogenous protein by functioning as a dominant negative. In fact, Tks5 knockdown in cells results in highly motile invadosomes that never mature into stable ones (Sharma et al., 2013). Because Tks proteins are unique to invadosomes, future studies should regulate their function by knockdown or mutant expression to elucidate their role in invadosome-mediated axon guidance.

Role of invadosomes as adhesion sites to the ECM

As mentioned above, invadosomes can act as adhesion sites. They do this by expressing integrins and associated adhesion proteins such as vinculin, talin, paxillin and FAK (Albiges-Rizo et al., 2009; Hoshino et al., 2013). In chapter 3, I demonstrate that growth cone invadosomes contain β1-integrin, paxillin and FAK. Furthermore, I show that paxillin localizes transiently, but continually, to most invadosomes throughout their lifetime. It would be interesting to determine if other adhesion proteins localize to growth cone invadosomes and assess their recruitment and dynamics over time. Additionally, it would also be interesting to assess if there exists a correlation between PCs and invadosomes in growth cones. In cancer cells, FAK has been shown to mediate a switch from focal adhesion formation to invadopodia formation by redistributing active Src and phosphotyrosine-containing proteins from adhesions to invadopodia (Chan et al., 2009). Importantly, the engagement of α3β1-integrin with LN-332 can mediate this switch (Liu et al., 2010), suggesting that molecules in the growth cone environment can regulate invadosome formation throughout guidance. Further work should go into finding additional interactions that may occur between the growth cone and its environment that can regulate the switch from PCs to invadosomes.

Similar to adhesions, invadosomes can function as mechanosensory structures, suggesting that mechanotransduction signaling can regulate their function (Collin et al., 2008). Likewise, substrate rigidity is known to control the number and activity of invadopodia in both cancer and endothelial cells (Alexander et al., 2008; Juin et al., 2013). Transduction of ECM-rigidity signals depended on the cellular contractile apparatus, given that inhibition of myosin II and Rho kinase abolished the increase in

invadopodia-dependent ECM degradation. Future studies consisting of traction force microscopy and ECM rigidity assays will be necessary to understand the role matrix-integrin interactions have in controlling invadosome activity. Moreover, it is imperative to determine if the matrix rigidity of different tissues can promote invadosome formation in growth cones navigating within the developing embryo. It is possible that during guidance, growth cones use invadosomes to sense and remodel tissue stiffness.

Invadosomal proteases in growth cones

Invadosomes of nonneuronal cells are reported to MMP2, 9, 14 and ADAM12, 15, 19 proteolytic activity (Murphy and Courtneidge, 2011). In chapter 3, I show the presence of MMP2, 9 and 14 in spinal neurons and the expression of MMP14 in growth cones. I also show that spinal neurons exhibit proteolytic activity within the intact spinal cord as well as in culture. To date there exists approximately 40 pericellular proteases known to remodel the ECM and membrane-bound proteins. Studies show that MMPs 2, 3, 7, 8, 9, 14, 24 and ADAMs 1, 9, 10, 11, 12, 17, 22, 23, 25 are expressed in neurons (Fujioka et al., 2012; Lin et al., 2010; Loers et al., 2012; Seals and Courtneidge, 2003; Tominaga et al., 2011; Zivraj et al., 2010). Due to the large amount of extracellular proteases present in neurons, a concerted research effort should go into elucidating the proteases relevant in axon guidance. When examining the expression profile of metalloproteases, much work will be needed to determine if distinct neuronal populations express specific proteases and if these proteases are expressed differentially over time during development. To assist in assessing the localization patterns of protease activity in the intact developing spinal cord, techniques such as

differential *in vivo* zymography (IVZ) can be used (Vandooren et al., 2013). In differential IVZ, FRET-quenched metalloprotease-substrate peptides are injected into different regions within developing embryos. Once these peptides are proteolytically cleaved, the quencher molecules diffuse away generating a dramatic increase in fluorescence. Currently, this technique has been used in both metamorphosing *Xenopus* tadpoles and zebrafish embryos and has successfully detected proteolytic activity in the developing brain and spinal cord (Keow et al., 2011). Once protease activity is mapped to specific regions, these regions can be molecularly dissected to elucidate the proteases and substrates in question. This approach may also assist in the discovery of possible combinatorial or synergistic effects of ECM and guidance cue signaling in the generation of protease activity in developing tissues.

The role of invadosome proteases on ECM remodeling

As mentioned in a previous section, the constitution of the ECM is known to regulate invadosome formation and protease secretion. Specific ECM components can either reduce [LN-332 via α3β1-integrin (Liu et al., 2010)] or enhance [FN via α5β1-integrin (Branch et al., 2012)] invadosomal-dependent protease secretion. This suggests that ECM proteins act as proteolytic regulators, promoting degradation in one tissue and halting it in another. Such a mechanism may exist to help axons traverse a tissue of specific ECM composition and then stop growth once the axon has reached its synaptic target where matrix proteolysis is no longer needed. The degradation of matrix molecules during neurite outgrowth may be to generate a barrier-free path, permissive to axon extension or to expose cryptic sites or growth factors and guidance cues within

the ECM (Yong et al., 2001). To aid in the understanding of substrate-mediated invadosome formation and activity regulation, the distribution of ECM proteins in the developing nervous system will need to be elucidated. Moreover, to determine the role of ECM degradation in growth cone motility, neurite outgrowth from spinal explants cultured on nonhydrolyzable ECM should be measured (Ehrbar et al., 2011).

Invadosomes and Metalloproteases in guidance

In addition to ECM regulation, invadosomes and proteases can act on guidance cues and their receptors to influence axon guidance. Many neuronal populations such as RGCs, motor axons and commissural interneuron axons depend on metalloprotease activity for guidance in developing tissues (McFarlane, 2003). Likewise, many guidance cue receptors and ligands are proteolytically regulated by MMPs and ADAMs, such as DCC, Ephs, Slits, Semaphorins and Ephrins. Additionally, proteases can also convert pro-neurotrophins into mature neurotrophins, which also regulate axon guidance (Marler et al., 2010). Because many guidance cues can regulate protease activity, it would be interesting to measure the formation of invadosomes and their proteolytic activity in growth cones treated with guidance cues and pro-neurotrophins such as pro-BDNF. To further characterize how metalloproteases regulate guidance cue signaling in growth cones, selective MMP and ADAM inhibitors can be administered to neurons growing in the presence of specific guidance cues. This assay should be done with neurons growing on fluorescent gelatin to assess whether there is an increase in protease activity in response to guidance cue addition. Similarly, 3D guidance assays where spinal explants are embedded in a collagen gel and exposed to a guidance cue gradient

can test the role of metalloproteases in 3D neurite outgrowth and guidance. As an alternative to embedding neurons in 3D ECM gels, modified chemotaxis assays can be employed. For example, a modified Boyden, Campenot or Dunn chamber with an added ECM barrier between the cells and guidance cue reservoir can be used to determine if matrix proteolysis is a factor in guidance towards a chemoattractant (Tominaga et al., 2011). This assay should be done with and without specific inhibitors to narrow down the proteases involved in mediating the guidance response. Additionally, whole embryos incubated in different metalloprotease inhibitor solutions can be analyzed for axon guidance defects resulting from protease inhibition.

Invadosomes and their associated proteases may also have a role in guiding the processes of newly born neurons in the adult brain. It is known that metalloproteases function in the adult brain as synaptic circuit remodelers by cleaving the synaptic adhesion proteins ICAM5 and neuroligin (Huntley, 2012; Suzuki et al., 2012). It is also known that similar guidance cue mechanisms, such as Slit-Robo signaling, regulate the migration of newly born neurons from the subventricular zone to the olfactory bulb in the adult brain (Kaneko et al., 2010). Interestingly, metalloproteases are known to regulate Slit-Robo signaling by proteolytically disrupting their interaction (Coleman et al., 2010; Schimmelpfeng et al., 2001), suggesting that invadosomes and proteases may regulate axon guidance in the adult brain as they do in the developing one.

The role of invadosomes and metalloproteases in regeneration

Injury to the CNS often results in permanent deficits because axons fail to undergo regeneration, which is attributed to both extrinsic and intrinsic factors. Extrinsic

factors include myelin-based proteins that inhibit neurite growth and components in the glial scar that aside from inhibiting growth, also act as an impenetrable barrier (Hur et al., 2012). Interestingly, in animals with high CNS regenerative capacity, like the Axolotl and zebrafish, MMPs are upregulated at the site of nerve damage and subside when recovery is near completion (Chernoff et al., 2000; McCurley and Callard, 2010). CNS injury-induced MMP upregulation has also been found in adult rats, where gelatinase activity was shown to assist neurite growth into the glial scar (Duchossoy et al., 2001). In both studies, however, it remains unclear if the source of metalloprotease activity is from the regenerating neurons or from the neuroglia surrounding the lesion. More experiments, where protease activity in neurons is either removed or elevated, will be needed to assess the role of neuronal versus glial metalloprotease activity in CNS regeneration.

Metalloproteases may modulate post-injury plasticity by hydrolyzing myelin-associated inhibitory ligands, the receptors to these ligands and components of the glial scar. Studies have demonstrated that MMP2 and 24 proteolytically process CSPG, a major constituent of the post-injury glial scar, allowing for axonal growth (Hayashita-Kinoh et al., 2001; Zuo et al., 1998). Moreover, cell culture assays demonstrate that myelin-associated glycoprotein (MAG), along with its receptors NGR1 and $p75^{NTR}$, can be cleaved by MMPs and ADAMs, attenuating growth cone collapse in response to these myelin-associated inhibitors (Ahmed et al., 2006; Ferraro et al., 2011; Milward et al., 2008; Walmsley et al., 2004). These studies suggest that metalloprotease-mediated proteolytic regulation of this inhibitory signaling system can directly influence the molecular cascade through which myelin-derived inhibitors and their receptors regulate

regeneration in the CNS. Future work will need to go into devising therapies where metalloprotease activity is promoted early on, within the onset of injury, to prevent scaring and allow for neurite regrowth but then decrease this activity as too much can further injure the regenerating CNS.

PAK-mediated control of invadosome formation

Although the studies described in chapter 2 and 3 focus on two distinct mechanisms, important in growth cone motility, numerous studies exist that demonstrate a role for PAK in the formation and metalloprotease activity of invadosomes. Specifically, both cancer cells and macrophages transfected with inhibitory PAK1 or PAK4 mutants exhibited a marked decrease in invadosome formation and ECM degradation (Ayala et al., 2008; Gringel et al., 2006). PAK activity is known to modulate invadosomes through phosphorylation of key components like the F-actin regulatory proteins, LIMK, myosin, and cortactin (Murphy and Courtneidge, 2011). For example, both LIMK activity and myosin-mediated contractility regulate invadosome formation and stability (Bhuwania et al., 2012; Scott et al., 2010; van Helden et al., 2008). Similarly, PAK phosphorylation of cortactin on Ser113, enhances invadosome formation and associated ECM degradation (Ayala et al., 2008). Because of the robust effects of PAK18 on neurite outgrowth, it would be interesting to assess whether disruption of the PAK-PIX interaction has effects on invadosome modulation in growth cones. Moreover, similar experiments such as LIMK inhibition and expression of cortactin mutants, S113D and S113A, should be used in growth cones to characterize the role of PAK targets in invadosome regulation and function.

References

Ahmed, Z., Mazibrada, G., Seabright, R. J., Dent, R. G., Berry, M. and Logan, A. (2006). TACE-induced cleavage of NgR and p75NTR in dorsal root ganglion cultures disinhibits outgrowth and promotes branching of neurites in the presence of inhibitory CNS myelin. FASEB J 20, 1939-41.

Albiges-Rizo, C., Destaing, O., Fourcade, B., Planus, E. and Block, M. R. (2009). Actin machinery and mechanosensitivity in invadopodia, podosomes and focal adhesions. J Cell Sci 122, 3037-49.

Alexander, N. R., Branch, K. M., Parekh, A., Clark, E. S., Iwueke, I. C., Guelcher, S. A. and Weaver, A. M. (2008). Extracellular matrix rigidity promotes invadopodia activity. Curr Biol 18, 1295-9.

Ang, L. H., Kim, J., Stepensky, V. and Hing, H. (2003). Dock and Pak regulate olfactory axon pathfinding in Drosophila. Development 130, 1307-16.

Antoku, S., Saksela, K., Rivera, G. M. and Mayer, B. J. (2008). A crucial role in cell spreading for the interaction of Abl PxxP motifs with Crk and Nck adaptors. J Cell Sci 121, 3071-82.

Ayala, I., Baldassarre, M., Giacchetti, G., Caldieri, G., Tete, S., Luini, A. and Buccione, R. (2008). Multiple regulatory inputs converge on cortactin to control invadopodia biogenesis and extracellular matrix degradation. J Cell Sci 121, 369-78.

Bhuwania, R., Cornfine, S., Fang, Z., Kruger, M., Luna, E. J. and Linder, S. (2012). Supervillin couples myosin-dependent contractility to podosomes and enables their turnover. J Cell Sci 125, 2300-14.

Boateng, L. R. and Huttenlocher, A. (2012). Spatiotemporal regulation of Src and its substrates at invadosomes. Eur J Cell Biol 91, 878-88.

Brown, M. C., Cary, L. A., Jamieson, J. S., Cooper, J. A. and Turner, C. E. (2005). Src and FAK kinases cooperate to phosphorylate paxillin kinase linker, stimulate its focal adhesion localization, and regulate cell spreading and protrusiveness. Mol Biol Cell 16, 4316-28.

Chahdi, A., Miller, B. and Sorokin, A. (2005). Endothelin 1 induces beta 1Pix translocation and Cdc42 activation via protein kinase A-dependent pathway. J Biol Chem 280, 578-84.

Chan, K. T., Cortesio, C. L. and Huttenlocher, A. (2009). FAK alters invadopodia and focal adhesion composition and dynamics to regulate breast cancer invasion. J Cell Biol 185, 357-70.

Chernoff, E. A., O'Hara, C. M., Bauerle, D. and Bowling, M. (2000). Matrix metalloproteinase production in regenerating axolotl spinal cord. Wound Repair Regen 8, 282-91.

Coleman, H. A., Labrador, J. P., Chance, R. K. and Bashaw, G. J. (2010). The Adam family metalloprotease Kuzbanian regulates the cleavage of the roundabout receptor to control axon repulsion at the midline. Development 137, 2417-26.

Collin, O., Na, S., Chowdhury, F., Hong, M., Shin, M. E., Wang, F. and Wang, N. (2008). Self-organized podosomes are dynamic mechanosensors. Curr Biol 18, 1288-94.

Courtneidge, S. A. (2012). Cell migration and invasion in human disease: the Tks adaptor proteins. Biochem Soc Trans 40, 129-32.

Decourt, B., Munnamalai, V., Lee, A. C., Sanchez, L. and Suter, D. M. (2009). Cortactin colocalizes with filopodial actin and accumulates at IgCAM adhesion sites in Aplysia growth cones. J Neurosci Res 87, 1057-68.

Duchossoy, Y., Horvat, J. C. and Stettler, O. (2001). MMP-related gelatinase activity is strongly induced in scar tissue of injured adult spinal cord and forms pathways for ingrowing neurites. Mol Cell Neurosci 17, 945-56.

Ehrbar, M., Sala, A., Lienemann, P., Ranga, A., Mosiewicz, K., Bittermann, A., Rizzi, S. C., Weber, F. E. and Lutolf, M. P. (2011). Elucidating the role of matrix stiffness in 3D cell migration and remodeling. Biophys J 100, 284-93.

Eisenmann, K. M., Harris, E. S., Kitchen, S. M., Holman, H. A., Higgs, H. N. and Alberts, A. S. (2007). Dia-interacting protein modulates formin-mediated actin assembly at the cell cortex. Curr Biol 17, 579-91.

Fan, X., Labrador, J. P., Hing, H. and Bashaw, G. J. (2003). Slit stimulation recruits Dock and Pak to the roundabout receptor and increases Rac activity to regulate axon repulsion at the CNS midline. Neuron 40, 113-27.

Ferraro, G. B., Morrison, C. J., Overall, C. M., Strittmatter, S. M. and Fournier, A. E. (2011). Membrane-type matrix metalloproteinase-3 regulates neuronal responsiveness to myelin through Nogo-66 receptor 1 cleavage. J Biol Chem 286, 31418-24.

Fujioka, H., Dairyo, Y., Yasunaga, K. and Emoto, K. (2012). Neural functions of matrix metalloproteinases: plasticity, neurogenesis, and disease. Biochem Res Int 2012, 789083.

Galisteo, M. L., Chernoff, J., Su, Y. C., Skolnik, E. Y. and Schlessinger, J. (1996). The adaptor protein Nck links receptor tyrosine kinases with the serine-threonine kinase Pak1. J Biol Chem 271, 20997-1000.

Gomez, T. M. and Letourneau, P. C. (1994). Filopodia initiate choices made by sensory neuron growth cones at laminin/fibronectin borders in vitro. J Neurosci 14, 5959-72.

Gringel, A., Walz, D., Rosenberger, G., Minden, A., Kutsche, K., Kopp, P. and Linder, S. (2006). PAK4 and alphaPIX determine podosome size and number in macrophages through localized actin regulation. J Cell Physiol 209, 568-79.

Hayashita-Kinoh, H., Kinoh, H., Okada, A., Komori, K., Itoh, Y., Chiba, T., Kajita, M., Yana, I. and Seiki, M. (2001). Membrane-type 5 matrix metalloproteinase is expressed in differentiated neurons and regulates axonal growth. Cell Growth Differ 12, 573-80.

Heckman, C. A., Demuth, J. G., Deters, D., Malwade, S. R., Cayer, M. L., Monfries, C. and Mamais, A. (2009). Relationship of p21-activated kinase (PAK) and filopodia to persistence and oncogenic transformation. J Cell Physiol.

Hines, J. H., Abu-Rub, M. and Henley, J. R. (2010). Asymmetric endocytosis and remodeling of beta1-integrin adhesions during growth cone chemorepulsion by MAG. Nat Neurosci 13, 829-37.

Hing, H., Xiao, J., Harden, N., Lim, L. and Zipursky, S. L. (1999). Pak functions downstream of Dock to regulate photoreceptor axon guidance in Drosophila. Cell 97, 853-63.

Hoffmann, B. and Schafer, C. (2010). Filopodial focal complexes direct adhesion and force generation towards filopodia outgrowth. Cell Adh Migr 4, 190-3.

Hoshino, D., Branch, K. M. and Weaver, A. M. (2013). Signaling inputs to invadopodia and podosomes. J Cell Sci 126, 2979-89.

Huntley, G. W. (2012). Synaptic circuit remodelling by matrix metalloproteinases in health and disease. Nat Rev Neurosci 13, 743-57.

Hur, E. M., Saijilafu and Zhou, F. Q. (2012). Growing the growth cone: remodeling the cytoskeleton to promote axon regeneration. Trends Neurosci 35, 164-74.

Johnson, S. A. and Hunter, T. (2005). Kinomics: methods for deciphering the kinome. Nat Methods 2, 17-25.

Juin, A., Planus, E., Guillemot, F., Horakova, P., Albiges-Rizo, C., Genot, E., Rosenbaum, J., Moreau, V. and Saltel, F. (2013). Extracellular matrix rigidity controls podosome induction in microvascular endothelial cells. Biol Cell 105, 46-57.

Kaneko, N., Marin, O., Koike, M., Hirota, Y., Uchiyama, Y., Wu, J. Y., Lu, Q., Tessier-Lavigne, M., Alvarez-Buylla, A., Okano, H. et al. (2010). New neurons clear the path of astrocytic processes for their rapid migration in the adult brain. Neuron 67, 213-23.

Kayser, M. S., Nolt, M. J. and Dalva, M. B. (2008). EphB receptors couple dendritic filopodia motility to synapse formation. Neuron 59, 56-69.

Keow, J. Y., Herrmann, K. M. and Crawford, B. D. (2011). Differential in vivo zymography: a method for observing matrix metalloproteinase activity in the zebrafish embryo. Matrix Biol 30, 169-77.

Kim, S., Kim, T., Lee, D., Park, S. H., Kim, H. and Park, D. (2000). Molecular cloning of neuronally expressed mouse betaPix isoforms. Biochem Biophys Res Commun 272, 721-5.

Kim, T. and Park, D. (2001). Molecular cloning and characterization of a novel mouse betaPix isoform. Mol Cells 11, 89-94.

Kreis, P. and Barnier, J. V. (2009). PAK signalling in neuronal physiology. Cell Signal 21, 384-93.

Lin, J., Yan, X., Markus, A., Redies, C., Rolfs, A. and Luo, J. (2010). Expression of seven members of the ADAM family in developing chicken spinal cord. Dev Dyn 239, 1246-54.

Liu, S., Yamashita, H., Weidow, B., Weaver, A. M. and Quaranta, V. (2010). Laminin-332-beta1 integrin interactions negatively regulate invadopodia. J Cell Physiol 223, 134-42.

Loers, G., Makhina, T., Bork, U., Dorner, A., Schachner, M. and Kleene, R. (2012). The interaction between cell adhesion molecule L1, matrix metalloproteinase 14, and adenine nucleotide translocator at the plasma membrane regulates L1-mediated neurite outgrowth of murine cerebellar neurons. J Neurosci 32, 3917-30.

Lucanic, M., Kiley, M., Ashcroft, N., L'Etoile, N. and Cheng, H. J. (2006). The Caenorhabditis elegans P21-activated kinases are differentially required for UNC-6/netrin-mediated commissural motor axon guidance. Development 133, 4549-59.

Manser, E., Huang, H. Y., Loo, T. H., Chen, X. Q., Dong, J. M., Leung, T. and Lim, L. (1997). Expression of constitutively active alpha-PAK reveals effects of the kinase on actin and focal complexes. Mol Cell Biol 17, 1129-43.

Manser, E., Loo, T. H., Koh, C. G., Zhao, Z. S., Chen, X. Q., Tan, L., Tan, I., Leung, T. and Lim, L. (1998). PAK kinases are directly coupled to the PIX family of nucleotide exchange factors. Mol Cell 1, 183-92.

Marler, K. J., Poopalasundaram, S., Broom, E. R., Wentzel, C. and Drescher, U. (2010). Pro-neurotrophins secreted from retinal ganglion cell axons are necessary for ephrinA-p75NTR-mediated axon guidance. Neural Dev 5, 30.

Mayhew, M. W., Jeffery, E. D., Sherman, N. E., Nelson, K., Polefrone, J. M., Pratt, S. J., Shabanowitz, J., Parsons, J. T., Fox, J. W., Hunt, D. F. et al. (2007). Identification of phosphorylation sites in betaPIX and PAK1. J Cell Sci 120, 3911-8.

McCurley, A. T. and Callard, G. V. (2010). Time Course Analysis of Gene Expression Patterns in Zebrafish Eye During Optic Nerve Regeneration. J Exp Neurosci 2010, 17-33.

McFarlane, S. (2003). Metalloproteases: carving out a role in axon guidance. Neuron 37, 559-62.

Milward, E., Kim, K. J., Szklarczyk, A., Nguyen, T., Melli, G., Nayak, M., Deshpande, D., Fitzsimmons, C., Hoke, A., Kerr, D. et al. (2008). Cleavage of myelin associated glycoprotein by matrix metalloproteinases. J Neuroimmunol 193, 140-8.

Mott, H. R., Nietlispach, D., Evetts, K. A. and Owen, D. (2005). Structural analysis of the SH3 domain of beta-PIX and its interaction with alpha-p21 activated kinase (PAK). Biochemistry 44, 10977-83.

Murphy, D. A. and Courtneidge, S. A. (2011). The 'ins' and 'outs' of podosomes and invadopodia: characteristics, formation and function. Nat Rev Mol Cell Biol 12, 413-26.

Murphy, D. A., Diaz, B., Bromann, P. A., Tsai, J. H., Kawakami, Y., Maurer, J., Stewart, R. A., Izpisua-Belmonte, J. C. and Courtneidge, S. A. (2011). A Src-Tks5 pathway is required for neural crest cell migration during embryonic development. PLoS One 6, e22499.

Myers, J. P. and Gomez, T. M. (2011). Focal adhesion kinase promotes integrin adhesion dynamics necessary for chemotropic turning of nerve growth cones. J Neurosci 31, 13585-95.

Myers, J. P., Santiago-Medina, M. and Gomez, T. M. (2011). Regulation of axonal outgrowth and pathfinding by integrin-ECM interactions. Dev Neurobiol 71, 901-23.

Nayal, A., Webb, D. J., Brown, C. M., Schaefer, E. M., Vicente-Manzanares, M. and Horwitz, A. R. (2006). Paxillin phosphorylation at Ser273 localizes a GIT1-PIX-PAK complex and regulates adhesion and protrusion dynamics. J Cell Biol 173, 587-9.

O'Connor, T. P., Duerr, J. S. and Bentley, D. (1990). Pioneer growth cone steering decisions mediated by single filopodial contacts in situ. J Neurosci 10, 3935-46.

Obermeier, A., Ahmed, S., Manser, E., Yen, S. C., Hall, C. and Lim, L. (1998). PAK promotes morphological changes by acting upstream of Rac. EMBO J 17, 4328-39.

Ohta, Y., Suzuki, N., Nakamura, S., Hartwig, J. H. and Stossel, T. P. (1999). The small GTPase RalA targets filamin to induce filopodia. Proc Natl Acad Sci U S A 96, 2122-8.

Renkema, G. H., Pulkkinen, K. and Saksela, K. (2002). Cdc42/Rac1-mediated activation primes PAK2 for superactivation by tyrosine phosphorylation. Mol Cell Biol 22, 6719-25.

Robles, E., Woo, S. and Gomez, T. M. (2005). Src-dependent tyrosine phosphorylation at the tips of growth cone filopodia promotes extension. J Neurosci 25, 7669-81.

Santiago-Medina, M., Gregus, K. A. and Gomez, T. M. (2013). PAK-PIX interactions regulate adhesion dynamics and membrane protrusion to control neurite outgrowth. J Cell Sci 126, 1122-33.

Schaffner, A. E., St John, P. A. and Barker, J. L. (1987). Fluorescence-activated cell sorting of embryonic mouse and rat motoneurons and their long-term survival in vitro. J Neurosci 7, 3088-104.

Schimmelpfeng, K., Gogel, S. and Klambt, C. (2001). The function of leak and kuzbanian during growth cone and cell migration. Mech Dev 106, 25-36.

Scott, R. W., Hooper, S., Crighton, D., Li, A., Konig, I., Munro, J., Trivier, E., Wickman, G., Morin, P., Croft, D. R. et al. (2010). LIM kinases are required for invasive path generation by tumor and tumor-associated stromal cells. J Cell Biol 191, 169-85.

Seals, D. F. and Courtneidge, S. A. (2003). The ADAMs family of metalloproteases: multidomain proteins with multiple functions. Genes Dev 17, 7-30.

Sharma, V. P., Eddy, R., Entenberg, D., Kai, M., Gertler, F. B. and Condeelis, J. (2013). Tks5 and SHIP2 Regulate Invadopodium Maturation, but Not Initiation, in Breast Carcinoma Cells. Current Biology 23, 2079-2089.

Shekarabi, M., Moore, S. W., Tritsch, N. X., Morris, S. J., Bouchard, J. F. and Kennedy, T. E. (2005). Deleted in colorectal cancer binding netrin-1 mediates cell substrate adhesion and recruits Cdc42, Rac1, Pak1, and N-WASP into an intracellular signaling complex that promotes growth cone expansion. J Neurosci 25, 3132-41.

Shin, E. Y., Shin, K. S., Lee, C. S., Woo, K. N., Quan, S. H., Soung, N. K., Kim, Y. G., Cha, C. I., Kim, S. R., Park, D. et al. (2002). Phosphorylation of p85 beta PIX, a Rac/Cdc42-specific guanine nucleotide exchange factor, via the Ras/ERK/PAK2 pathway is required for basic fibroblast growth factor-induced neurite outgrowth. J Biol Chem 277, 44417-30.

Shin, E. Y., Woo, K. N., Lee, C. S., Koo, S. H., Kim, Y. G., Kim, W. J., Bae, C. D., Chang, S. I. and Kim, E. G. (2004). Basic fibroblast growth factor stimulates activation of Rac1 through a p85 betaPIX phosphorylation-dependent pathway. J Biol Chem 279, 1994-2004.

Srivastava, N., Robichaux, M. A., Chenaux, G., Henkemeyer, M. and Cowan, C. W. (2013). EphB2 receptor forward signaling controls cortical growth cone collapse via Nck and Pak. Mol Cell Neurosci 52, 106-16.

Stofega, M. R., Sanders, L. C., Gardiner, E. M. and Bokoch, G. M. (2004). Constitutive p21-activated kinase (PAK) activation in breast cancer cells as a result of mislocalization of PAK to focal adhesions. Mol Biol Cell 15, 2965-77.

Suzuki, K., Hayashi, Y., Nakahara, S., Kumazaki, H., Prox, J., Horiuchi, K., Zeng, M., Tanimura, S., Nishiyama, Y., Osawa, S. et al. (2012). Activity-dependent proteolytic cleavage of neuroligin-1. Neuron 76, 410-22.

ten Have, S., Boulon, S., Ahmad, Y. and Lamond, A. I. (2011). Mass spectrometry-based immuno-precipitation proteomics - the user's guide. Proteomics 11, 1153-9.

ten Klooster, J. P., Jaffer, Z. M., Chernoff, J. and Hordijk, P. L. (2006). Targeting and activation of Rac1 are mediated by the exchange factor beta-Pix. J Cell Biol 172, 759-69.

Tominaga, M., Tengara, S., Kamo, A., Ogawa, H. and Takamori, K. (2011). Matrix metalloproteinase-8 is involved in dermal nerve growth: implications for possible application to pruritus from in vitro models. J Invest Dermatol 131, 2105-12.

Toriyama, M., Kozawa, S., Sakumura, Y. and Inagaki, N. (2013). Conversion of a signal into forces for axon outgrowth through Pak1-mediated shootin1 phosphorylation. Curr Biol 23, 529-34.

Turner, C. E., Brown, M. C., Perrotta, J. A., Riedy, M. C., Nikolopoulos, S. N., McDonald, A. R., Bagrodia, S., Thomas, S. and Leventhal, P. S. (1999). Paxillin LD4 motif binds PAK and PIX through a novel 95-kD ankyrin repeat, ARF-GAP protein: A role in cytoskeletal remodeling. J Cell Biol 145, 851-63.

Vadlamudi, R. K., Li, F., Adam, L., Nguyen, D., Ohta, Y., Stossel, T. P. and Kumar, R. (2002). Filamin is essential in actin cytoskeletal assembly mediated by p21-activated kinase 1. Nat Cell Biol 4, 681-90.

van Helden, S. F., Oud, M. M., Joosten, B., Peterse, N., Figdor, C. G. and van Leeuwen, F. N. (2008). PGE2-mediated podosome loss in dendritic cells is dependent on actomyosin contraction downstream of the RhoA-Rho-kinase axis. J Cell Sci 121, 1096-106.

Vandooren, J., Geurts, N., Martens, E., Van den Steen, P. E. and Opdenakker, G. (2013). Zymography methods for visualizing hydrolytic enzymes. Nat Methods 10, 211-20.

Walmsley, A. R., McCombie, G., Neumann, U., Marcellin, D., Hillenbrand, R., Mir, A. K. and Frentzel, S. (2004). Zinc metalloproteinase-mediated cleavage of the human Nogo-66 receptor. J Cell Sci 117, 4591-602.

Woo, S. and Gomez, T. M. (2006). Rac1 and RhoA promote neurite outgrowth through formation and stabilization of growth cone point contacts. J Neurosci 26, 1418-28.

Woodring, P. J., Meisenhelder, J., Johnson, S. A., Zhou, G. L., Field, J., Shah, K., Bladt, F., Pawson, T., Niki, M., Pandolfi, P. P. et al. (2004). c-Abl phosphorylates Dok1 to promote filopodia during cell spreading. J Cell Biol 165, 493-503.

Xie, Y., Tan, E. J., Wee, S., Manser, E., Lim, L. and Koh, C. G. (2008). Functional interactions between phosphatase POPX2 and mDia modulate RhoA pathways. J Cell Sci 121, 514-21.

Yong, V. W., Power, C., Forsyth, P. and Edwards, D. R. (2001). Metalloproteinases in biology and pathology of the nervous system. Nat Rev Neurosci 2, 502-11.

Zheng, J. Q., Wan, J. J. and Poo, M. M. (1996). Essential role of filopodia in chemotropic turning of nerve growth cone induced by a glutamate gradient. J Neurosci 16, 1140-9.

Zivraj, K. H., Tung, Y. C., Piper, M., Gumy, L., Fawcett, J. W., Yeo, G. S. and Holt, C. E. (2010). Subcellular profiling reveals distinct and developmentally regulated repertoire of growth cone mRNAs. J Neurosci 30, 15464-78.

Zuo, J., Ferguson, T. A., Hernandez, Y. J., Stetler-Stevenson, W. G. and Muir, D. (1998). Neuronal matrix metalloproteinase-2 degrades and inactivates a neurite-inhibiting chondroitin sulfate proteoglycan. J Neurosci 18, 5203-11.